HEP Laboratory I

Author: Angelo Serrecchia
Prof.: Gianluca Cavoto

Disclaimer:
The following notes have not been fully reviewed, they could contain inaccuracies in physical arguments and may be present grammatical/ syntax english errors.
The author takes full responsibility for everything wrong that's written in this work and by no means the professor should be held accountable.

If you find any inaccuracies/typos you can send me an email to the address: angeloserrecchia.physics@gmail.com

Enjoy the reading and enjoy physics!

Angelo Serrecchia

NATURAL UNITS

Quantity	Dimensions: SI Units	Dimensions: Natural Units	Conversions
mass	kg	E	1 GeV = 1.8×10^{-27} kg
length	m	1/E	1 GeV^{-1} = 0.197×10^{-15} m
time	s	1/E	1 GeV^{-1} = 6.58×10^{-25} s
energy	$kg\cdot m^2/s^2$	E	1 GeV = 1.6×10^{-10} Joules
momentum	kg·m/s	E	1 GeV = 5.39×10^{-19} kg·m/s
velocity	m/s	none	1 = 2.998×10^{8} m/s (c)
angular momentum	$kg\cdot m^2/s$	none	1 = 1.06×10^{-34} J·s (ħ)
cross-section	m^2	$1/E^2$	1 GeV^{-2} = 0.389 mb = 0.389×10^{-31} m^2
force	$kg\cdot m/s^2$	E^2	1 GeV^2 = 8.19×10^{5} Newton
charge	C=A·s	none	1 = 5.28×10^{-19} Coulomb; e=0.303=1.6×10^{-19} C

$$[Q] = [s]^{\alpha}[v]^{\beta}[\varepsilon]^{\delta} \;\Big\}\; \hbar = c = 1 \;\rightarrow [Q] = [\varepsilon]^{\delta}$$

$$\hbar c = 197\ \text{MeV}\cdot\text{fm}$$

$$\hbar c = \frac{e^2}{4\pi\alpha} = \frac{e^2\,137}{4\pi}$$

CROSS SECTION

$$\text{Prob(to have 1 interaction)} = \frac{\sigma\cdot N}{S} = \frac{\sigma\cdot n\cdot \Delta\ell\cdot S}{S} = \sigma\cdot n\cdot v_{rel}\cdot\Delta t \longrightarrow \frac{dP}{dt} = \sigma\cdot n\cdot v_{rel}$$

- **Density of targets:** $n_{\text{molecules}} = N_A\frac{\rho}{PM}$ $\qquad n_{\text{subparticles}} = N_A\frac{\rho}{PM}\cdot(\#\ \text{subparticles inside the molecule})$
- **Reduction of the beam intensity through ℓ:** $\lambda^{-1} \equiv n\cdot\sigma$ (Absorbtion length) $\longrightarrow N(\ell) = N_0\, e^{-\frac{\ell}{\lambda}}$
- $1\,b = 10^{-24}\,cm^2$

LORENTZ TRANSFORMATIONS

CMS ← LAB

$$\begin{bmatrix} ct' \\ x' \\ y' \\ z' \end{bmatrix} = \begin{bmatrix} \gamma & -\frac{v}{c}\gamma & 0 & 0 \\ -\frac{v}{c}\gamma & \gamma & 0 & 0 \\ 0 & 0 & 1 & 0 \\ 0 & 0 & 0 & 1 \end{bmatrix} \begin{bmatrix} ct \\ x \\ y \\ z \end{bmatrix}$$

$$\begin{bmatrix} \epsilon' \\ k'_x \\ k'_y \\ k'_z \end{bmatrix} = \begin{bmatrix} \gamma & -\beta\gamma & 0 & 0 \\ -\beta\gamma & \gamma & 0 & 0 \\ 0 & 0 & 1 & 0 \\ 0 & 0 & 0 & 1 \end{bmatrix} \begin{bmatrix} \epsilon \\ k_x \\ k_y \\ k_z \end{bmatrix}$$

LAB ← CMS

$$\begin{bmatrix} ct \\ x \\ y \\ z \end{bmatrix} = \begin{bmatrix} \gamma & +\frac{v}{c}\gamma & 0 & 0 \\ +\frac{v}{c}\gamma & \gamma & 0 & 0 \\ 0 & 0 & 1 & 0 \\ 0 & 0 & 0 & 1 \end{bmatrix} \begin{bmatrix} ct' \\ x' \\ y' \\ z' \end{bmatrix}$$

$$\begin{bmatrix} \epsilon \\ k_x \\ k_y \\ k_z \end{bmatrix} = \begin{bmatrix} \gamma & +\beta\gamma & 0 & 0 \\ +\beta\gamma & \gamma & 0 & 0 \\ 0 & 0 & 1 & 0 \\ 0 & 0 & 0 & 1 \end{bmatrix} \begin{bmatrix} \epsilon' \\ k'_x \\ k'_y \\ k'_z \end{bmatrix}$$

- **Connecting 2 frames of ref.**

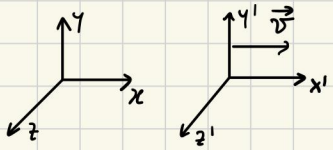

- **Particle Lorentz parameters:** $\beta = \frac{P}{E}$ $\qquad \gamma = \frac{E}{M}$
- **Particle Lorentz parameters in a fixed target experiment:**

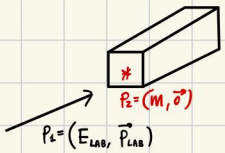

$$\begin{cases} \beta_{CMS} = \dfrac{|\vec{P}_{LAB}|}{E_1+E_2} = \dfrac{|\vec{P}_{LAB}|}{E_{LAB}+m} \\ \gamma_{CMS} = \dfrac{E_1+E_2}{\sqrt{s}} = \dfrac{E_{LAB}+m}{\sqrt{s}} \\ s = |\underline{P}_1+\underline{P}_2|^2 \end{cases}$$

- **Angles transformation:**

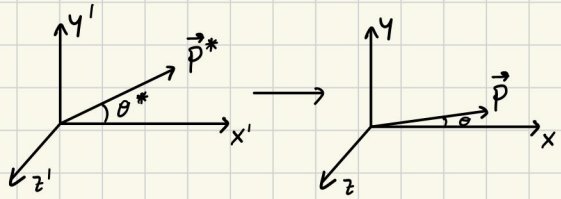

$$\tan\theta = \frac{P^*\sin\theta^*}{\beta\gamma E^* + \gamma P^*\cos\theta^*} = \frac{\sin\theta^*}{\gamma\left(\frac{\beta}{\beta^*}+\cos\theta^*\right)}$$

- **Decaying particle:**
  - **Lifetime** $\tau = \frac{1}{\Gamma}$ where

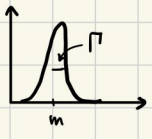

  - **Survived particles**

$$N(t') = N_0\, e^{-\frac{t'}{\tau}} \qquad t' : \text{time in the CoM frame}$$

$$N(t) = N_0\, e^{-\frac{t}{\gamma\tau}} \qquad t : \text{time in the LAB frame}$$
$$N(x) = N_0\, e^{-\frac{x}{\beta\gamma c\tau}} \qquad x : \text{decay length in the LAB frame}$$

useful to infer τ →

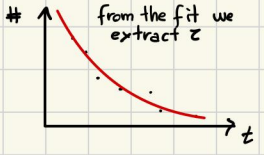

§2 SOURCE OF PARTICLES

- radioactive source decays
- cosmic rays
- collisions in accelerators

COSMIC RAYS

- They are made of:
  - 99% nuclei
    - 90% protons
    - 9% α particles
    - 1% heavy nuclei
  - 1% solitary electrons

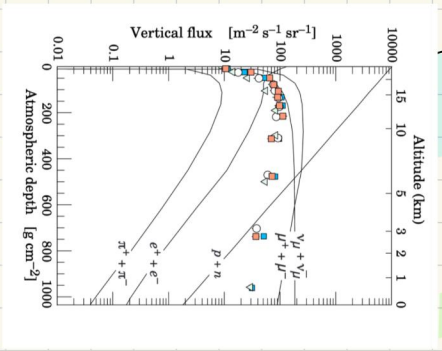

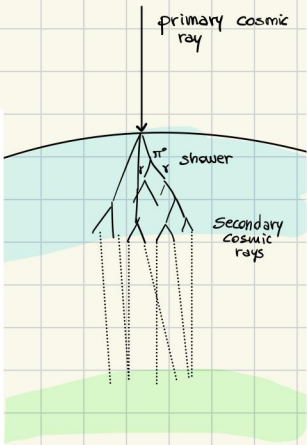

- Energy : very high
- Origin : Sun, other galaxies, ...

- What we see? : cosmic rays interact with atmosphere producing other particles which can be seen on the Earth surface and underground (secondary cosmic rays) from which we can reconstruct the energy, the direction and the composition of the incident particle

- Intensity on the surface : $I \sim 1\ cm^{-2}\ min^{-1}$ (horizontal detectors)

DECAYS

GAMMA DECAYS

$$ {}^{A}_{Z}N^{*} \longrightarrow {}^{A}_{Z}N + \gamma $$

- Interaction : hadronic
- Source of : γ
- Spectrum : monocromatic

BETA DECAYS

$$ \beta^- : \quad n \to p + e^- + \bar{\nu}_e, \qquad {}^{N}_{Z}A \to {}^{N}_{Z+1}A + e^- + \bar{\nu}_e $$

$$ \beta^+ : \quad p \to n + e^+ + \nu_e, \qquad {}^{N}_{Z}A \to {}^{N}_{Z-1}A + e^+ + \nu_e $$

- Interaction : Weak
- Sources of : $e^-, e^+, \nu, \bar{\nu}, \gamma$
- Spectrum : continuum

Theoretical pure β spectrum

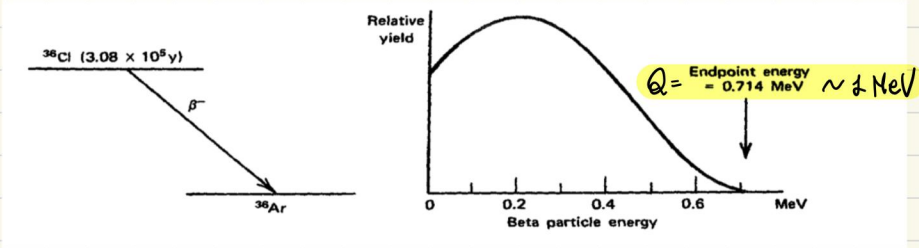

Real spectrum

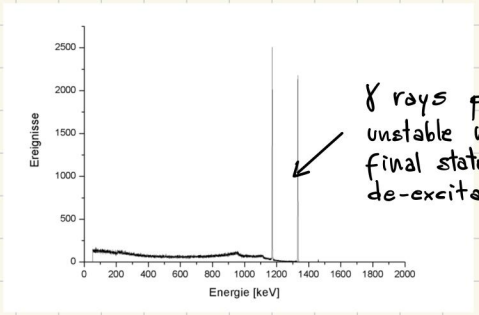

γ rays produced by unstable nucleus in the final state or by de-excitations

Common γ sources

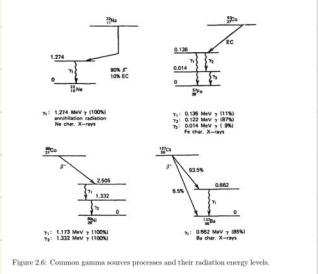

Figure 2.6: Common gamma sources processes and their radiation energy levels.

Table 1.1 Some "Pure" Beta-Minus Sources

Nuclide	Half-Life	Endpoint Energy (MeV)
^{3}H	12.26 y	0.0186
^{14}C	5730 y	0.156
^{32}P	14.28 d	1.710
^{33}P	24.4 d	0.248
^{35}S	87.9 d	0.167
^{36}Cl	3.08 × 10^5 y	0.714
^{45}Ca	165 d	0.252
^{63}Ni	92 y	0.067
^{90}Sr/^{90}Y	27.7 y/64 h	0.546/2.27
^{99}Tc	2.12 × 10^5 y	0.292
^{147}Pm	2.62 y	0.224
^{204}Tl	3.81 y	0.766

Figure 2.7: Summary of some beta-minus sources.

INTERNAL CONVERSION

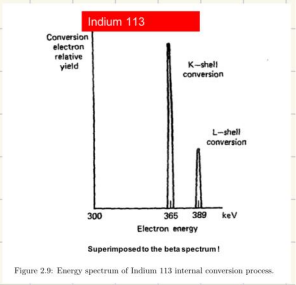

Figure 2.9: Energy spectrum of Indium 113 internal conversion process.

- Cause : $\Psi_{nucleus}$ has a large overlap with Ψ_{1s}
- Primary effect : monocromatic high energetic electron ejected with $E_e = E_{ex\ nucleus} - E_{binding}$
- Secondary effect : emission of x-rays or Auger electrons due to the descending of the other electrons to the lower empty level

ELECTRON CAPTURE

$$p + e^- \longrightarrow n + \nu_e$$

- Cause : unstable nucleus absorbs an inner atomic electron
- Secondary effect : emission of x-rays due to the replacing of the captured electron by an outer electron

AUGER ELECTRONS

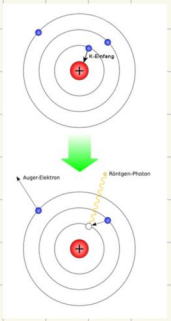

- Electrons ejected by the atom thanks to the energy released by the replacing of a core hole by higher electrons.

ALPHA DECAY

$$^{A}_{Z}N \longrightarrow ^{A-4}_{Z-2}N + ^{4}_{2}He$$

- Most common source : ^{243}Am

NEUTRON PRODUCTION

- from neutron-rich nuclides
- from the spontaneous or induced fission
- from the reaction between nuclei and α-particles $^{4}_{2}\alpha + ^{9}_{4}Be \rightarrow ^{12}_{6}C + n$
- fusion of : $D + D \longrightarrow {}^{3}He + n$ (2.5 MeV) ; $D + T \longrightarrow {}^{4}He + n$ (14.1 MeV)

§3 PARTICLE INTERACTION WITH MATTERS

CHARGED PARTICLES

- Interaction with the electrons of the material → excitation / ionization of the material atoms
  → non negligible energy loss
- Bremsstrahlung effect → emission of photons due to deacceleration of charged particles
  → dominant for low mass charged particles
  → non negligible energy loss

CHARGED OR NEUTRAL PARTICLES

- Coulomb scattering with the nuclei → sizeable deflection
  → negligible energy loss

- Photons interaction → totally absorbed in the matter
  → the effect is described by the attenuation length $\lambda = 1/n\sigma_{em}$
  (σ_{em} is the total cross section : $\sigma_{photo\ electric} + \sigma_{Compton} + \sigma_{pair\ prod}$ and n is the numeric density of scattering centers).

ENERGY LOSS BY CHARGED PARTICLES

Bohr's model : • interaction of a fast moving particle and the electrons of the medium
• bynary collision picture: the particle interacts with 1 atomic electron at the time
• 2 ASSUMPTIONS : atomic electrons at rest and free

↳ Are these 2 assumptions valid?
↳ $P_{atomic\ e^-} \sim$ KeV ($\sim$ rest) $\longrightarrow$ $E_{binding\ \text{outer shells}} \sim$ eV ($\sim$ free)

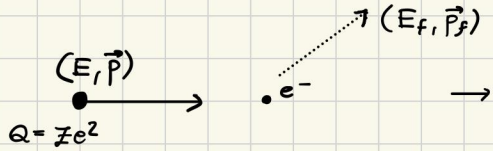

$\longrightarrow$ Momentum transfer: $\Delta\vec{P} = \int_{-\infty}^{+\infty} \vec{F}(t')\,dt'$

Strategy : we go in the CoM frame where it's easy to find the Coulomb force of the moving particle and then transform it with a Lorentz boost

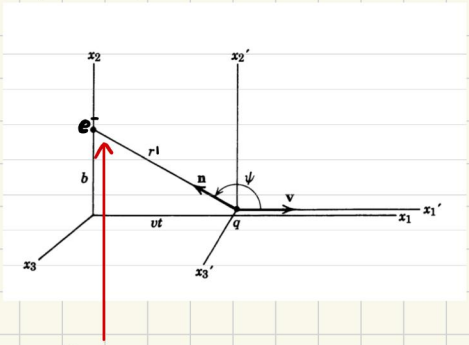

The $\vec{E}'$ field measured here in the CoM frame:

$$\left(\frac{Ze}{r'^2}\frac{(vt')}{r'}, \frac{Ze}{r'^2}\frac{b}{r'}, 0\right)$$

To find $\vec{E}$ in the Lab frame we need to transform the coordinates: The boost has the effect of squeezing the $\vec{E}$ field lines in the x direction, while the transverse (y) component gets enhanced by the boost

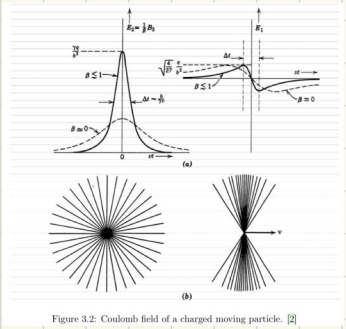

Figure 3.2: Coulomb field of a charged moving particle. [2]

$$\begin{cases} E_{\parallel} = E_{\parallel}' \\ E_{\perp} = \gamma E_{\perp}' \end{cases}$$

n.b. $r' = \sqrt{b^2 + x'^2} = \sqrt{b^2 + (v\gamma t)^2}$

$$\longrightarrow \Delta P_x = \int_{-\infty}^{+\infty} dt\, \frac{v\gamma t \cdot Ze^2}{\left(\sqrt{b^2 + (v\gamma t)^2}\right)^3} = 0$$

$$\Delta P_y = \int_{-\infty}^{+\infty} dt\, \gamma \frac{b \cdot Ze^2}{\left(\sqrt{b^2 + (v\gamma t)^2}\right)^3} \neq 0$$

$$\longrightarrow \boxed{\Delta E = \frac{|\Delta\vec{P}|^2}{2m_e} = \frac{4Z^2e^4}{2m_e}\frac{1}{b^2v^2}}$$

Now we have to sum all the single energy loss ΔE for each electrons inside the medium. So we need :
- Integral over all the possible b
- Incoherent sum over the Z electrons in each atom

$\longrightarrow$ we need the number density of electrons in the target material

We consider a volume element $dV = 2\pi b\,db\,dx$ and an electron number density n_e :

$$\longrightarrow -dE = \Delta E \cdot n_e \cdot dV = \frac{4\pi Z^2e^4}{m_e v^2} n_e \frac{db}{b} dx$$

$$\longrightarrow -\frac{dE}{dx}(b) = \frac{4\pi Z^2e^4}{m_e v^2} n_e \frac{db}{b} \longrightarrow -\frac{dE}{dx} = \frac{4\pi Z^2e^4}{m_e v^2} n_e \int_{b_{min}}^{b_{max}} \frac{db}{b}$$

$$b_{max} = \frac{\gamma v}{\omega}\ ; \quad b_{min} = \frac{Ze^2}{\gamma m_e v^2}$$

$$\longrightarrow \boxed{-\frac{dE}{dx} = \frac{4\pi Z^2e^4}{m_e v^2} n_e \ln\left(\frac{\gamma^2 m_e v^3}{Ze^2\omega}\right)} \quad \text{where } n_e = \frac{\rho N_A Z}{A}$$

Bethe-Bloch formula

Considerin the quantum correction, the mean energy loss per unit length by moderately relativistic heavy particles with charge Ze is well described by:

$K \equiv 0.307\ \text{MeV g}^{-1}\text{cm}^2$ (=)

if $M \gg m_e$ $W_{max} \sim 2m_e(\beta\gamma)^2$ — max kinematic energy transferred

density correction due to polarisation (relevant at high E)

$$-\frac{1}{\rho}\frac{dE}{dx} = (4\pi N_A r_e^2 m_e c^2)\frac{z^2}{\beta^2}\frac{Z}{A}\left(\frac{1}{2}\ln\frac{2m_e c^2\beta^2\gamma^2 W_{max}}{I^2} - \beta^2 - \frac{\delta(\beta\gamma)}{2} - \frac{C}{Z}\right) \quad \left[\text{MeV g}^{-1}\text{cm}^2\right]$$

$r_e = \frac{e^2}{4\pi\varepsilon_0 m_e c^2} = 2.8\ \text{fm} = 0.0143\ \text{MeV}^{-1}$

I: mean excitation energy of the material

Rule of thumb: $I \sim 10Z\,\text{eV}$ if $Z > 20$

C/Z: correction close to shell boundaries (relevant at small E)

Easy version to remember:

$$-\frac{1}{\rho}\frac{dE}{dx} \simeq 0.307\ \text{MeV g}^{-1}\text{cm}^2 \cdot Z^2\left(\frac{Z}{A}\right)\frac{1}{\beta^2}\left[\frac{1}{2}\ln\left(\frac{(2m_e(\beta\gamma)^2)^2}{I^2}\right) - \beta^2\right]$$

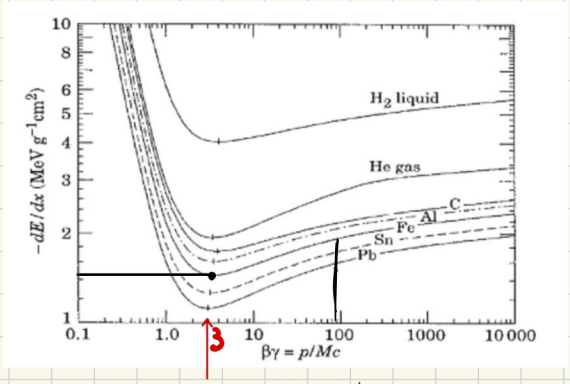

Table 1.1. *Average energy loss of minimum-ionising particles in various materials [10–12]; gases for standard pressure and temperature*

Absorber	$\frac{\langle dE\rangle}{dx}\big\vert_{\min}$ [MeV g^{-1}cm^2]	$\frac{\langle dE\rangle}{dx}\big\vert_{\min}$ [MeV cm^{-1}]
Hydrogen (H_2)	4.10	$0.37 \cdot 10^{-3}$
Helium	1.94	$0.35 \cdot 10^{-3}$
Lithium	1.64	0.87
Beryllium	1.59	2.94
Carbon (Graphite)	1.75	3.96
Nitrogen	1.82	$2.28 \cdot 10^{-3}$
Oxygen	1.80	$2.57 \cdot 10^{-3}$
Air	1.82	$2.35 \cdot 10^{-3}$
Carbon dioxide	1.82	$3.60 \cdot 10^{-3}$
Neon	1.73	$1.56 \cdot 10^{-3}$
Aluminium	1.62	4.37
Silicon	1.66	3.87
Argon	1.52	$2.71 \cdot 10^{-3}$
Titanium	1.48	6.72
Iron	1.45	11.41
Copper	1.40	12.54
Germanium	1.37	7.29
Tin	1.26	9.21
Xenon	1.25	$7.32 \cdot 10^{-3}$
Tungsten	1.15	22.20
Platinum	1.13	24.24
Lead	1.13	12.83
Uranium	1.09	20.66
Water	1.99	1.99
Lucite	1.95	2.30

Normlazied to density

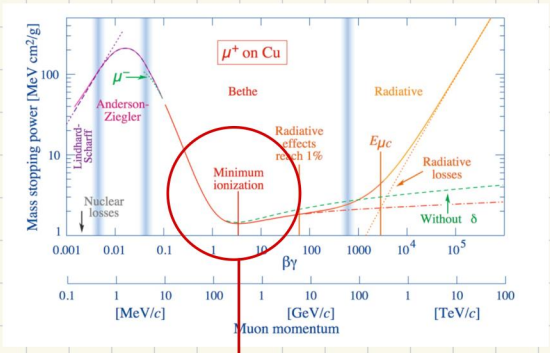

For practical cases most relativistic particles (e.g cosmic μ) have $\frac{dE}{dx} \sim \frac{dE}{dx}\big\vert_{min}$ → they are called MIP

RULE OF THUMB: for $\beta\gamma = 3$ $\quad \frac{dE}{dx} = 2\ \text{MeV g}^{-1}\text{cm}^2$

RANGE: maximum distance before that the particle stops:

$$R = \int_E^M \frac{dE}{-\frac{dE}{dx}}$$

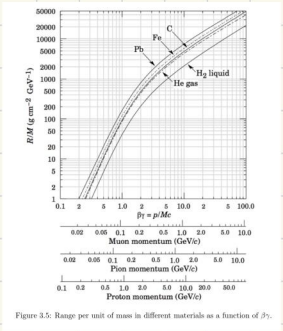

Figure 3.5: Range per unit of mass in different materials as a function of $\beta\gamma$.

n.b. At very low energies $-\frac{dE}{dx} \sim \frac{1}{\beta^2} \sim \frac{1}{K^2}$

→ $\boxed{R \sim K^2}$

BRAGG PEAK: peak located at a distance where the release of energy is maximum (usually before the particle stops) This is because $-\frac{dE}{dx} \propto \frac{1}{v^2}$

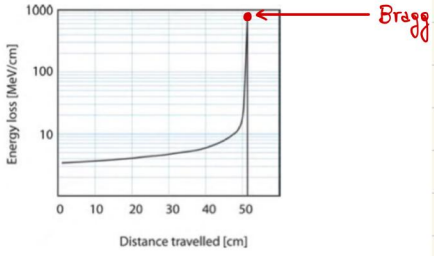

Figure 3.6: Energy loss as a function of travelled distance. the curve clearly exhibits the typical Bragg peak. This qualitative behavior can be understood in term of the non-linear Bethe-Bloch function ($\sim \frac{1}{\beta^2}$).

PARTICLE IDENTIFICATION : When the Bethe curve is plotted as a function of the momentum of the particle the energy loss is described by different curves depending on the particle type (i.e. its mass)

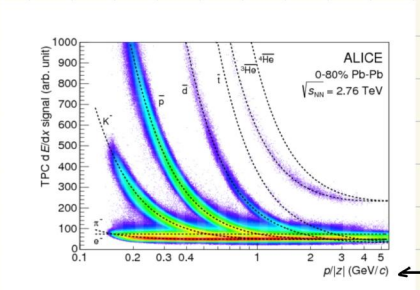

Figure 3.7: Energy loss in the Time Projection Chambers of the ALICE experiment for different particles. This picture describes the theoretical expectation of the average energy loss given by the Bethe-Bloch function and shown with the dashed curves. Each line corresponds to different masses starting from electron up to more massive anti-Helium.

← rigidity

$\longrightarrow$ we can perform P.I.D. seeing which curve is closest to the measured point $(p, \frac{\Delta E}{\Delta x})$.

NO FREE ELECTRONS : . the e^- are not free ! They are bounded to atoms and we can approximate them as quantum harmonic oscillators of similar energy ω_j. We have to consider the interaction of an $\vec{E}$ field with an harmonically bound oscillating e^-. By solving the eq. with Fourier transform we find an average energy $\langle\omega\rangle$. N.B. Oscillators are still classical.

- Since is a quantum effect the energy transfer is discrete. So the $\Delta E(b_{max})$ could be smaller than the smallest quantum of energy $\longrightarrow$ so $\Delta E(b)$ must be interpreted as the average over several single quantum energy transfer

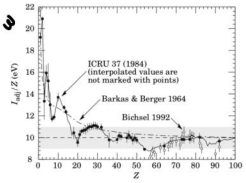

Figure 3.8: Mean excitation energy (divided by Z). The grey point is for liquid H_2, the black point at 19.2 eV is for gaseous H_2.

SOFT COLLISIONS : they need quantum treatment

$$\frac{dE}{dx}(T<\varepsilon) = 2\pi N Z \frac{z^2 e^4}{mc^2\beta^2}\{\ln[B_q^2(\varepsilon)] - \beta^2\}$$

$$B_q(\varepsilon) = \frac{\gamma v (2me)^{1/2}}{\hbar\langle\omega\rangle}.$$

ENERGY LOSS PROBABILITY DISTRIBUTION : . For detectors of moderate thickness x the energy loss probability distribution is described by the highly-skewed Landau distribution $f(\Delta)$ from which we can extrapolate the most probable value :

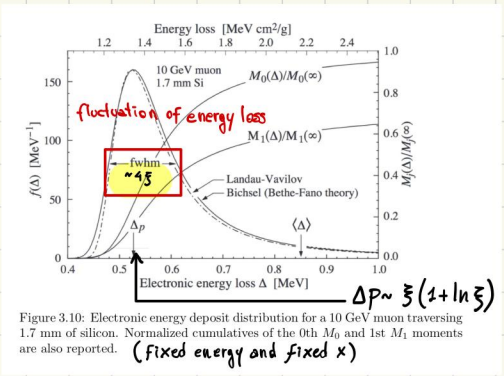

Figure 3.10: Electronic energy deposit distribution for a 10 GeV muon traversing 1.7 mm of silicon. Normalized cumulatives of the 0th M_0 and 1st M_1 moments are also reported. (fixed energy and fixed x)

$$\Delta_p = \xi\left[\ln\frac{2mc^2\beta^2\gamma^2}{I} + \ln\frac{\xi}{I} + j - \beta^2 - \delta(\beta\gamma)\right]$$

$j = 0.2$

take into account material properties

$$\xi = \frac{K}{2}\left\langle\frac{Z}{A}\right\rangle Z^2\left(\frac{x}{\beta^2}\right)$$

- For Si detectors $Z=14$, $A=28$, $\rho = 2.3\ g/cm^3$, $x \sim 300\,\mu m$ $\quad \left.\frac{\xi}{x}\right|_{MIP} = 1.7\cdot10^{-2}\ KeV/\mu m \xrightarrow{x=300\mu m} \xi = 5.1\ KeV$

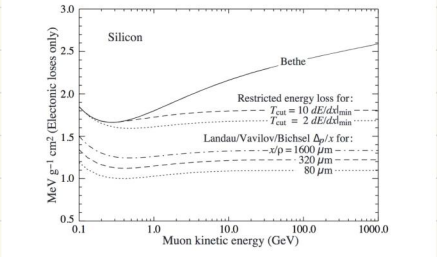

Figure 3.9: Bethe dE/dx, two examples of restricted energy loss, and the Landau most probable energy per unit thickness in silicon.

- Here we can see the most probable energy loss v.s. the mean energy loss (Bethe). The most probable energy loss can be found deriving the Landau p.d.f.

Energy loss for electrons and positrons

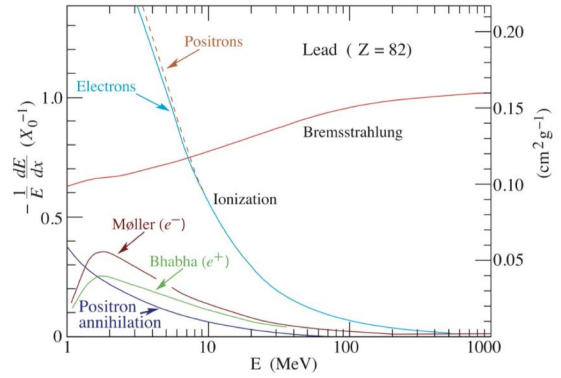

Figure 3.11: Fractional energy loss per radiation length in lead as a function of electron or positron energy. Electron (positron) scattering is considered as ionization when the energy loss per collision is below 0.255 MeV.

Proccsses involved during $e^{-/+}$ energy loss. The rule of thumb is:

- Low energy : ionization
- High energy: Bremsstrahlung

BREMSSTRAHLUNG (relevant for e^+/e^- and very high energetic μ)

- While the charged particles travel in the $\vec{E}$ field of a nuclei they can be bent: this deflection causes the emission of E.M. radiation
- The acceleration increases decreasing the mass of the charged particle $\longrightarrow$ dominant for light particles.

- Typical emission angle $\theta_{Brems} \sim \frac{1}{\gamma}$
- Radiation length:
  - It is the mean distance in which a high-energy $e^{-/+}$ is reduced to $1/e$ of its energy by Brems
  - (7/9 of the mean free path for pair production by a high-energy photon

$$X_0 = \frac{1}{n\sigma_{Brems}} = \frac{A}{4r_e^2 \alpha N_A Z^2 \rho Z(Z+1)\ln(183 Z^{-1/3})} \simeq \frac{180\,A}{\rho Z^2}$$

Material	Z	A	X_0 [g/cm^2]	X_0 [cm]	E_c [MeV]
Hydrogen	1	1.01	61.3	731 000	350
Helium	2	4.00	94	530 000	250
Lithium	3	6.94	83	156	180
Carbon	6	12.01	43	18.8	90
Nitrogen	7	14.01	38	30 500	85
Oxygen	8	16.00	34	24 000	75
Aluminium	13	26.98	24	8.9	40
Silicon	14	28.09	22	9.4	39
Iron	26	55.85	13.9	1.76	20.7
Copper	29	63.55	12.9	1.43	18.8
Silver	47	109.9	9.3	0.89	11.9
Tungsten	74	183.9	6.8	0.35	8.0
Lead	82	207.2	6.4	0.56	7.40
Air	7.3	14.4	37	30 000	84
SiO_2	11.2	21.7	27	12	57
Water	7.5	14.2	36	36	83

- If the medium is a compound $\longrightarrow$ $\frac{1}{X_0} = \sum_i \frac{w_i}{X_i}$ w_i: fraction of elem. X_i: singles rad. length

- Energy loss: $\left.\frac{dE}{dx}\right|_{Brems} \simeq -\frac{E}{X_0}$

- Critical energy: E such that $\left.\frac{dE}{dx}\right|_{Bethe\ Bloch} = \left.\frac{dE}{dx}\right|_{Brems}$

$$\begin{cases} E_{cr}^{e^-/e^+} = \frac{610\ MeV}{Z+1.24} \simeq \frac{600}{Z} \text{ (gas)} \\ E_{cr}^{e^-/e^+} = \frac{710\ MeV}{Z+0.92} \simeq \frac{700}{Z} \text{ (solid)} \end{cases}$$

- Total radiated power relativistic formula: $P = \frac{q^2 a^2 \gamma^4}{6\pi\varepsilon_0 c^3}$

Multiple Coulomb Scattering

The angle measurements are important in P.P.

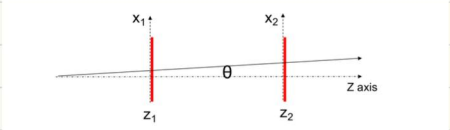

Figure 3.12: Scheme of two conceptual detectors measuring "transverse position" x of a charged particle at fixed "longitudinal position" z.

This kind of measurement can be affected by an uncertainty due to <u>multiple scattering</u>.
A charged particle traversing a medium can be deflected by many small scattering angles
This is due mainly by Coulomb scattering described by Rutherford cross section:

$$\frac{d\sigma}{d\Omega} \sim \left(\frac{2Z\mathcal{I}e^2}{pv}\right)^2 \frac{1}{\theta^4}$$

The problem is that for $\theta \to 0$ $\frac{d\sigma}{d\Omega} \to \infty$ a moreover at small b the point-like approx. of nucleus is not more valid So we need to add the structure factor.

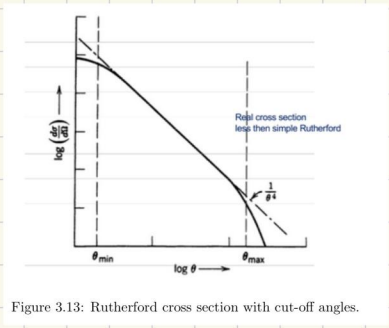

Figure 3.13: Rutherford cross section with cut-off angles.

Since $\Delta p \Delta x \sim \hbar \longrightarrow \frac{\Delta p}{p}\Delta x \sim \frac{\hbar}{p} \longrightarrow \theta \cdot \Delta x \sim \frac{\hbar}{p}$

$\longrightarrow \theta_{min} \sim \frac{\hbar}{pa}$

$\longrightarrow \theta_{max} \sim \frac{\hbar}{pR}$

→ The cut off for the scattering angle are then:

$$\theta_{max} = \frac{\hbar}{pR} \approx \frac{274}{A^{1/3}} \frac{mc}{p} \; ; \; \theta_{min} = \frac{\hbar}{pa} \simeq \frac{Z^{1/3}}{192} \frac{mc}{p}$$

$R = R_0 A^{1/3}$

$a = 1.4 \cdot a_0 Z^{-1/3}$

θ_j is a random variable

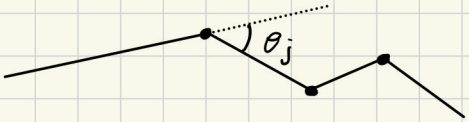

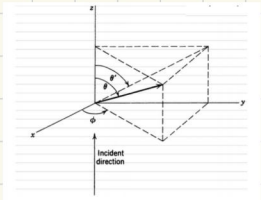

Figure 3.14: Scheme of projected scattering angles.

$$\langle \theta_j \rangle = 0$$

$$\langle \theta^2 \rangle = \frac{\int \theta^2 \frac{d\sigma}{d\Omega} d\Omega}{\int \frac{d\sigma}{d\Omega} d\Omega} = 2\theta_{min}^2 \ln\left(\frac{\theta_{max}}{\theta_{min}}\right)$$

$$\langle \theta_{ij}^2 \rangle = \langle \theta_{kj}^2 \rangle = \frac{\langle \theta^2 \rangle}{2}$$

if the incident particle is along the j axis

The cumulative effect of multiple scatterings by T.L.C. is described by a Gaussian:

$$pdf(\textcircled{H}) \sim \prod_i pdf(\theta_i)$$

where $pdf(\theta_i) \sim \mathcal{N}(0, \langle\theta^2\rangle)$

Therefore the random variable $\textcircled{H}$ will have:

$$\langle \textcircled{H} \rangle = 0$$

$$\langle \textcircled{H}^2 \rangle = N\langle\theta^2\rangle = 2\pi n \left(\frac{2Z\mathcal{I}e^2}{pv}\right)^2 \ln\left(\frac{\theta_{max}}{\theta_{min}}\right) \cdot x$$

where $N = n \cdot \sigma \cdot x$

σ: total Rutherford cross-section

x: thickness of the medium

n: density of scattering centers

We can define a lot of projected angles:

$$\theta_0 = \frac{1}{\sqrt{2}}\sqrt{\langle \textcircled{H}^2 \rangle}$$

n.b. θ_0 is θ_{rms}^x

$$\psi = \frac{1}{\sqrt{3}}\theta_0$$

$$y = \frac{1}{\sqrt{3}} x\theta_0$$

$$s = \frac{1}{4\sqrt{3}} x\theta_0$$

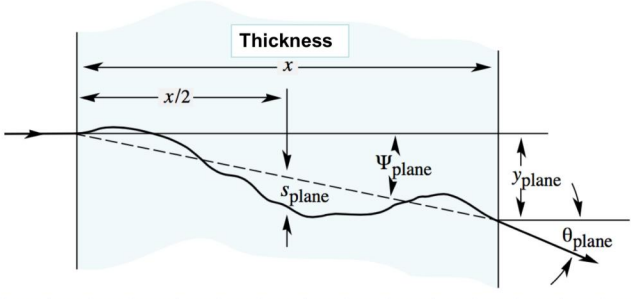

For many small deflections the net effect is described by a Gaussian (ideally). However scattering from the Coulomb field of the atomic nucleus does not obey exactly the T.L.C. The single scattering σ falls of only as $\sim \theta^{-4}$ generating a very small, but non zero, probability for single events with very large scattering angles.

$\longrightarrow$ The actual prob. distribution is Gaussian only for small angles.

Moliere developed a model that was able to predict the whole distribution, taking into account the target thickness. His model was interpolated by Highland who found a Gaussian approx. to the full Moliere model using

$$\theta_0 = \frac{13.6\ \text{MeV}}{\beta c p} z \sqrt{\frac{x}{X_0}} \left(1 + 0.038 \ln\left(\frac{x z^2}{X_0 \beta^2}\right)\right) \simeq \frac{13.6\ \text{MeV}}{\beta p} z \sqrt{\frac{x}{X_0}}$$

as σ for the Gaussian which describes the p.d.f of the angle projected to a plane after a thickness x of material.

X_0 : parametrize properties of the medium related to interaction with nuclei (both angular deflection and radiation emission)

Table 2.1 Radiation length X_0 for some common materials

Material	Radiation length X_0
Air	304 m
Water	36 cm
Shielding concrete	10.7 cm
Nylon	36.7 cm
Aluminium (Al)	8.9 cm
Silicon (Si)	9.36 cm
Iron (Fe)	1.76 cm
Lead (Pb)	0.56 cm
Uranium (U)	0.32 cm

PHOTON INTERACTION IN MATTER

Photon energy is not continuously lost in the medium (as for charged particles): a photon can be either totally absorbed or travel in a medium without any release of energy. So is the intensity the variable that is decreasing not the energy:

$$I = I_0 e^{-\frac{x}{\lambda}} \qquad \lambda = \frac{1}{n\sigma} \text{ mean free path}$$

3 processes: Photoelectric effect
Pair production
Compton

Photoelectric effect

$$\gamma + A \longrightarrow e^- + A^+$$

- It is the absorbtion of a γ with $E_\gamma = h\nu$ by an atomic e^- (E_b = binding energy with the emission of an e^- with $E_{e^-} = E_\gamma - E_b$
- Constraint: $E_\gamma > E_{e^-\text{binding}}$; requires the presence of a nucleus.
- Strongly dependent on the material and relevant at small energies:

$$\begin{cases} \sigma_{p.E} \propto Z^5/E^3 & E \gtrsim m_e c^2 \\ \sigma_{p.E} \propto Z^5/E & E \gg m_e c^2 \end{cases}$$

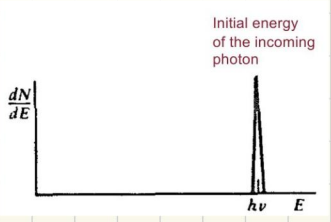

Compton effect

$$\gamma + e^- \longrightarrow \gamma + e^-$$

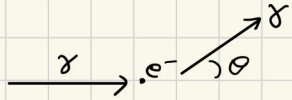

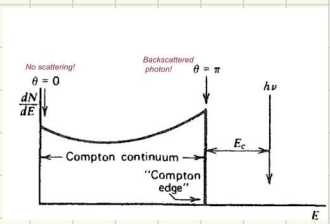

- It is the scattering of a γ (with $E_\gamma = h\nu$) off an atomic electron (at rest). The γ in the final statte will have an energy

$$E_{\gamma'} = \frac{E_\gamma}{1 + \frac{E_\gamma}{m_e}(1+\cos\theta)} \quad ; \quad \lambda' - \lambda = \frac{h}{m_e c}(1-\cos\theta)$$

- **Compton cross section (Q.E.D.):**

$$\frac{d\sigma}{d\Omega} = \frac{r_e^2 Z E_\gamma'}{2 A E_\gamma}\left(1 + \left(\frac{E_\gamma'}{E_\gamma}\right)^2 + \frac{E_\gamma'}{E_\gamma}\sin^2\theta\right)$$

~ incoherent sum of the γ int. with each atomic e^- (this explains the Z presence)

- $\sigma_c \propto \sigma_{Th}\left(1 - 2\frac{E_\gamma}{m_e}\right)$ $\quad E_\gamma \ll m_e c^2$
- $\sigma_c \propto Z \frac{\ln\left(\frac{E_\gamma}{m_e}\right)}{\frac{E_\gamma}{m_e}}$ $\quad E_\gamma \gg m_e c^2$

- **Transferred energy to electron:**

$$K = E_\gamma - E_\gamma' = E_\gamma \frac{\frac{E_\gamma}{m_e}(1-\cos\theta)}{1 + \frac{E_\gamma}{m_e}(1-\cos\theta)} \overset{\theta=\pi}{=} E_\gamma \frac{2\frac{E_\gamma}{m_e}}{1+2\frac{E_\gamma}{m_e}} \equiv K^{max} < E_\gamma$$

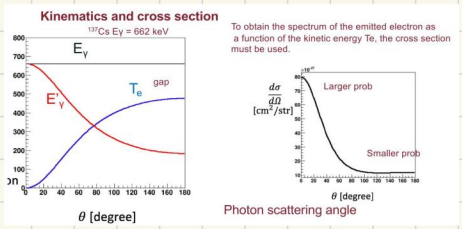

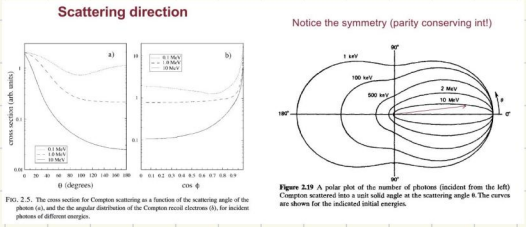

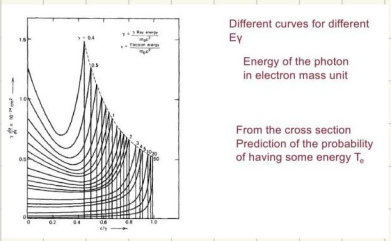

Pair production $\quad \gamma \rightarrow e^+e^-$

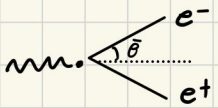

- **Threshold effect:** $E_\gamma > 2 m_e c^2 = 1.022$ MeV, medium needed

- $\sigma_{pair} = 4\alpha r_e^2 Z_{nucl}(Z_{nucl}+1)\left[\frac{7}{9}\ln\left(\frac{183}{Z^{1/3}}\right) - \frac{1}{54}\right]$ cm²/atom $\quad E \gg 1$ GeV $\rightarrow$ $\sigma_{pair} \sim \frac{7}{9}\frac{1}{X_0}\frac{A}{\rho N_A}$

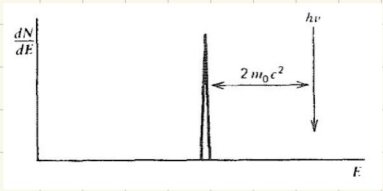

- **Pair length:** $\lambda^{pair}_{\text{mean free path}} \equiv \frac{9}{7} X_0$; **Mean opening angle:** $\bar{\theta} = \frac{m_e c^2}{E_\gamma}$

- **Fraction of energy carried away by the e^+ (e^-):**

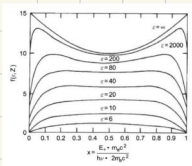

- x: fraction of energy of the photon carried away by the positron(electron)
- Symmetric around 0.5

TOTAL ABSORBTION CROSS SECTION FOR PHOTONS

$$I = I_0 e^{-\frac{x}{\lambda}} = I_0^{-x n \sigma}$$

$$\sigma = \sigma_{P.E.} + \sigma_C + \sigma_{pair} + \sigma_{elastic}$$

Very small contribution

- Dominant process depends on Energy of the photon and Z of the material
- Compton scattering largely dominat at 1 MeV for low Z

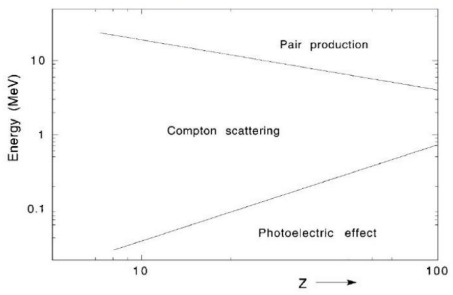

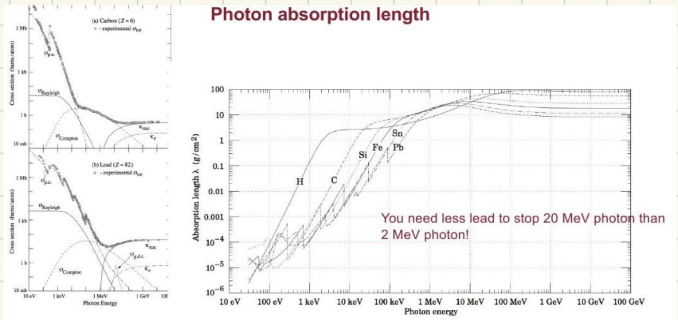

- **MULTIPLE INTERACTIONS IN THE SAME MATERIAL**

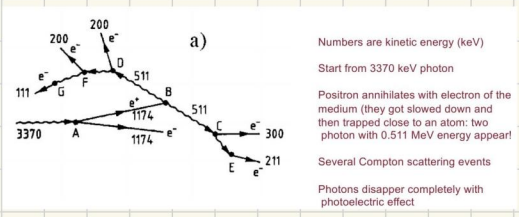

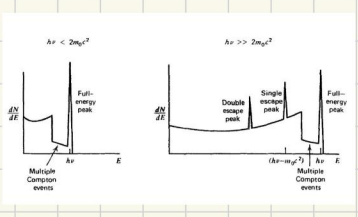

A TOO SMALL DETECTOR? Simply geometry : sphere

- radius must be compared with the photon absorbtion length.
- If $\lambda_{abs} < R$ the size of the detector is big enough to make all the photon interacting. Of course we have to take into account the range of the emitted e^- but usually are $< \lambda_{abs}$.

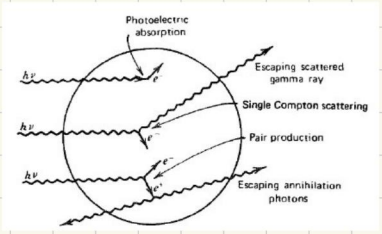

FULLY CONTAINED

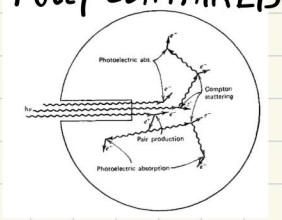

PARTIALLY CONTAINED

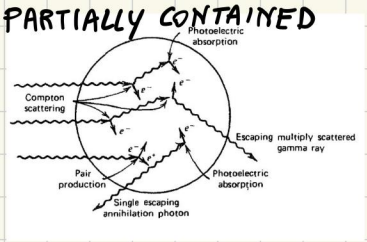

NUCLEAR CROSS SECTION

- Hadron can interact with nuclei via strong interaction

$$\sigma_{tot} = \sigma_{elastic} + \sigma_{inelastic}$$

$$\sigma_{in} \sim 4 \cdot 10^{-26} \cdot A^{2/3}\ cm^2 = 4 \cdot A^{2/3}\ mb$$

- Interaction length :

$$\lambda_I = \frac{A}{N_A \rho \sigma_{inelastic}} \simeq \left(\frac{A}{\rho}\right)^{1/3} \cdot \frac{1}{N_A \cdot 4 \cdot 10^{-26}} = \left(\frac{A}{\rho}\right)^{1/3} \cdot 35\ g/cm^2$$

Material	Z	A	σ_{total} [barn]	σ_{inel} [barn]	$\lambda_I \cdot \rho$ [g/cm^2]	$\lambda_\gamma \cdot \rho$ [g/cm^2]
Hydrogen	1	1.01	0.0387	0.033	43.3	50.8
Helium	2	4.0	0.133	0.102	49.9	65.1
Beryllium	4	9.01	0.268	0.199	55.8	75.2
Carbon	6	12.01	0.331	0.231	60.2	86.3
Nitrogen	7	14.01	0.379	0.265	61.4	87.8
Oxygen	8	16.0	0.420	0.292	63.2	91.0
Aluminium	13	26.98	0.634	0.421	70.6	106.4
Silicon	14	28.09	0.660	0.440	70.6	106.0
Iron	26	55.85	1.120	0.703	82.8	131.9
Copper	29	63.55	1.232	0.782	85.6	134.9
Tungsten	74	183.85	2.767	1.65	110.3	185
Lead	82	207.19	2.960	1.77	116.2	194
Uranium	92	238.03	3.378	1.98	117.0	199

Total meams including also the elastic (or Quasi elastic) interactions

ELECTROMAGNETIC SHOWERS

- Rossi model

- Starting point: γ with E_0
- After X_0 a e^+e^- pair is produced (Pair prod.)
- After X_0 each e^-/e^+ produces a γ (Brems)

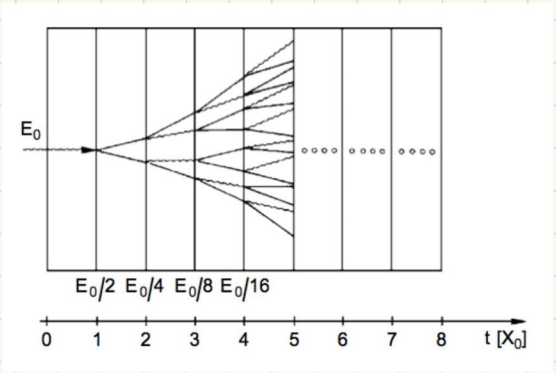

- For E_0 large enough this process keeps repeating
- # of particles $N(t) = 2^t$ $\quad t = \frac{x}{X_0}$
- Each particle is carrying a smaller and smaller energy : $E(t) = \frac{E_0}{2^t}$
- When E(t) is equal to the E_{cr} the shower stops (n.b. E_{cr} is the energy where $\left.\frac{dE}{dx}\right|_{ion} = \left.\frac{dE}{dx}\right|_{Brems}$)

$$E_{cr} = \frac{E_0}{2^{t_{max}}} \rightarrow t_{max} = \frac{\ln\left(\frac{E_0}{E_c}\right)}{\ln(2)}$$

- Below E_c (At the end of the shower)

▸ γ are stopped by Compton and ph.elec. effect. They are not absorbed quickly : we need to compare the absorbtion length with the radiation length X_0.

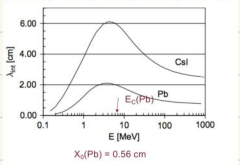

▸ e^-/e^+ release all their energy (E_c) in one X_0 by ionization.

- # of positrons

Table 2.1 *The numbers of positrons that are generated in em shower development and the fraction of the total energy deposited by these particles. Results of EGS4 simulations.*

Shower energy →	10 GeV		100 GeV	
Absorber ↓	$\#e^+$	E^+/E_{tot}	$\#e^+$	E^+/E_{tot}
Aluminium ($Z = 13$)	191	26%	1750	27%
Iron ($Z = 26$)	285	27%	2920	26%
Tin ($Z = 50$)	427	24%	4330	25%
Lead ($Z = 82$)	554	22%	5730	23%
Uranium ($Z = 92$)	612	23%	5970	23%

- Example of a 10 GeV e.m. shower energy deposit

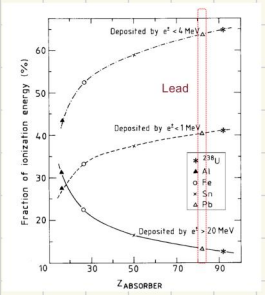

- Most of the energy deposit is due to slow e^-/e^+
- In lead more than 60% of E_0 is deposited by e^+/e^- with an energy < 4 MeV (by ionization since below critical energy)

- <u>Shower profile</u> :

- the shower has a 3D profile : → longitudinal extension, → lateral extension

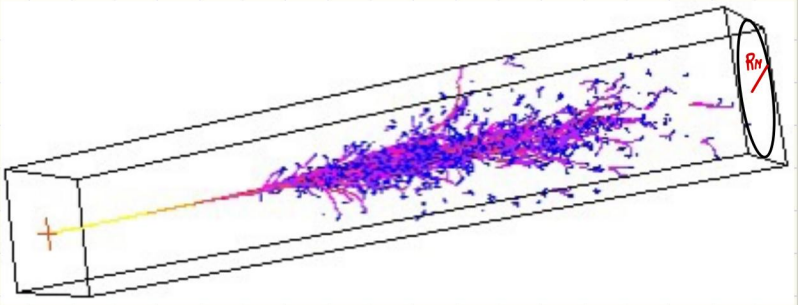

<u>Moliere radius</u>: $R_M = \frac{21}{E_c\,(\text{MeV})} X_0 \quad [\text{g cm}^{-2}]$

- <u>Energy deposit as function of the lateral and longitudinal depth</u>

more in detail

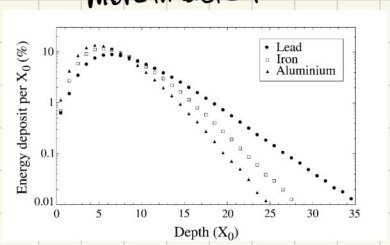

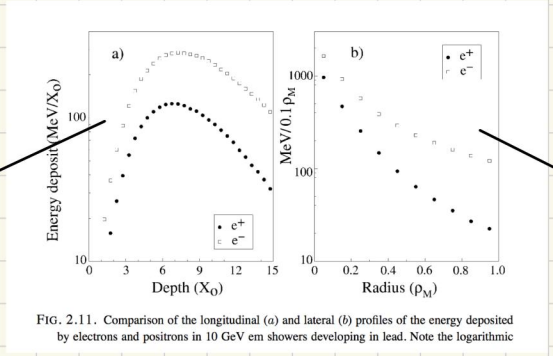

FIG. 2.11. Comparison of the longitudinal (*a*) and lateral (*b*) profiles of the energy deposited by electrons and positrons in 10 GeV em showers developing in lead. Note the logarithmic

more in detail

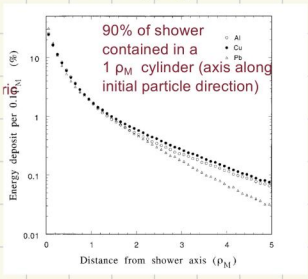

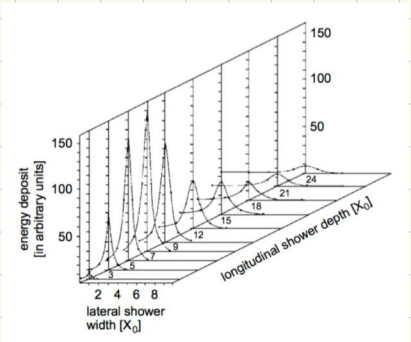

- Energy is measured by "counting" the low energy e^-/e^+. Resolution improves with statistics:

$$\frac{\sigma(E_0)}{E_0} \propto \frac{1}{\sqrt{n}} \propto \frac{1}{\sqrt{E_0}}$$

FERNI ENERGY LOSS CALCULATION

Bohr's and Bethe's result works under the assumption that medium is not affected by the charged particles
Actually the particle produces an $\vec{E}(\vec{x},t)$ that acts on medium atoms (molecules causing *polarization* of it.
This effect is parametrized by the *dielectric constant* of the medium ε.

- Isotropic medium $\rightarrow$ $\varepsilon \in \mathbb{C}$ $\quad \sqrt{\varepsilon} = n + i\alpha$
  - n: refraction index
  - α: absorption parameter (it describes the propagation of E.M. waves in that medium)

ε is a function of the frequency ω of the E.M. waves (i.e. the $E_\gamma = \hbar\omega$). Therefore it's convenient to introduce the ω (contained in $\vec{E}$) dependence by using a Fourier transform formalism

1. We compute the work done by the $\vec{E}(\vec{x},t)$ generated by the moving charged p. ($\vec{v}$; ze) on one e^- of the medium:

$$\Delta E = -e \int_{-\infty}^{+\infty} \vec{E}(\vec{x},t) \cdot \vec{v}_e(t)\, dt \qquad \text{where } d\vec{x}(t) = \vec{v}_e(t)\, dt \text{ is the } e^- \text{ displacement}$$

2. We perform the Fourier transform rewritint $\vec{E}(\vec{x},t)$ as:

$$\vec{E}(\vec{x},t) = \frac{1}{(2\pi)^2} \int d^3k \int d\omega\, \vec{E}(\vec{k},\omega)\, e^{-i(\vec{k}\cdot\vec{x} - \omega t)}$$

3. Rememberin that for real functions $f(t)$ the F.T. is such that $f(\omega) = f^*(-\omega)$ and using Parseval theorem:

$$\Delta E(b) = ze\, Re \int_0^{+\infty} i\omega\, \vec{x}(\omega) \cdot \vec{E}^*(\omega)\, d\omega \qquad \text{where} \qquad \vec{E}(\omega) \equiv \frac{1}{(2\pi)^{3/2}} \int d^3k\, \vec{E}(\vec{k},\omega)\, e^{i\vec{k},b} \quad *$$

This is the contribution of 1 electron at some impact parameter b to the energy loss.

4. We need to sum up over all the electrons in the medium assuming isotropic density n.
We use the infinitesimal volume $b\,d\phi\,db\,dx$ to counts e^- (which are $n \cdot b \cdot d\phi \cdot db \cdot dx$).
We need therefore to integrate over a range of **b** and over all angles.
Before doing that we recall that the molecular polarizability can be expressed as:

$$-e \sum_i f_i \vec{x}_i = \frac{1}{4\pi n} [\varepsilon(\omega) - 1] \vec{E}(\omega) \qquad \text{where } f_i \text{ is the \# of } e^- \text{ in the } i^{th} \text{ orbital}$$

So:

$$\left.\frac{dE}{dx}\right|_{b>a} = \frac{-1}{2\pi n} Re \int_a^{+\infty} i\omega\, \varepsilon(\omega)\, \vec{E}(\omega) \cdot \vec{E}^*(\omega)\, d\omega$$

Therefore $\left.\frac{dE}{dx}\right|_{b>a} \neq 0 \longleftrightarrow$ there exist ω where $Im(\varepsilon(\omega)) \neq 0$ (absorbing medium)

5. To compute $\vec{E}(\omega)$ we can use $\phi(\vec{x},t)$ and $\vec{A}(\vec{x},t)$ wave equations with non-zero source

The motion of the charged particle can be expressed by a charge density $\rho(\vec{x},t) = ze\,\delta(\vec{x} - vt)$ and a current density $\vec{J}(\vec{x},t) = \vec{v}\rho(\vec{x},t)$. Actually is convenient to solve the eq. in the Fourier space:

$$\begin{cases} \phi(\vec{k},\omega) = \dfrac{2ze}{\varepsilon(\omega)} \dfrac{\delta(\omega - \vec{k}\cdot\vec{v})}{k^2 - \frac{\omega^2}{c^2}\varepsilon(\omega)} \\ \vec{A}(\vec{k},\omega) = \varepsilon(\omega) \dfrac{\vec{v}}{c} \phi(\vec{k},\omega) \end{cases}$$

So $\vec{E} = -\vec{\nabla}\phi - \frac{1}{c}\frac{\partial \vec{A}}{\partial t}$:

$$\vec{E}(\vec{k},\omega) = \left(-i\vec{k} - \frac{1}{c}\frac{\vec{v}}{c}\varepsilon(\omega)(-i\omega)\right)\phi(\vec{k},\omega)$$

6. Using * and evaluating the integral eliminating the δ function we obtain $\omega = \vec{k}\cdot\vec{v} = k_x v$
The components of $\vec{E}(\omega)$ can be now evaluated and a complex function λ (with dimension of L^{-1}) emerges:

$$\lambda^2 = \frac{\omega^2}{v^2} - \frac{\omega^2}{c^2}\varepsilon(\omega)$$

λ depends on ω through $\varepsilon(\omega)$: it can emerge an imaginary part for some specific intervals in frequency where $n = \mathrm{Re}\sqrt{\varepsilon(\omega)}$ has large values. N.B. The velocity of the E.M. in the medium emerges as $\frac{c}{\sqrt{\mathrm{Re}(\varepsilon(\omega))}}$

7. The result can be summarized as:

$$\left.\frac{dE}{dx}\right|_{b>a} = \frac{2}{\pi}\frac{(Ze)^2}{c^2}\,\mathrm{Re}\int_0^\infty i\omega\,\lambda^* a\,K_1(\lambda^* a)\,K_0(\lambda a)\left(\frac{1}{\beta^2\varepsilon(\omega)} - 1\right)d\omega$$

energy loss per unit length of a charged p. with $\vec{v}$ and transverse distance from its path larger than a

where K_0 and K_1 are the modified Bessel functions:

- for $z \ll 1 \longrightarrow K_0 \sim -\ln\frac{z}{2} - 0.5772 \qquad K_1 \sim \frac{1}{z}$
- for $z \gg 1 \longrightarrow K_0, K_1 \sim \sqrt{\frac{\pi}{2}}\frac{e^{-z}}{\sqrt{z}}$

LIMITS:

- $\lambda a \sim \frac{\omega a}{c} \ll 1$ $\left(\omega \sim 10^{14}\,Hz;\ a \sim a_0 = 0.5\,10^{-10}\,m;\ v \sim c\right)$ $\left(\frac{dE}{dx}\right)_{b>a} = \frac{2}{\pi}\frac{(ze)^2}{v^2}\Re\int_0^{+\infty} i\omega\,\ln\left(\frac{1.123}{\lambda a}\right)\frac{1}{\epsilon(\omega)}\left(1-\beta^2\epsilon(\omega)\right)d\omega.$
- $\lambda a \ll 1$ $\beta \to 1$: $\left(\frac{dE}{dx}\right)_{b\gg a} = \frac{(Ze)^2\omega_p^2}{c^2}\left(\ln\left(\frac{1.123c}{a\omega_p}\right)\right.$ with $\omega_p = \frac{4\pi Z n e^2}{m}$
- $\lambda a \gg 1$: → if λ is real $\longrightarrow$ $\frac{dE}{dx} = 0$ (exp. damping)
  → if λ is purely imaginary there is no exp (when $\beta > \frac{1}{\sqrt{\varepsilon(\omega)}}$)

$$\longrightarrow \frac{d^2E}{dx\,d\omega} = \omega\left(1 - \frac{1}{\beta^2\varepsilon(\omega)}\right)$$

In this limit there is no a dependence in $\frac{dE}{dx}$ and then there is an energy loss even at infinite distance. The interpretation is that the energy can be lost in form of EM waves, i.e γ are produced and emitted from the charged particles. This is the explaination of Cherenkov effect.

CHERENKOV EFFECT

- Cherenkov radiation is an E.M. radiation emitted when charged particles pass through a dielectric medium at a speed greater than the speed of light in that medium

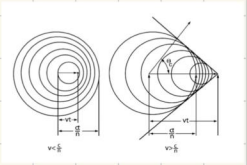

- Constraint : $v > \frac{c}{n} \longrightarrow \boxed{\beta > \beta_{threshold} \equiv \frac{1}{n}}$ where $n = Re\sqrt{\varepsilon}$
- Cherenkov emission angle : $\boxed{\cos\theta_c = \frac{1}{\beta n}}$ or $\boxed{\tan\theta_c = \sqrt{\beta^2 n^2 - 1}}$
- For gases : $\boxed{n = 1+\delta \quad \text{with} \quad \delta \ll 10^{-3}} \longrightarrow \beta_{threshold} = \frac{1}{1+\delta} \sim 1-\delta \longrightarrow p_{threshold} = \frac{m}{\sqrt{2\delta}}$
- Cherenkov angle close to the threshold : $\cos\theta_c \sim 1 - \frac{\theta_c^2}{2}$; $\beta \sim \frac{1}{n} + \varepsilon \longrightarrow \theta_c \sim \sqrt{2n\varepsilon}$
- # of Cherenkov γ (in unit energy and space) : $\frac{d^2N}{dEdx} = \frac{\alpha z^2}{\hbar c}\sin^2\theta_c = \frac{\alpha^2 z^2}{r_e m_e c^2}\left(1 - \frac{1}{\beta^2 n^2(E)}\right) \simeq 370 \sin^2\theta_c(E)\ eV^{-1}cm^{-1}$ $(z=1)$
- N.B. $\beta = \frac{p}{E} = \frac{1}{\sqrt{1+\frac{m^2}{p^2}}}$; in the case of $p \gg m$ $\beta \sim \frac{1}{1+\frac{1}{2}\frac{m^2}{p^2}} \sim 1 - \frac{1}{2}\frac{m^2}{p^2}$

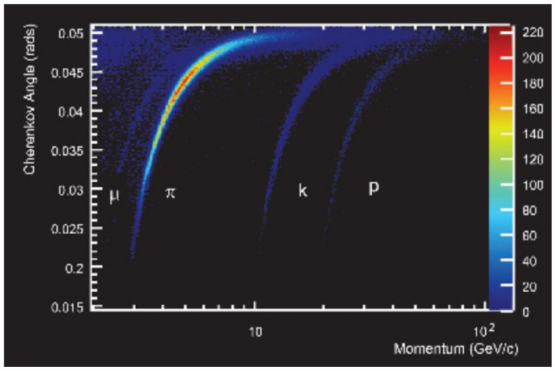

Figure 3.20: Cherenkov angle as a function of the momentum for different particles.

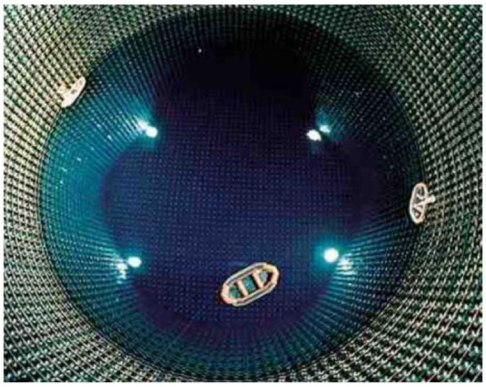

Figure 3.19: Inside the SuperKamiokande detector, that is based on Cherenkov radiation in water.

Mezzo o sostanza	Indice di rifrazione	Velocità di propagazione
vuoto	1	$3 \cdot 10^8$ m/s
aria	1,00029	$2{,}999 \cdot 10^8$ m/s
acqua	1,33	$2{,}26 \cdot 10^8$ m/s
ghiaccio	1,31	$2{,}29 \cdot 10^8$ m/s
sale	1,54	$1{,}95 \cdot 10^8$ m/s
alcool	1,36	$2{,}2 \cdot 10^8$ m/s
vetro (Crown)	1,5	$2 \cdot 10^8$ m/s
vetro (Flint)	1,65	$1{,}82 \cdot 10^8$ m/s
solfuro di carbonio	1,63	$1{,}84 \cdot 10^8$ m/s
sodio liquido	4,22	$0{,}7 \cdot 10^8$ m/s
arseniuro di gallio	3,6	$0{,}83 \cdot 10^8$ m/s
silicio	3,4	$0{,}88 \cdot 10^8$ m/s
diamante	2,417	$1{,}24 \cdot 10^8$ m/s
quarzo	1,51	$1{,}98 \cdot 10^8$ m/s

In a gas $\frac{n^2+1}{n^2+2} = \rho$

Densità di alcuni solidi

(a 0°C, 1 atm)

Nome	Densità (g/cm³)
Alluminio	2.70
Argento	10.49
Acciaio	7.81
Cemento	2.7-3.0
Ferro	7.96
Ghiaccio	0.92
Gomma	1.34
Legno (densità media)	0.75
Legno di cedro	0.31-0.49
Legno d'ebano	0.98
Legno d'olmo	0.54-0.60
Legno di pino bianco	0.35-0.50
Legno di quercia	0.6-0.9
Marmo	2.71
Nichel	8.8
Oro	19.3
Ottone	8.44-9.70
Osso	1.7-2.0
Piombo	11.34
Platino	21.37
Rame	8.96
Stagno	7.28
Sughero	0.22-0.26
Terra (valor medio*)	5.52
Tungsteno	19.3
Vetro	2.4-2.8
Zinco	7.1

Densità di alcuni liquidi

(a 0°C, 1 atm)

Nome	Densità (g/cm³)
Acqua	1.00
Acqua di mare	1.025
Acetone	0.79
Alcool (etilico)	0.806
Ammoniaca	0.77
Benzina	0.68
Glicerina	1.261
Mercurio	13.6
Olio d'oliva	0.92
Olio di paraffina	0.8

Densità di alcuni gas

(a 0°C, 1 atm)

Nome	Formula	Densità (g/dm³)
Acetilene	C_2H_2	1.173
Aria		1.292
Ammoniaca	NH_3	0.771
Diossido di carbonio	CO_2	1.976
Monossido di carbonio	CO	1.250
Elio	He	0.178
Idrogeno	H_2	0.089
Ossigeno	O_2	1.429
Ozono	O_3	2.144

DETECTORS PROPERTIES

In a detector there are some concepts to keep in mind:

- Signal formation
- efficiency
- resolution
- rate and timing
- linearity

COUNTING DETECTOR : · Simplest detector
· binary information (YES/NO)
· can measure an event rate
· useful only if the theory provides some prediction about the rate

CONCEPTUAL DETECTORS AND DETECTOR CHAIN

DETECTOR CONCEPT #1

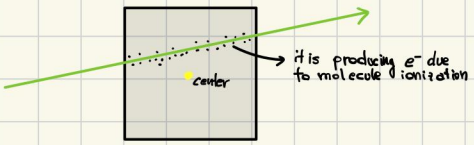

- Box filled with thin/light material (gas)
  - When the particle is crossing the volume it produces a signal proportional to $\Delta E \ll T_0$
  - The walls of the detector are passive: the energy lost in the walls cannot be used for detection but that energy should be taken into account
  - Measuring the position of the box (e.g its center) we can measure the position of a point on the trajectory of a charged particle

DETECTOR CONCEPT #2

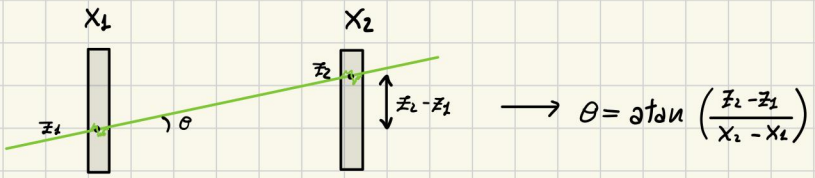

- Two detectors that measure the transverse position x of a charged particle at fixed z
  - We are able to measure the beam divergence (angles)
  - The detector thickness adds an uncertainty due to Multiple Coulomb scattering

DETECTOR CONCEPT #3

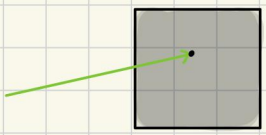

- Box filled with heavy/dense material
  - Particles are stopped inside the volume $\Delta E = T_0$ and the signal is proportional to T_0
  - Destructive measurement
  - Concept of range is relevant (only ionization energy loss is important).

DETECTOR CONCEPT #4

- Box filled with heavy/dense material with a radioactive source inside
  - Also here $\Delta E = T_0$
  - The walls of the detector can be a source of noise.

DETECTOR CONCEPT #5 :

- Multi channels detectors : a single system made of several replicas of the same unit (the channel)

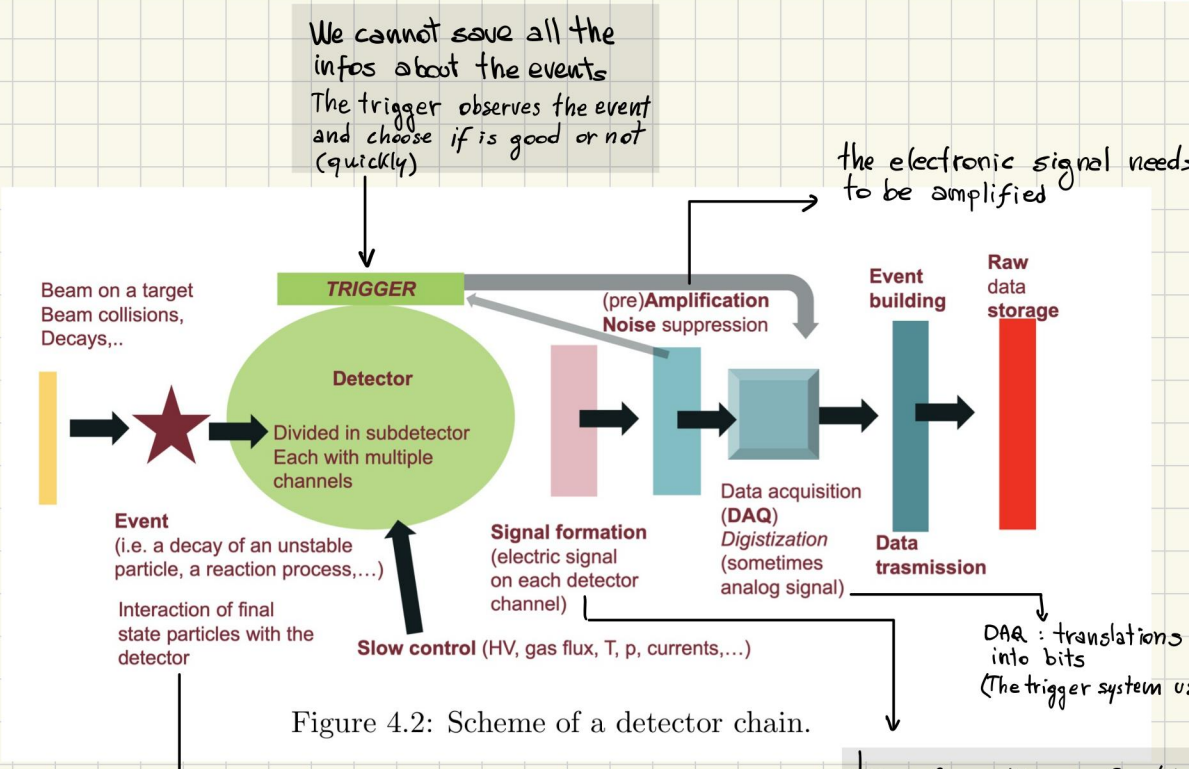

Figure 4.2: Scheme of a detector chain.

transformation of the physical event in an electronic signal

- in p.p. we look for single events
- Each event is identified by its final state. that need to be reconstructed

Example of detector divided into multiple subdetectors (BaBar exp. SLAC)

1) Vertex tracker
2) Spectrometer (drift chamber)
3) Hadron PID (Cherenkov det)
4) γ / e^- detector (em calorimeter)
5) Spectrometer magnet (sc)
6) Muon id

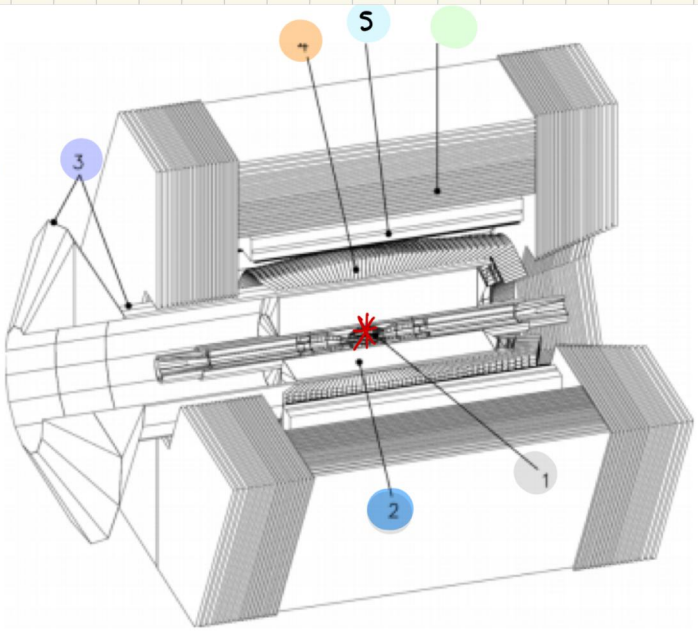

Figure 4.3: Scheme of the BaBar experiment.

UNCERTAINTY: measurement of the deviation of the measured value from the exoected true value. Can be statistical or systematic.

RESOLUTION: smallest number we can resolve

PRECISION: how close are different measurements of the same quantity? In other words it measure the repeatibility of the measurement. (statistical uncertainty)

ACCURACY: how close is your measurement to the true value? (bias? Need good calibration)

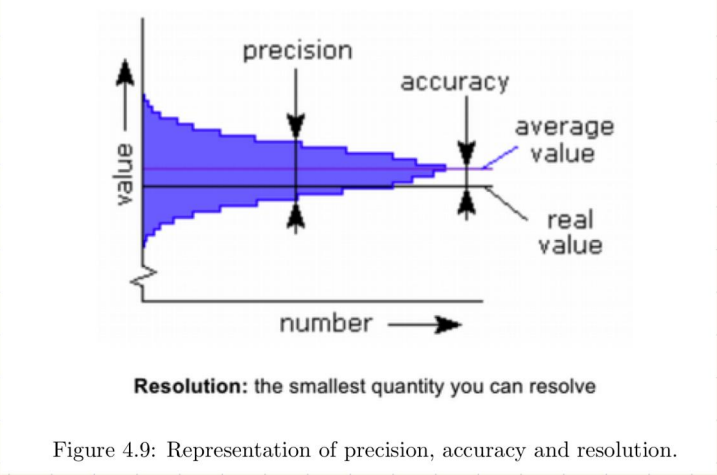

Figure 4.9: Representation of precision, accuracy and resolution.

DEAD TIME

If we want to measure the rate of signals we need to compare the duration of the signal with the rate at which it appears. : if the signals are very close in time the detector may not be fully efficient to detect them.
The detector may be <u>not totally active</u> during a recovery time τ_R or may be completely inactive during a certain time τ_D (data processing, ...)

$\longrightarrow$ the detector cannot accept events at a rate $> \dfrac{1}{\tau_D + \tau_R}$

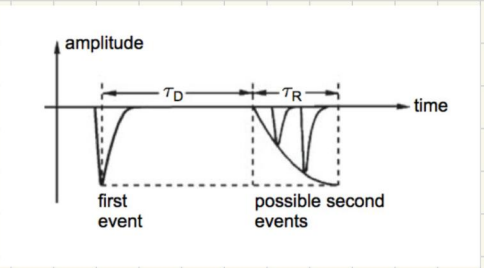

MODELS FOR DEAD TIME

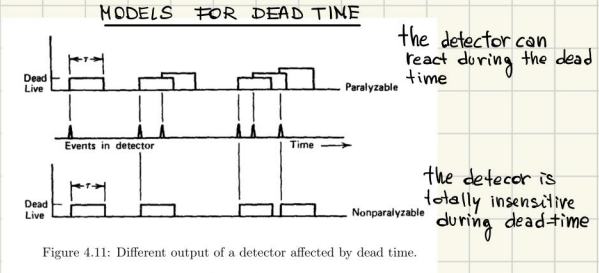

Figure 4.11: Different output of a detector affected by dead time.

we can find the true rate having measured the rate r_m for a detector with dead time τ_D as

$$r_{true} = \frac{r_m}{1 - r_m \tau_D}$$

TIMING PROPERTIES: - Capability of a detector to determine the time when some event has happened
- Fast time to transfer the electronic signal info. to a memory
- Livetime: the detector can be on only for some tim

LINEARITY

- We usually want to measure an observable by measuring phenomena well correlated with that observable e.g obs. = ΔE, correlated quantity = # charge carriers)
- It is important to verify that the correlation is linear! In fact non-linearity can introduce limitations in qeration and resolution:

- extreme effect of non linearity : saturation, i.e. independently on the value of the obs. the measurement is giving always the same outcome.

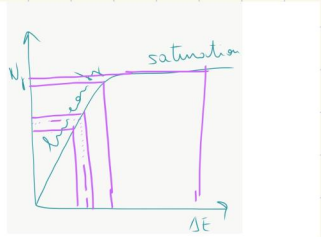

Figure 4.12: Representation of the observation of a value for ΔE using the counting of N_1 as a proxy for it. The linearity and saturation conditions are shown to see the effect on the extrapolated value of ΔE. In the case of linear condition the larger is the slope the better is the sensitivity to the ΔE value. In the case of saturation (slope equal to zero) very little or none sensitivity is present for ΔE even for a very precise counting of N_1.

EFFICIENCY :

- Ratio between the number of particles actually counted and the number which is expected.

$$\varepsilon = \frac{\#\,counts}{\#\,expected}$$

- Two types:
  - ACCEPTANCE : - geometrical coverage : is the detector in the right position?
    - can be calculated evaluating the solid angle percentage covered by the detector
  - INTRINSIC : - is the detector able to see a signal whenever for sure it should see something!
    - is there a particle - matter interaction mechanisme active in the detector?

- HOW DO YOU MEASURE EFFICIENCY :

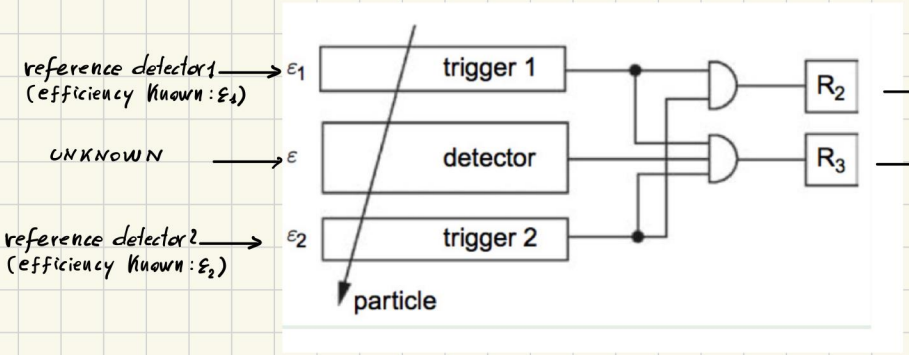

$$\varepsilon = \frac{R_3}{R_2} \qquad \left(= \frac{\varepsilon_1 \varepsilon_2 \varepsilon \cdot R}{\varepsilon_1 \varepsilon_2 \cdot R} = \varepsilon \right)$$

- Notice that a time coincidence among these 2 detectors must be defined: a good signal is accepted if and only if the 2 triggers happens within a finite chosen amount of time.

- N.B. in this way we are measuring the intrinsic acceptance under the assumption that the 3 detector have a geom. arrangement such that every event detected in the trig 1 and trig 2 must leave a signal in the detector. Otherwise acceptance corrections need to be applied.

- Which is the error on ε :

$$B(K; N, p) = \binom{N}{K} p^K (1-p)^{N-K} \qquad \begin{cases} Exp(K) = Np \\ Var(K) = Np(1-p) \end{cases}$$

$$If \quad \varepsilon = \frac{K}{N} \longrightarrow \begin{cases} Exp(\varepsilon) = \frac{Np}{N} = p \\ Var(\varepsilon) = \frac{Np(1-p)}{N} = p(1-p) \end{cases} \longrightarrow \frac{\delta\varepsilon}{\varepsilon} = \frac{\delta\varepsilon}{\frac{R_3}{R_2}} = \frac{\sqrt{\frac{R_3}{R_2}\left(1-\frac{R_3}{R_2}\right)}}{\frac{R_3}{R_2}}$$

ACCIDENTAL COINCIDENCE :

- We want to deduce the causal relationship from correlated events : e.g. I have 2 detectors, if they both give an electric signal I have a signal event

- Suppose there is some process (radioactivity, thermal exc, electric noise, ...) that is producing the same electric signal ⟶ noise event
Both det. are sensitive to that noise but there is no causal connection between the 2 electric noise signals.

- Accidental coincidence rate :

R_1 : rate of noise in detector 1 $\quad\quad$ Δt : coincidence gate
R_2 : rate of noise in detector 2

To detect a signal I need to have an el. signal in ① then wait within a time Δt another signal in ②. But this can be due to the accidental coincidences of the noises

$$\longrightarrow \boxed{R_{Acc} = 2R\,(1 - e^{-R\Delta t}) \;;\quad R_1 = R_2}$$

- Practical solution :- majority logic, we acquire the event only when a majority of channels have fired (to suppress accidentals)

  - Among n detectors (with same ε) the prob. to have k detectors with signal is given by

$$\sum_{i=1}^{n-k} P(k; n, \varepsilon)$$

IONIZATION CHAMBERS

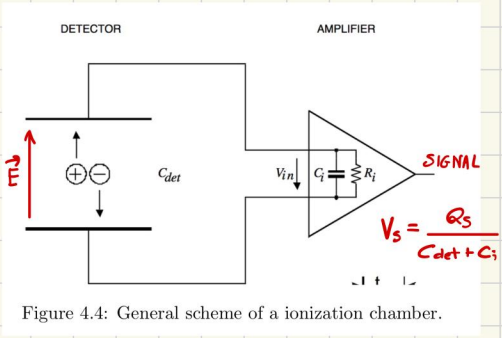

Figure 4.4: General scheme of a ionization chamber.

- Realization of detector concep #1
- A particle loses its energy inside the sensitive material of the detector
- The energy loss transforms into charge carriers which can be collected using an $\vec{E}$
- The collected charges can be read using an amplifier and forms the electric signal

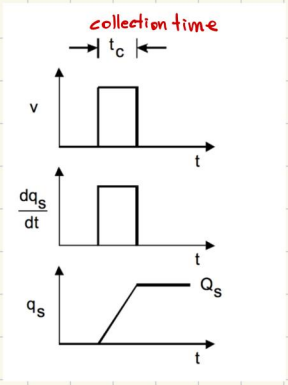

- The general scheme of charge collection process is:
- How many charge carriers: $$\text{Signal} = N_c = \frac{\text{Energy lost}}{\text{Cost of one carrier}}$$
- The cost of one carrier depends on the energy loss mechanism:
  - IONIZATION: carrier: e^-/ion pair cost: {~ eV (semiconductors); ~ 30eV (gases)}
  - SCINTILLATION: carrier: photons cost: ~ 10-100 eV (optical - UV band)
  - LATTICE VIBRATION: carrier: phonons cost: ~ meV
- Statistical model: Poissonian describes the process $\mu = N_c$ $\sigma = \sqrt{N_c}$
  - The relative fluctuation of # carriers and therefore energy loss fluctuation is $\frac{\sigma}{\mu} = \frac{1}{\sqrt{N_c}}$

FANO FACTOR

- Not all the energy loss goes into visible carriers

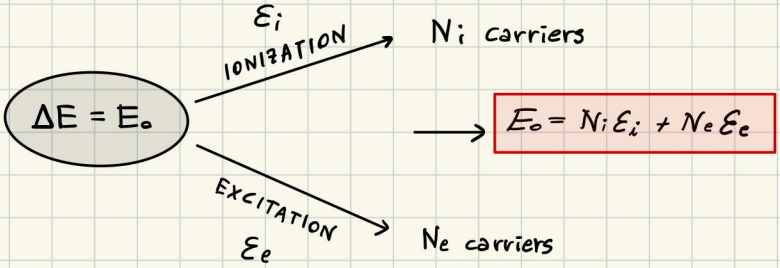

$$\longrightarrow E_0 = N_i \varepsilon_i + N_e \varepsilon_e$$

N_i and N_e are 2 poissonian variable so there are a lot of way to have E_0 fixed. (N_i can be smaller than N_e) If E_0 is fixed for any N_i fluctuation we can always find a N_e such that exactly E_0 is absorbed:

$$\longrightarrow \sigma_i \varepsilon_i = \sigma_e \varepsilon_e \qquad \text{where} \quad \begin{cases} \sigma_i = \sqrt{N_i} \\ \sigma_e = \sqrt{N_e} \end{cases}$$

Combining these expressions together:

$$\longrightarrow \sigma_i = \frac{\varepsilon_e}{\varepsilon_i}\left[\frac{E}{\varepsilon_e} - \frac{\varepsilon_i}{\varepsilon_e} N_i\right]^{1/2}$$

Defining the energy to produce one single pair (ionization) as $\varepsilon_0 = \frac{E}{N_i}$ we have:

$$\sigma_i = \left[\frac{\varepsilon_e}{\varepsilon_i}\left(\frac{\varepsilon_0}{\varepsilon_i} - 1\right)\frac{E}{\varepsilon_0}\right]^{1/2} \equiv \sqrt{F \cdot N_i} \quad \rightarrow \quad F = \frac{\varepsilon_e}{\varepsilon_i}\left(\frac{\varepsilon_0}{\varepsilon_i} - 1\right)$$ Fano factor

Even though we assumed that the individual processes of exc. and ion. to be Poissonian the process of creating pairs is actually a Poissonian only once a multiplicative factor F is introduced. This is because the physical processes are not entirely uncorrelated as it should be for 2 independent Poiss. process. The Fano factor was introduced to explain the difference betweeen the expected and exp variance of the counting.

COUNTING DETECTOR

- Examples of counting
  - ACCELERATORS COLLISIONS: $N = \varepsilon T \sigma L$ $\longrightarrow$ measurement of σ in collision process
  - DECAYING OBJECTS: $N = \varepsilon \Gamma T \left(V \frac{N_A \rho}{A}\right)$ $\longrightarrow$ measurement of lifetime $1/\Gamma$
  - FIXED TARGET COLLISIONS $N = \varepsilon \sigma \left(\frac{N_A \rho}{A}\right) \ell$ $\longrightarrow$ measurement o of σ at fixed target
- Comments
  - Total error on σ/Γ depends on N, on the lifetime, efficiency, ...
  - We are not assuming the B.G. presence. (that need to be subtracted)

GAS DETECTORS

- Important because charged particles, especially MIP, leave a small amount of energy in the gas. Hence gas is the best candidate to be the least perturbing device for charged particles detection.
- Based on the concept of drift velocity
- Very thin in order to not modify the momentum of the p.
- Usually they are inserted in a magnetic field as part of a magnetic spectrometer to measure p.
- By localizing the ionization clusters along the trajectory we can reconstruct the track → able to measure positions in space

GAS IONIZATION

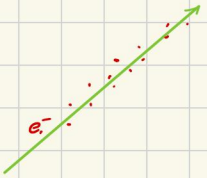

- The passage of a charged particle produces a trail of electrons (by ionization)
- Absorbtion length (mean free path) among 2 ionizations λ : $\boxed{\frac{1}{\lambda} = \rho\sigma}$ ($\lambda \sim o(mm)$)
- The # e^- produced in a distance L has a Poisson distribution with $\boxed{\mu = \frac{L}{\lambda}}$
- 2 principal GAS standards :
  - STP (Standard Temperature and Pressure) $T = 273.15\,K = 0°C$, $P = 10^5\,Pa = 1\,bar$
  - NTP (Normal Temperature and Pressure) $T = 293.15\,K = 20°C$, $P = 101.325\,KPa = 1\,atm$, $K_BT = 25meV$
- PHASES :
  - Primary ionization : the charge particle extracts an e^- from a gas molecule. E.g.: $\pi A \longrightarrow \pi A^+ e^-$
  - Secondary ionization : the extracted e^- has sufficient energy to ionize other gas molecules: E.g.: $e^- A \longrightarrow e^- A^+ e^-$
  - Penning effect : the gas molecule is excited to a metastable state. The de-excitation happens through a collision with a nearby molecule which results in the retarded emission of a e^-. Prevalent in mixtures with noble gases. E.g. $\pi\,(\text{or } e^-)\,A \longrightarrow \pi\,(\text{or } e^-)\,A^*$
    or $A^*B \longrightarrow AB^+e^-$
    or $A^*A \longrightarrow A_2^* \longrightarrow A_2^+ e^-$

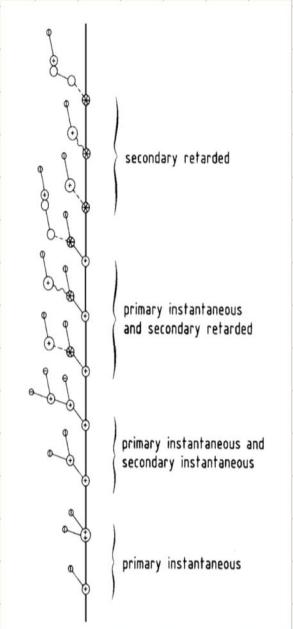

- The cost W to produce an electron is connected to the E loss as:

$$W\langle N_I\rangle = L\left\langle \frac{dE}{dx}\right\rangle \longrightarrow \boxed{W = \frac{L}{\langle N_I\rangle}\left\langle \frac{dE}{dx}\right\rangle}$$

(path length; # e^- created along the ion. path)

- Usually W > ionization potentials

Gas	W_α(eV)	W_β(eV)	I(eV)	Gas mixture[a]	W_α(eV)
H_2	36.4	36.3	15.43	Ar (96.5%) + C_2H_6 (3.5%)	24.4
He	46.0	42.3	24.58	Ar (99.6%) + C_2H_2 (0.4%)	20.4
Ne	36.6	36.4	21.56	Ar (97%) + CH_4 (3%)	26.0
Ar	26.4	26.3	15.76	Ar (98%) + C_3H_8 (2%)	23.5
Kr	24.0	24.05	14.00	Ar (99.9%) + C_6H_6 (0.1%)	22.4
Xe	21.7	21.9	12.13	Ar (98.8%) + C_3H_6 (1.2%)	23.8
CO_2	34.3	32.8	13.81	Kr (99.5%) + C_4H_8-2 (0.5%)	22.5
CH_4	29.1	27.1	12.99	Kr (93.2%) + C_2H_2 (6.8%)	23.2
C_2H_6	26.6	24.4	11.65	Kr (99%) + C_3H_6 (1%)	22.8
C_2H_2	27.5	25.8	11.40		
Air	35.0	33.8	12.15		
H_2O	30.5	29.9	12.60		

adding a second gas in the mixture helps to reduce the cost (and increase the stability)

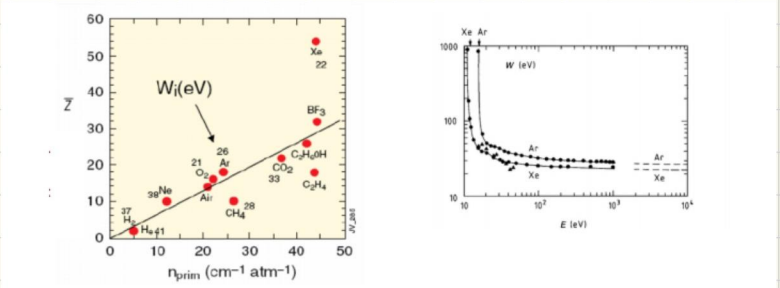

Figure 5.2: Left: number of ionization per cm. The cost is shown along with the molecule/atom name. This value scales with the pressure of the gas. Right: cost of an electron as a function of the energy. Notice that it does not depend on the energy of the particles.

- Probability of e⁻ emission by ionization of a gas as a function of its energy.

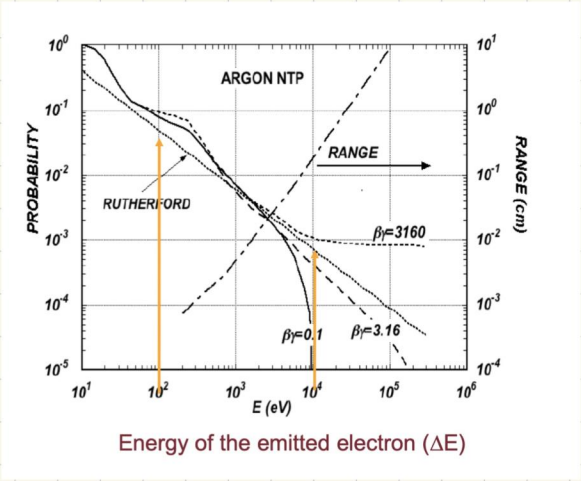

- Range of primary electrons produced from ionization:

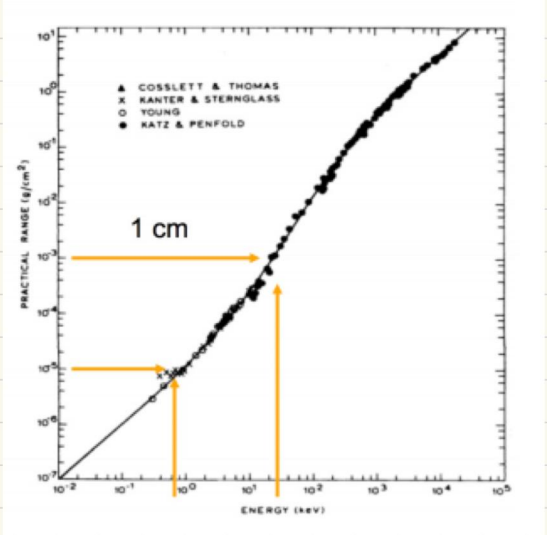

- Path of the electrons produced by the ionization in a wire chamber:

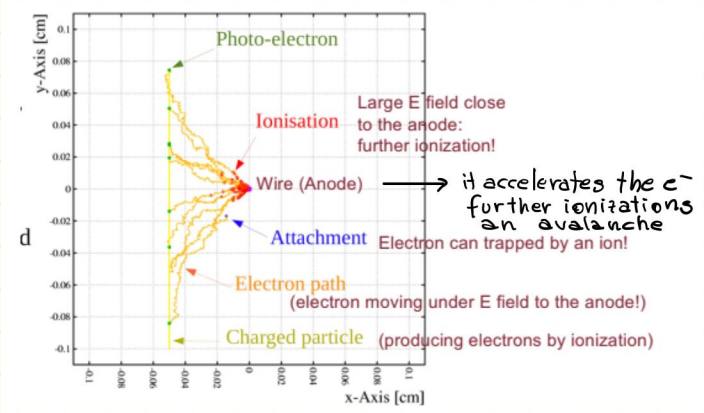

- Cluster size distribution (percentage)

Primary and secondary Electrons are close together!

They appear experimentally as a cluster of **few** (k) electrons

k	CH_4	Ar	He	CO_2
1	78.6	65.6	76.60	72.50
2	12.0	15.0	12.50	14.00
3	3.4	6.4	4.60	4.20
4	1.6	3.5	2.0	2.20
5	0.95	2.25	1.2	1.40
6	0.60	1.55	0.75	1.00
7	0.44	1.05	0.50	0.75
8	0.34	0.81	0.36	0.55
9	0.27	0.61	0.25	0.46
10	0.21	0.49	0.19	0.38
11	0.17	0.39	0.14	0.34
12	0.13	0.30	0.10	0.28
13	0.10	0.25	0.08	0.24
14	0.08	0.20	0.06	0.20
15	0.06	0.16	0.048	0.16
16	(0.050)	0.12	(0.043)	0.12
17	(0.042)	0.095	(0.038)	0.09
18	(0.037)	0.075	(0.034)	(0.064)
19	(0.033)	(0.063)	(0.030)	(0.048)
≥20	$(11.9/k^2)$	$(21.6/k^2)$	$(10.9/k^2)$	$(14.9/k^2)$

Little dependence on gas type

DRIFT VELOCITY MODEL

- The ionization clusters can be collected by an $\vec{E}$, inducing an electric signal on the electrodes. The e^- are moving towards the anode and at the same time they're bouncing against the molecules

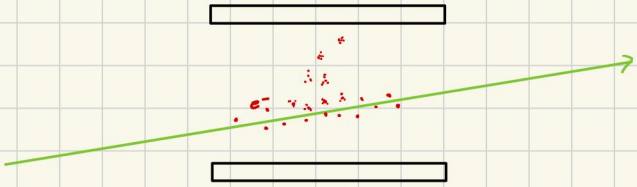

On average: $$m\frac{d\vec{v}_d}{dt} = e\vec{E} + q\vec{v}_d \times \vec{B} - K\vec{v}_d \qquad K \equiv \frac{m}{\tau}$$ τ is a typical friction time scale

- We can define the mobility μ such that $\boxed{\vec{v}_d = \mu \vec{E}}$

- If $B=0$ motion can reach constant drift velocity

$$m\frac{d\vec{v}_d}{dt} = e\vec{E} - K\vec{v}_d \longrightarrow \frac{d\vec{v}_d}{dt} = 0 \longleftrightarrow \boxed{\vec{v}_d = \frac{e}{K}\vec{E}} \longrightarrow \boxed{\mu = \frac{e}{K} = \frac{e}{m}\tau}$$

μ: MACRO; τ: MICRO

- What is τ?

  - It is the typical time scale of the friction.
  - It can be represented by the average time between 2 collisions of the particle with mass m under the action of the external force

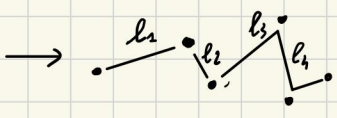

$$\rightarrow \bar{l} = \sum \frac{l_i}{N} \longrightarrow \tau = \frac{\bar{l}}{v}$$

- How to estimate $\bar{\ell}$: $n = \rho \frac{N_A}{PM} \longrightarrow \boxed{\bar{\ell} \sim \frac{1}{\sqrt[3]{n}}}$ (roughly estimation, see below for the more correct one)

- What about the behaviour of the electrons?
  - If we compute the $\lambda_{compt} = \frac{\hbar}{m} \sim 10^{-12} m$ (that is the scale where the quantum effect is important). However the intermolecular distance $\bar{\ell} \gg \lambda_{compt} \longrightarrow$ SAFE ZONE

- It should be connected with the cross section of the process. We know that the mean free path is $\frac{1}{n\sigma}$ and a good guess for ℓ is it: $\ell = \frac{1}{n\sigma}$. Therefore: assuming $v = v_c$:

$$\longrightarrow \boxed{\frac{1}{\tau} \simeq n\sigma \cdot v_c}$$

DRIFT OF ELECTRONS

- Each time the particle collides with the molecules it releases some energy. We could compute the work done by the external $\vec{E}$ field as

$$eEx$$

and it should be equal to (# collisions × energy lost in 1 collision) (for the energy conservation)

$$\bigstar \quad eEx = N \lambda \varepsilon$$

- the number of collisions in a distance L can be evaluated as $N_c = \frac{L}{v_d \cdot \tau}$
- ε: energy of the e^- in this motion $\longrightarrow \mathcal{E} = \mathcal{E}_{ER} + \cancel{\frac{3}{2} kT} \approx \frac{1}{2} m v^2$ (we can neglet thermal energy at NPT ~25meV)
- λ: fraction of energy lost in a single collision

Putting all together:

$$v_d^2 = \frac{\ell}{m} \left(\frac{E}{n}\right) \frac{1}{\sigma(\varepsilon)} \sqrt{\frac{\lambda(\varepsilon)}{2}}$$

← depends on the gas

↑ larger E, lesser n → larger v_d

- v_d is a function of the reduced field E/n. For a gas in a vdume at some fixed pressure n is equivalent to the pressure and therefore $\frac{E}{n} = \frac{[kV]}{[cm][Torr]}$. The condition where $v_d \sim const$ at $\frac{E}{n}$ means the detector is more stable → important.

- λ an σ are function of $\mathcal{E}$. They do nd drastically change with $\mathcal{E}$

- Ramsauer effect: for electron with $\mathcal{E} \sim 1eV$ the σ decreases $\longrightarrow$ v_d reachs a maximum

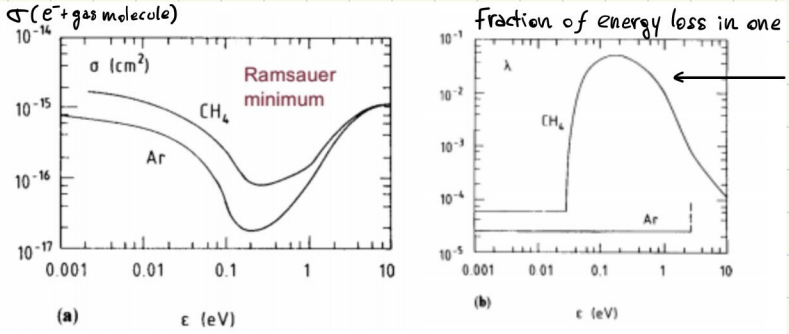

← big (organic) molecule absorbs energy in the collision under roto-vibrational excitation states.

Figure 5.7: Ramsauer effect in CH_4 and Ar.

- λ is largely affected by the gas nature. If $\mathcal{E}$ is below any molecular level λ has an average value given by elastic scattering. If $\mathcal{E}$ is larger than a molecular energy level, larger λ are possible → change on v_d. This can be used to tune the v_d to a desired value adding components in the gas mixtures (especially organic ones since they have several roto vib. states accesible even withe energies < 1eV)

▶ Typical numbers for e^- : $v_d \sim 2\text{-}10 \frac{cm}{\mu s}$ in a typical $\vec{E}$ field of $E \sim 1\text{-}10 \frac{kV}{cm}$

DRIFT OF IONS

- Much heavier than electrons
  - ▶ In each collision they loss a substantial amount of energy $\lambda \sim 1$ (the eq condition ★ cannot be reached)
  - ▶ We can derive λ from elastic scattering kinematics : $\lambda = \frac{P^2}{M}\frac{2m}{P^2} = \frac{2mM}{(M+m)^2}$
  - ▶ It cannot be easily accelerated $\longrightarrow$ $\mathcal{E}_{ion} \sim \mathcal{E}_{thermal} = \frac{3}{2}K_B T$

▶ Typical values $v_d \sim 0.01 \frac{cm}{\mu s}$

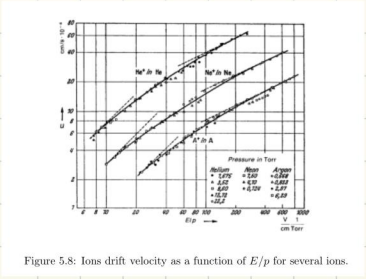

Figure 5.8: Ions drift velocity as a function of E/p for several ions.

DIFFUSION

- The motion description of e^-/ions in the gas is statistical : v_d is the average value of an ensamble of drifting e^-/ions. Each e^- will cover in principle the same distance L in a different time ΔT
- The e^-/ions are indeed subject to a diffusive process

- The diffusive process can be described, in 1D, by a Gaussian p.d.f. $G(r_i; 0, \sigma_x(t))$ (prob to find an e^- at some $r = X + (Z - v_d t)$ after a time t) (ISOTROPIC DIFFUSION)

$$\boxed{\sigma_x^2 = 2Dt} \longrightarrow p.d.f \sim \left(\frac{1}{\sqrt{2\pi \cdot 2Dt}}\right)^3 \exp\left(\frac{-r^2}{4Dt}\right) \qquad r^2 = X^2 + (Z - v_d t)^2$$

D: diffusion coefficient

▶ D can be determined by calculating the variance of the sum of the X_i displacements :

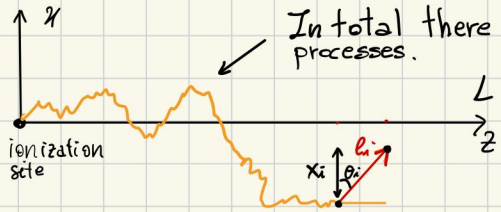

$$X = \sum_i^{N_c} x_i = \sum_i l_i \cos\theta_i$$

$$\begin{cases} pdf(l_i) \sim e^{-\frac{l_i}{l_c}} \\ pdf(\cos\theta_i) \sim \frac{1}{2} \quad \text{if } -1 < \theta_i < 1 \end{cases}$$

$$\longrightarrow Var(X) = \langle X^2 \rangle - \cancel{\langle X \rangle^2} = \langle X^2 \rangle = \int \left(\sum_i^{N_c} X_i\right)^2 \cdot \prod_i^{N_c} f(X_i)\, dX_i$$

$\langle X \rangle = X - v_0 \Delta T = 0$

To compute it we assume that : $\boxed{f(X_i) = \frac{1}{l_i} e^{-\frac{l_i}{l_c}}}$ where $l_c = \frac{1}{n\sigma} = v_c \tau$ (mean free path)

$$\rightarrow \quad \sigma_x^2 = N_c \frac{2}{3} l_c^2 = \frac{\Delta t}{\tau} \frac{2}{3} (v_c \cdot \tau)^2 = \frac{\Delta t}{\tau} \frac{2}{3} \tau^2 \frac{2\mathcal{E}}{m} = 2\left(\frac{2}{3}\frac{\mathcal{E}}{m}\tau\right)\Delta t \quad \left(\mathcal{E} = \tfrac{1}{2} m v_c^2\right) \rightarrow \boxed{D = \frac{2}{3}\frac{\mathcal{E}}{m}\tau} \quad \boxed{D = \frac{1}{3} v_c \lambda}$$

By using $\mu = \frac{e}{m}\tau$ and $v_d = \mu E$ and $\Delta t = \frac{L}{v_d}$ we obtain:

$$\boxed{\sigma_x = \sqrt{\frac{4}{3}\frac{\mathcal{E}}{e}\frac{L}{E}}}$$

- electrons: $\mathcal{E} = \mathcal{E}_q \rightarrow \sigma_x^{electron} = \sqrt{\frac{4}{3}\frac{\mathcal{E}_q}{e}\frac{L}{E}}$
- ions: $\mathcal{E} = \frac{3}{2} K_B T \rightarrow \sigma_x^{ion} = \sqrt{\frac{2 K_B T L}{e E}}$

Larger is L, lesser is E, hotter are the electrons (ions) $\rightarrow$ larger is the diffusion

▶ Diffusion is active in 3D

- **Longitudinal diffusion**: - along the drift direction
  - consequences on drift length L and drift time Δt
- **Transverse diffusion**: - along the direction transverse to drift direction
  - consequences on spatial resolution in case of segmented readout electrodes

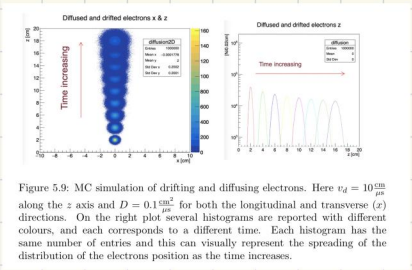

Figure 5.9: MC simulation of drifting and diffusing electrons. Here $v_d = 10 \frac{cm}{\mu s}$ along the z axis and $D = 0.1 \frac{cm^2}{\mu s}$ for both the longitudinal and transverse (x) directions. On the right plot several histograms are reported with different colours, and each corresponds to a different time. Each histogram has the same number of entries and this can visually represent the spreading of the distribution of the electrons position as the time increases.

DETECTORS BASED ON THE DRIFT TIME MEASUREMENTS

- **Idea**: Knowing the drift velocity v_d (with high accuracy) we can infer the distance d of the track from the anode position

$$\rightarrow \quad \boxed{d = v_d \cdot (t_a - t_0)}$$

- t_a: start time of the signal induced to the anode by the e^- moving
- t_0: time when the e^- are produced (measured by an auxiliary detector, fast scintillation detector, $\sigma_{t_0} \sim 1ns$)

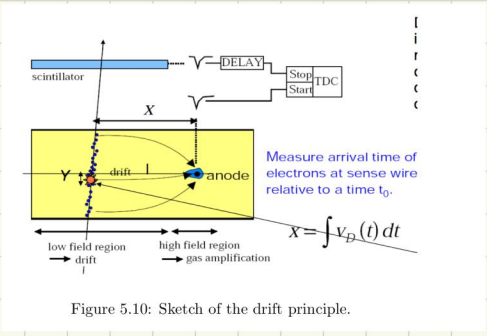

Figure 5.10: Sketch of the drift principle.

- **Resolution**: since $v_d \sim 10 \frac{cm}{\mu s}$ and $\sigma_{t_a} \sim 1ns \rightarrow \sigma_d \sim 0{,}14$ mm

- **CYLINDRICAL GAS DETECTOR**
  - Radial $\vec{E}$ field used to collect on the central anode wire the ionization e^- formed along the trajectory
  - External tube kept at ground voltage while the central wire at positive voltage (respect to ground) $V_0 \sim$ KV
  - The $\vec{E}$ field is not really uniform: it diverges close to the anode surface.
  - Problem: AVALANCHES

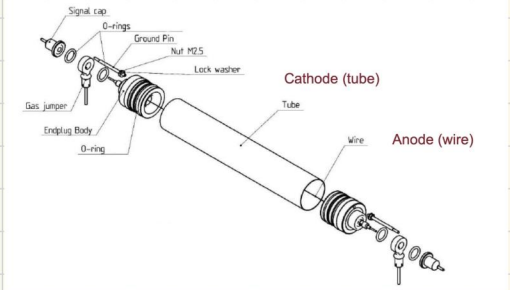

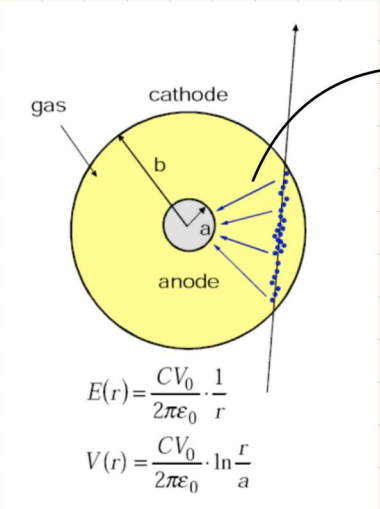

→ The high electric field around the wire is able to accelerate the e^- well beyond the equilibrium energy reached during the drift. → <u>production of avalanches</u> (in the form of e^- and ions) due to electrons which are ionizing!

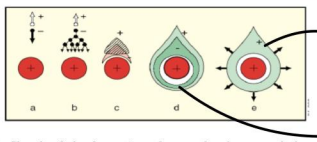

→ they start to moving slowly back to the cathode $v_d^{ion} \sim 0.01 \frac{cm}{\mu s}$

→ e^- distribution is sucked into the wire

Figure 5.13: Sketch of the formation of an avalanche around the anode wire (red circle). (a) Production of ion-electron pair by a ionizing particle; (b) the electron gets close to the anode, acquires a large kinetic energy much larger than the equilibrium energy of the drift and starts to ionize the gas by itself; (c) two charge distribution develop in the space close to the anode, one negative due to the electrons produced in the cascade (pink) and one positive (grey) due to ions; (d) the charge distributions continue to grow and extend around the wire; the electron are quickly absorbed by the anode wire (that is a very good conductor) and disappear, while the ions are slowly moving to the cathode, not shown in this figure.

▶ SIDE EFFECTS OF AVALANCHE

- <u>Photon emission</u> : • excited molecules and atoms isotropically emit photons that can induce other avalanches ⟶ discharges, detector breakdown
  • solution: addition of quenchers (hydrocarbon) to the gas mixture which can absorb the photons emitted.

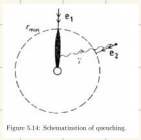

Figure 5.14: Schematization of quenching.

- <u>Space charge</u> : • a lot of e^- and ions close to the anode can change the local $\vec{E}$ field.

• <u>Resolution σ_d as function of the distance d</u>

- <u>Longitudinal diffusion effect</u> $\sigma_d(d) \propto \sqrt{d}$ (along $\vec{E}$ direction)

- <u>Geometrical effect</u>: If the charged particle is crossing the drift tube far from the anode wire, the average trajectory of the ionization clusters is almost ⊥ to the charged particle track. (⟶ domination of diffusion effect)

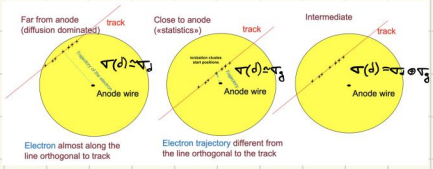

If the charged particle is crossing the drift tube close to the anode wire, the average trajectory of the ionization clusters is far from being ⊥. (⟶ domination of geom. effect).

- These 2 points lead to <u>different effects on the resolution σ_d</u> :

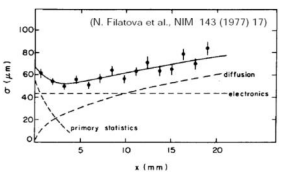

Figure 5.16: Resolution on the distance from the anode (σ_d in the text) as a function of the distance from the anode (d in the text).

• <u>Gain</u> : • most important quantity in a gas detector
• amplitude of the signal for a single e^- drifted to the anode
• increasing V_0 does not mean always to increase the gain : the best is when this happens (where an increase of V_0 results in an increase in the gain):

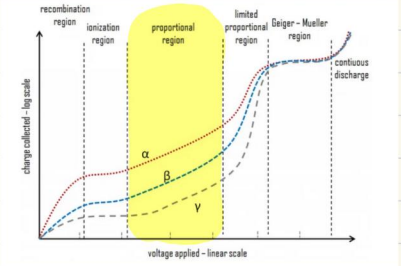

- **LIMITATIONS OF A GAS DETECTOR**

  - Rate capability : it is limited to the e^- drift velocity $\sim 10\ ^{cm}/_{\mu s}$
  - Proportionality : the applied voltage needs to be in the proportional region
  - Spatial resolution : it is limited by the lateral diffusion
  - Timing resolution : it is limited by the longitudinal diffusion that can be partially mitigated by the presence of a magnetic field

- To overcome these problems we can modify the detector geometry (micro-pattern gas det.)

DRIFT CHAMBER

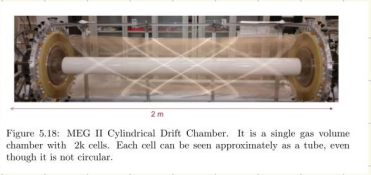

Figure 5.18: MEG II Cylindrical Drift Chamber. It is a single gas volume chamber with 2k cells. Each cell can be seen approximately as a tube, even though it is not circular.

- Multi cell detector
  - Each cell has an anode wire kept at high voltage and surrounded by cathode wires kept at ground voltage
  - High segmentation : The more cells → the better is the performance (more points to reconstruct the track.

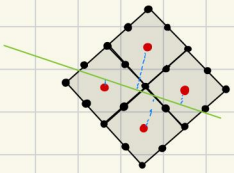

- Segmented anodes detector

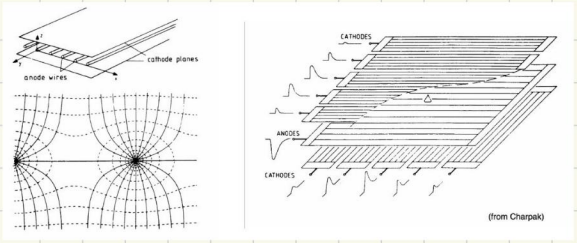

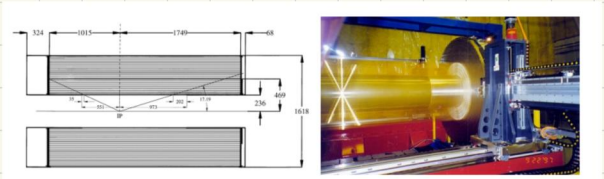

Figure 5.19: BaBar Cylindrical Drift Chamber. It has several segmented anode and cathode planes.

- What happens if I put a magnetic field ? The field lines are distorted

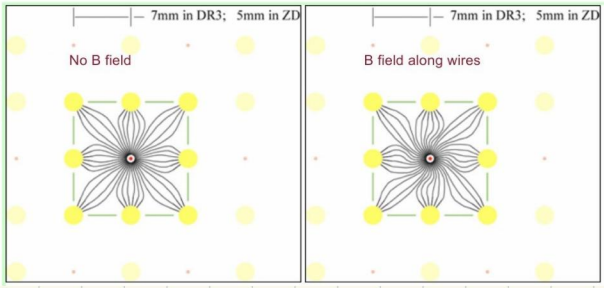

TIME PROJECTION CHAMBER (TPC)

- Large volume of gas contained in a vessel with two faces kept at a potential difference such to have a uniform $\vec{E}$ field.

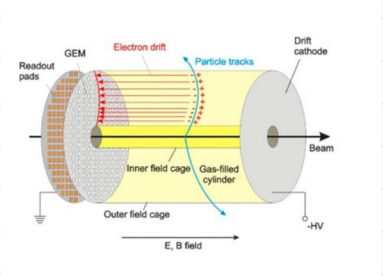

- Ionizing particles to be detected comes from an internal interaction point and leave a trail of ionization clusters which drift to the anode

- 3D reconstruction of particle trajectory

  - longitudinal drift distance z (by measuring Δt) $z_i = v_d (t_{a_i} - t_0)$
    RESOLUTION : given by diffusion in the gas $\sigma_z = v_d \sqrt{\sigma_{t_{a_i}}^2 + \sigma_{t_0}^2}$
  - x,y measured by the segmentation of the anode through an amplification stage
    RESOLUTION : given by the size of readout pad. $\sigma_x = \sigma_y = \frac{\ell}{\sqrt{12}}$

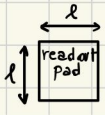

Different pad read out system geom.

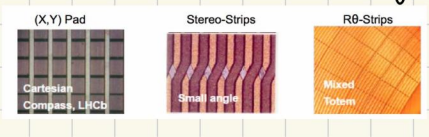

- **G.E.M. (Gas Electron Multiplier)** : amplification stage in the TPC

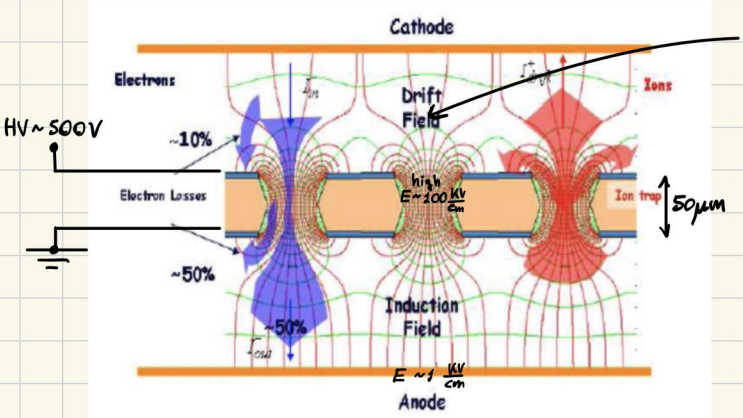

Figure 5.22: Sketch of the operation of a Gas Electron Multiplier element, frequently used as amplification stage in a TPC.

- The high electric field induces an avalanche full of new others e^- and ions. Ions are trapped by the GEM itself avoiding them to drift to the cathode

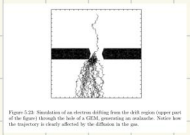

- The avalanche is local i.e. it involves only one hole (the rest of the GEM is not affected by it → the RATE CAPABILITY is high because the dead region contributing to dead time is very limited

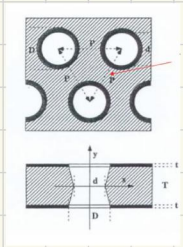

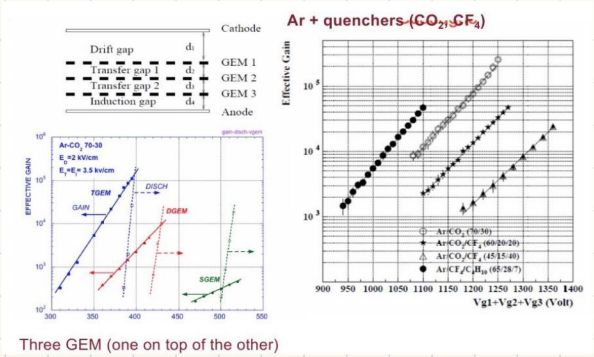

Three GEM (one on top of the other)

- The gain is proportional to the applied voltage (prop. region).

- **Alternative to GEM** : the amplification is made throug a mesh of wires (instead of having planar foils)

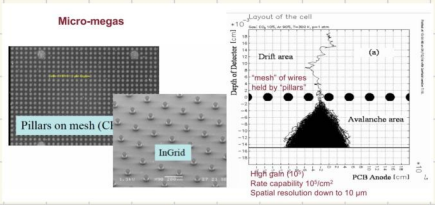

- **Limitation and operational problems**

  - Back plane insulator cannot discharge quickly : charge build up field distortion
  - Discharge between strip : mainly due to spike-edges on the strip
  - Use of gas mixture with hydrocarbons : Organic compounds tend to form on the electrodes. Local deposition of (+) charge : continuous extraction of e^- due to the high $\vec{E}$ in the insulating layer generated by this (+) charge and then spontaneous avalanches (Malter effect).

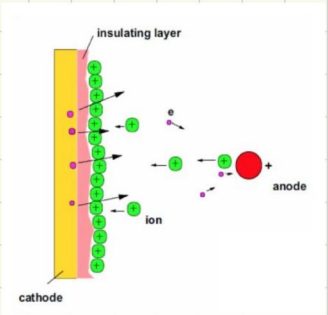

- **MICRO-STRIP GAS CHAMBER**

  - Strip-like geometry. very narrow conductive ribbon as insulator
  - Thin anode to collect electrons ; nearby cathode strips to collect ions.
  - Compact readout : spatial resolution of 50 μm
  - Efficiency reaches a plateau increasing V_0 while the gain increases exponentially (n.b. it's impossible to increase the gain ∞ because the discharge prob. increases as well)

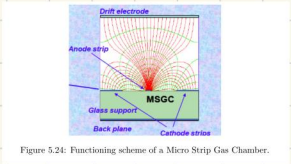

Figure 5.24: Functioning scheme of a Micro Strip Gas Chamber.

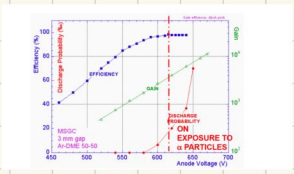

MOMENTUM MEASUREMENT

- The trick is to use a magnetic field $\vec{B}$ to bend the trajectory of a charged particle. In fact:

$$\begin{cases} \vec{F} = q\,\vec{v}\times\vec{B} = q\,\dfrac{\vec{p}\times\vec{B}}{m} = \dfrac{q\,p\cdot B}{m}\,\hat{r}_\perp \\ \vec{F} = m\dfrac{v^2}{R}\,\hat{r}_\perp \end{cases} \longrightarrow \boxed{p_\perp\,[\text{GeV}] = 0.3\cdot z\cdot R\,[\text{m}]\cdot B\,[\text{T}]}$$

- The track can be reconstructed by a gas detector from which we measure the radius of curvature R

- Rigidity: defined as $\dfrac{p_\perp}{ze}$ is the quantity measured in general. Only with the knowledge of ze we can infer $p_\perp$

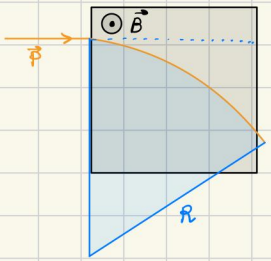

- Approximation: in general B and L (detector length) are such that θ is very small and the trajectory length $\ell = R\theta \sim L$. A pitch angle θ is usually approximated as $\theta \sim \arctan\left(\frac{p_\perp}{p_\parallel}\right)$

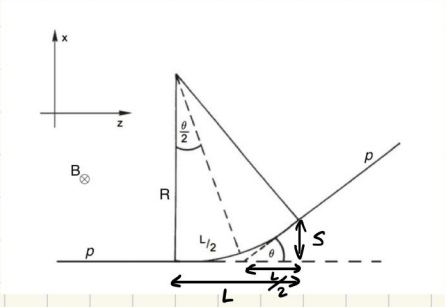

$$\begin{cases} \dfrac{s}{L/2} \simeq \tan\theta \simeq \theta \rightarrow s = \dfrac{L}{2}\theta \\ \dfrac{\frac{L}{2}}{R} \simeq \tan\dfrac{\theta}{2} \simeq \dfrac{\theta}{2} \rightarrow \theta \simeq \dfrac{L}{R} \end{cases} \longrightarrow s \simeq \frac{L^2}{2R} \rightarrow R \simeq \frac{L^2}{2s}$$

$$\longrightarrow \boxed{p_\perp \simeq 0.3\cdot z\cdot \frac{L^2}{2s}\cdot B}$$

- Example of a magnetic spectrometer

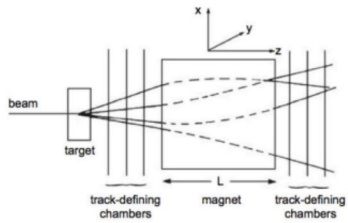

Figure 5.27: Scheme of a magnetic spectrometer in a fixed target geometry. The magnetic field is perpendicular to the page, parallel to y. The *track-defining chambers* can measure the position of the passage of the particle, thus the deflection of the track due to the magnetic field.

- Different magnetic field configurations

  - DIPOLE MAGNETIC FIELDS: preferred for fixed target experiments (what we've used above)

    - R is inferred measuring the deflection angle $\Delta\theta$ by measuring the direction of the particle before θ_{IN} and after the magnetic field θ_{OUT}

$$\boxed{\Delta\theta = \theta_{out} - \theta_{in} \simeq \frac{x_4 - x_3}{d} - \frac{x_2 - x_1}{d}}$$

$$\Delta\theta = \frac{\ell}{R} \simeq \frac{L}{R} \longrightarrow R \simeq \frac{L}{\Delta\theta}$$

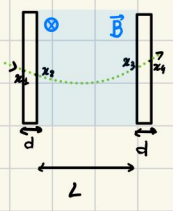

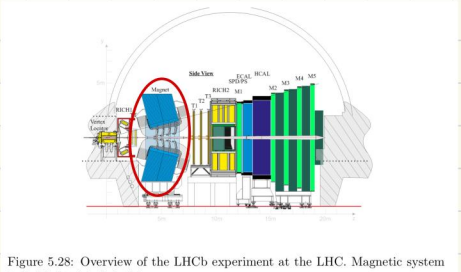

Figure 5.28: Overview of the LHCb experiment at the LHC. Magnetic system is highlighted in light blue.

▶ Resolution (V. Vanilla)

- $\sigma(\Delta\theta) \simeq \frac{2\sigma_x}{d}$ $\quad p_\perp = \frac{0.3\,BL}{\Delta\theta} \longrightarrow \frac{\sigma_{p_\perp}}{p_\perp} = \frac{\sigma_{\Delta\theta}}{\Delta\theta} \longrightarrow$ $\boxed{\frac{\sigma_{p_\perp}}{p_\perp} = \frac{2\sigma_x}{0.3\,BLd}\,p_\perp}$

▶ Resolution (multiple scattering)

- $\Delta p_\perp^{MS} = p \sin\theta_{rms} \simeq p\,\theta_{rms} = 19.2\sqrt{\frac{L}{X_0}}$ MeV/c $\longrightarrow$ $\boxed{\left.\frac{\sigma(p_\perp)}{p_\perp}\right|^{MS} = \frac{4.5\cdot10^{-3}}{\beta\cdot B[T]\cdot\sqrt{L[m]\cdot X_0[m]}}}$

- SOLENOIDAL MAGNET

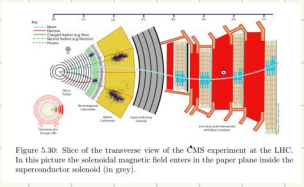

Figure 5.30: Slice of the transverse view of the CMS experiment at the LHC. In this picture the solenoidal magnetic field enters in the paper plane inside the superconductor solenoid (in grey).

▶ R is inferred using many more points than with the dipole magnet $\longrightarrow$ better $\frac{\sigma_{p_\perp}}{p_\perp}$.
The detector is placed inside the magnetic volume allowing a precise tracking and a precise measurement of the sagitta s.
For a smal Fraction of the track (3 consecutive measured points) tha sagitta is:

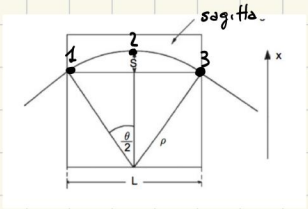

$$\boxed{s = x_2 - \frac{x_1 + x_3}{2}}$$

$s = R\left(1-\cos\frac{\Delta\theta}{2}\right) \sim R\,\frac{(\Delta\theta)^2}{8} = \frac{\ell^2}{8R} \longrightarrow R \simeq \frac{\ell^2}{8s}$ with ℓ the small length of a piece of trajectory between 3 points

▶ Resolution:

$$\boxed{\sigma_s = \sqrt{\frac{3}{2}}\,\sigma_x} \;;\; p_\perp = \frac{0.3B\ell^2}{8s} \longrightarrow \frac{\sigma_{p_\perp}}{p_\perp} = 8\sqrt{\frac{3}{2}}\,\frac{p_\perp}{0.3B\ell^2}\,\sigma_x \xrightarrow{\text{for N points (entire track)}} \boxed{\frac{\sigma_{p_\perp}}{p_\perp} = \sqrt{\frac{720}{N+4}}\,\frac{p_\perp}{0.3BL^2}\,\sigma_x}$$

▶ Can be preferred because can be arranged around a collision point of a circular accelerator.

- TOROIDAL MAGNET

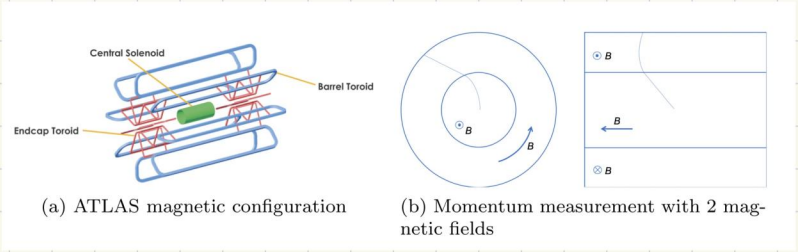

(a) ATLAS magnetic configuration

(b) Momentum measurement with 2 magnetic fields

- HOW TO CHOOSE THE LAYOUT:

- We must use a small space (short L) with a large B $\longrightarrow$ solenoidal
- We must use a long track length with a smaller B $\longrightarrow$ toroidal

- OVERALL MOMENTUM RESOLUTION

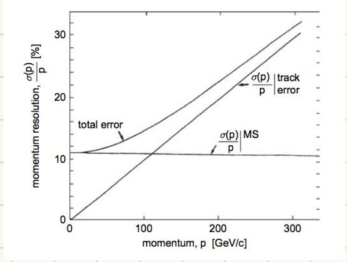

PARTICLE IDENTIFICATION : i.e determine the mass of a particle

- Most relevant techniques:
  - dE/dx measurements
  - Time of Flight measurements
  - Cherenkov effect - based detectors
  - Absorbtion of hadrons

ENERGY LOSS MEASUREMENTS

- The Bethe-Bloch curve as a function of p is no more universal : it depends on the type of particle. Measuring a point $(p, \frac{dE}{dx})$ we can perform a PID.
- N.B. Since the curve is not linear they can be present degenerate points → PID difficult Moreover the intrinsic fluctuation of $\frac{dE}{dx}$ have to be taken into account.

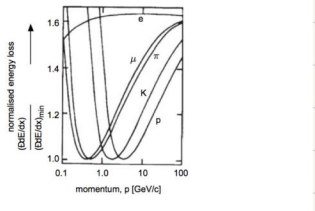

Figure 6.1: $\frac{dE}{dx}$ normalized to the its minimum value as a function of momentum of the particles. Different curves for the different masses are displayed.

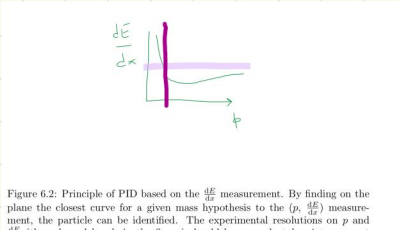

Figure 6.2: Principle of PID based on the $\frac{dE}{dx}$ measurement. By finding on the plane the closest curve for a given mass hypothesis to the $(p, \frac{dE}{dx})$ measurement, the particle can be identified. The experimental resolutions on p and $\frac{dE}{dx}$ (the coloured bands in the figure) should be properly taken into account in a hypothesis test. Bayes theorem can help in defining this properly from a statistical point of view.

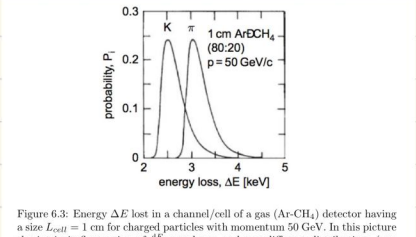

Figure 6.3: Energy ΔE lost in a channel/cell of a gas (Ar-CH_4) detector having a size $L_{cell} = 1$ cm for charged particles with momentum 50 GeV. In this picture the intrinsic fluctuation of $\frac{dE}{dx}$ are shown and two different distributions (one for kaon and one for pion) are shown.

- In gas detector we have various cells. Each cell with a signal due to a particle can be used to measure the # of e^- released by the particle in that cell. They are subject to Poisson fluctuation (due to counting) and to Landau fluctuation.
  Usually a truncated mean algorithm is used to build an estimator of ΔE. (removing the sample with highest dE/dx → better estimation)

- EXAMPLE : ALICE experiment

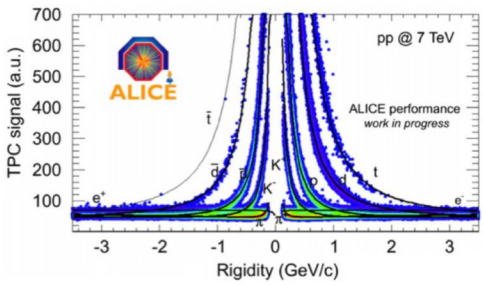

Figure 6.4: Signal from the ALICE TPC as a function of the rigidity.

- $\frac{dE}{dx}$ estimated counting the ion. clusters N_e in some cell of gas detector. If the detector signal amplitude is prop. to # ion. clusters (through the gain value G), the value of ΔE in that cell can be obtained. as:

$$\Delta E = G \cdot N_e$$

By estimating the path length of the charged particle trajectory in the cell : $l \simeq L_{cell}$

$$\rightarrow \frac{dE}{dx} \simeq \frac{\Delta E}{L_{cell}}$$

TIME OF FLIGHT

- Usually it is used a scintillator because it is fast. Measuring the arrival time of a signal t_A and by subtracting the collision event time t_0 it is possible to measure the TOF of the particle:

- Using :

$$\delta t = t_1 - t_2 = \frac{L}{v_1} - \frac{L}{v_2} = \frac{L}{c}\left(\frac{1}{\beta_1} - \frac{1}{\beta_2}\right) = \frac{L}{c}\left(\frac{\sqrt{P^2+m_1^2}}{P} - \frac{\sqrt{P^2+m_2^2}}{P}\right)$$

if is possible to distinguish 2 particles with same p

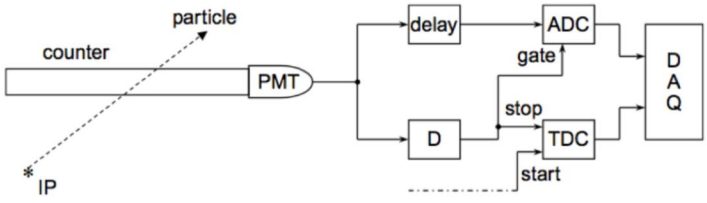

Figure 6.6: Scheme of a time of flight measurement with the DAQ chain.

- If σ_t is the time resolution, the separation power is $\boxed{n_\sigma = \frac{\delta t}{\sigma}}$. We can use it to distinguish different particles:

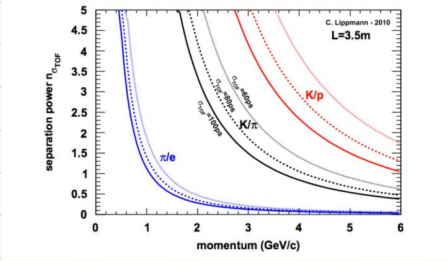

CHERENKOV DETECTORS

- RECAP:
  - Threshold effect $\beta > \frac{1}{n}$ $\longrightarrow$ emission of γ at $\cos\theta_c = \frac{1}{\beta n}$ $\begin{cases} \theta_c^{max} \text{ for } \beta = 1 \\ \theta_c = 0 \text{ for } \beta = \frac{1}{n} \end{cases}$
  - n for liquid and solid is $1.1 < n < 2.5$
    n for gases goes like $n = \frac{n^2-1}{n^2+2} \sim \rho + 1$ (or $n \sim \delta + 1$)

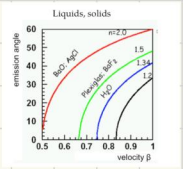

medium	n	θ_{max} (β=1)	N_{ph} (eV^{-1} cm^{-1})
air	1.000283	1.36	0.208
isobutane	1.00127	2.89	0.941
water	1.33	41.2	160.8
quartz	1.46	46.7	196.4

  - Useful relations:
    - $\beta_t = \frac{1}{n} \longrightarrow \beta_t \gamma_t = \frac{1}{\sqrt{n^2-1}} = \frac{1}{\sqrt{(n-1)(n+1)}}$
    - For gases we define $\delta = n-1$
      - $\beta_t \gamma_t = \frac{1}{\sqrt{\delta(\delta+2)}} \longrightarrow \beta_t = m\beta_t\gamma_t = \frac{m}{\sqrt{\delta(\delta+2)}} \overset{\delta \ll 1}{\sim} \frac{m}{\sqrt{2\delta}}$

Medium	δ=n-1	γ_t
helium	3.3×10^{-5}	123
CO_2	4.3×10^{-4}	34
H_2O	0.33	1.52
glass	0.46-0.75	1.37-1.22

  - Cherenkov light yeald
    - $\frac{dN}{dx} = 2\pi\alpha z^2 \sin^2\theta_c \frac{\lambda_2 - \lambda_1}{\lambda_2 \lambda_1}$ (z: charge of the particle) range blue-UV 350–550 nm $\boxed{\frac{dN}{dx} = 490 \sin^2\theta_c \ (cm^{-1})}$

- RING CHERENKOV DETECTOR PID
  - Detecting the angle at which the cherenkov light is produced we can do a PID

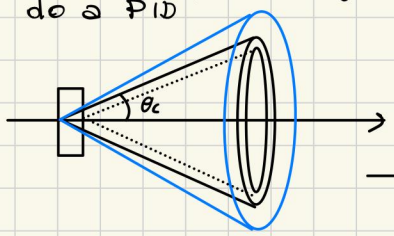

$$\cos\theta_c = \frac{1}{n\beta} \longrightarrow m = \frac{p \cdot n \cdot \cos\theta_c}{\gamma}$$

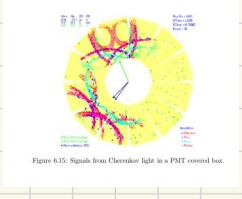

Figure 6.15: Signals from Cherenkov light in a PMT covered box.

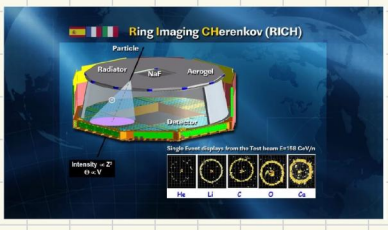

- **CHERENKOV THRESHOLD COUNTERS PID**

  - Using the threshold condition $\beta > \frac{1}{n}$ we can discriminate particles with same momentum putting a series of Cherenkov counters with different material (different n)

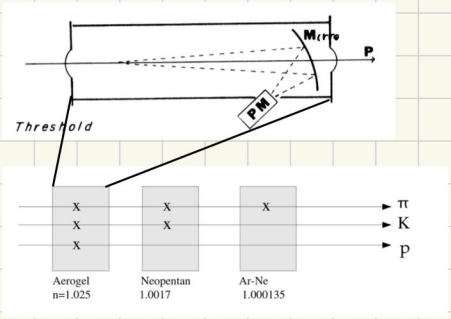

- **Example 1 : DIRC** (Detector of Internally Reflected Cherenkov light)

  - Synthetic quartz as radiator, by internal reflection, traps a good fraction of Cherenkov light. This can be understood comparing $\theta_C^{max} = \arccos\left(\frac{1}{n_2}\right)$ with the angle of internal reflection $\theta_r = \arcsin\left(\frac{1}{n_1}\right)$

  - Multiple reflections can propagate the light to the end of the radiator (it is working as a light guide).

  - At the end of the bars ther is H_2O with $n_2 \sim n_1$.

  - The cherenkov γ are then imaged to a surfaced covered by PMTs.

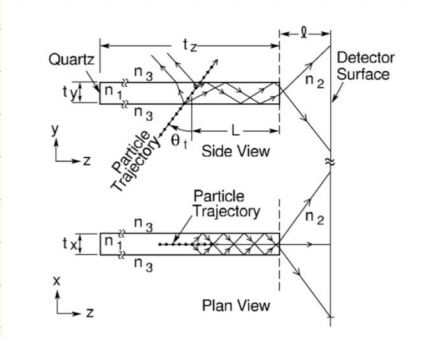

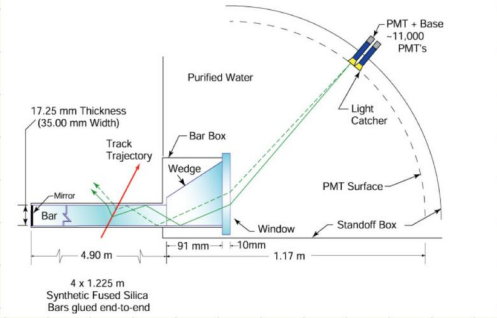

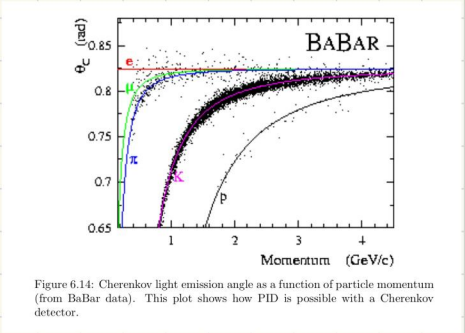

Figure 6.14: Cherenkov light emission angle as a function of particle momentum (from BaBar data). This plot shows how PID is possible with a Cherenkov detector.

- **Example 2 : CEDAR (CERN)**

  - If the beam has very high energy and a gas is used as radiator a long path is needed Therefore we can use mirrors to have longer light paths :

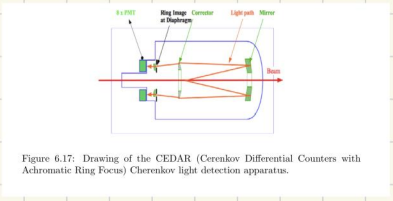

Figure 6.17: Drawing of the CEDAR (Cerenkov Differential Counters with Achromatic Ring Focus) Cherenkov light detection apparatus.

PHOTO - DETECTORS

- **SCINTILLATOR**

  - How is it made:

    + scintillating material
    + light guide
    + photo sensor (PMT, ...)

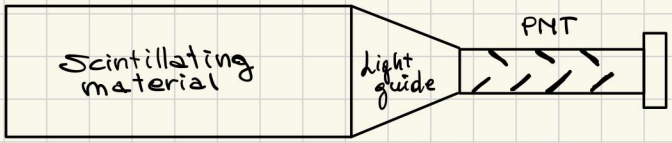

  - How does it work:

    1) A particle excites the scintillator molecules
    2) Light is transferred to the PMT where it is converted in photoelectrons which are amplified through a dynodes cascade
    3) Current signal by amplified electrons

- **SCINTILLATING MATERIAL** : luminous material : fluorescense (fast 10ns), phospohorence (slower)

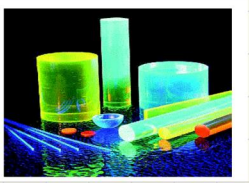

  - Basic properties :

    1. It should convert the E_{kin} of the charged particle into detectable light with high scintillation efficiency
    2. Linear conversion : light yield $\propto$ deposited energy
    3. Medium should be transparent to the wavelength of its own emission
    4. Short decay time of the induced luminescence $\rightarrow$ fast pulse generated
    5. Good optical quality material
    6. Index of refraction near ~ 1.5 (glass) to permit efficient coupling of the scintillation light to a photomultiplier tube or other light sensor.

  - Light yield

$$N(t) = N_f e^{-\frac{t}{\tau_f}} + N_s e^{-\frac{t}{\tau_s}}$$

There can be different time-scale for different emission

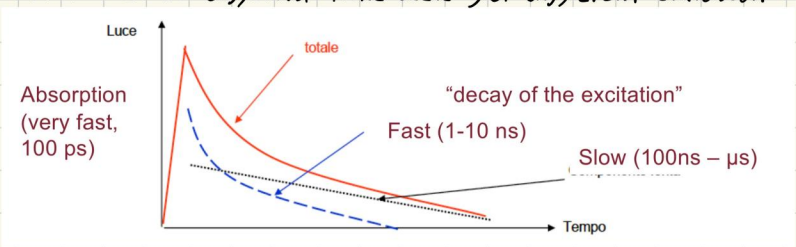

- 2 CATEGORIES :

  - ▶ ORGANIC (hydrocarbons) : sizeable amount of light, fast, easy to be handled (plastic)
    Scintillation mechanism : transition between molecular or atomic en. levels
  - ▶ INORGANIC : lot of light, usually slower, crystals
    Scintillation mechanism : driven by the band structure

• ORGANIC SCINTILLATORS

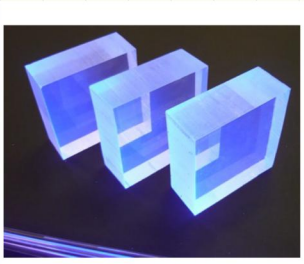

General Technical Data –

Base ..... Polyvinyltoluene

Density (g/cc) ..... 1.032 g/cc

Refractive Index 1.58

Expansion Coefficient (per°C,<67°C): 7.8X10⁻⁵

Softening Point ..... 70°C

Vapor Pressure ..... May be used in vacuum

Solubility ..... Soluble in aromatic solvents, chlorinated solvents, acetone, etc. Unaffected by water, dilute acids, lower alcohols, alkalis and pure silicone fluids or grease.

Light Output ..... At +60°C = 95% of that at+20°C. Independent of temperature from -60°C to +20°C

- EMISSION WAYS :

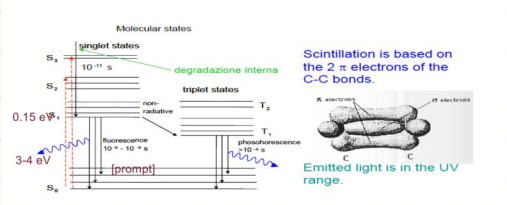

1) Particle excitation : molecules excited (both electronic and vibrational model)
2) Singlet decay : < 10 ps - no emission (internal degradation)
3) fluorescence : S_1 to S_0 (1-10 ns)
4) phosphorescence : T_1 to S_0 (100 μs) . n.b. Triplet state accesible via internal degradation

- WAVELENGTH SHIFTING : we can shift the emission wavelength doping the scintillator

- Ex. polimeric material (polystirene) can be doped with fluors

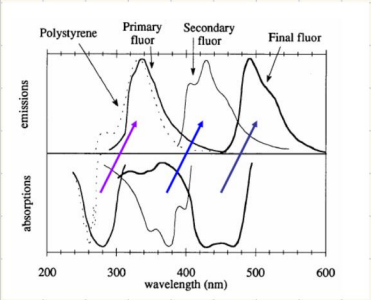

	Polystyrene (PST)
Density [g/cm^3]	1.06
Refractive index	1.06
Absorption coefficient [cm^{-1}]	0.01-0.003
Softening temperature [K]	355-360
Hygroscopic	no
Wavelength of emission maximum [nm]	430
Light output [% of anthracene]	56
H/C ratio	1.0
Decay time [ns]	2-3

In
rld

- NON LINEARITY (and saturation)

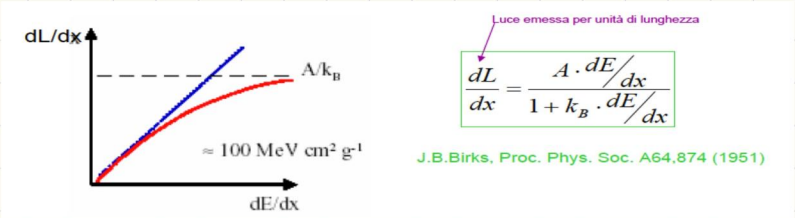

Organic scintillators

Name	density [g/cm^3]	refractive index	typical λ [nm]	time const. [ns]	Relative LY to anthracene			Relative LY to NaI(Tl)
naphthalene	1.15	1.58	348	11	11	0.800	monocrist.	
anthracene	1.25	1.59	448	30-32	100	0.714	monocrist.	0.5
NE 102 A	1.032	1.58	425	2.5	65	1.105	Nucl. Ent.	
NE 104	1.032	1.58	405	1.8	68	1.100	Nucl. Ent.	
NE 110	1.032	1.58	437	3.3	60	1.105	Nucl. Ent.	
BC 412	1.032	1.58	434	3.3	60	1.104	Bicron	
BC 414	1.032	1.58	392	1.8	68	1.110	Bicron	
BC 416	1.032	1.58	434	4.0	50	1.110	Bicron	

• INORGANIC SCINTILLATORS

- EMISSION WAYS :

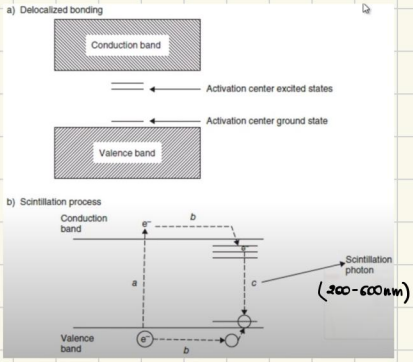

- Crystal can contain impurity : i.e. additional level in the band gap the so called ACTIVATORS CENTERS

Excitation induced by the passage of a particle could lead to:

a) e^- can jump to the conduction band leaving a hole in the valence band

b) one of the e^- from the activation center could come to the hole leaving a hole in the activation center.

b) the e^- in the cond. band jump down to the nearest activation c.

c) this last e^- can jump to the activation c. below and emit a scintillation γ.

- LIGHT SPECTRUM :

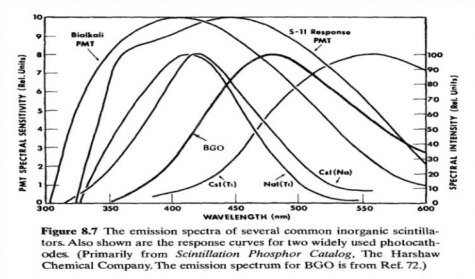

Figure 8.7 The emission spectra of several common inorganic scintillators. Also shown are the response curves for two widely used photocathodes. (Primarily from *Scintillation Phosphor Catalog*, The Harshaw Chemical Company. The emission spectrum for BGO is from Ref. 72.)

- LIGHT YIELD V.S. TEMPERATURE

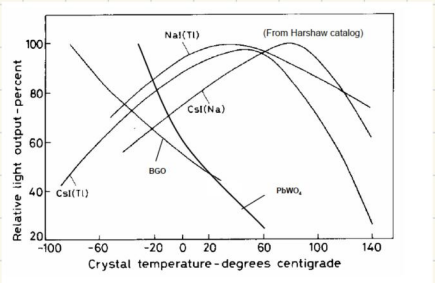

A list of inorganic scintillators

Name	density [g/cm^3]	refractive index	typical λ [nm]	time const. [μs]	Relative LY to NaI(Tl)	Absolute LY	
NaI	3.67	1.78	303	0.06	190		
NaI(Tl)	3.67	1.85	410	0.25	100	a 80 K	4x10^4
CsI	4.51	1.80	310	0.01	6	a 80 K	
CsI(Tl)	4.51	1.80	565	1.0	45	a 80 K	1.1x10^4
^{6}LiI(Eu)	4.06	1.96	470-485	1.4	35	a 80 K	1.4x10^4
BaF_2	4.88	1.49	190/220 310	0.0006 0.63	5 15		6.5x10^3 2x10^3
$Bi_4Ge_3O_{12}$	7.13	2.15	480	0.30	10		2.8x10^3
$PbWO_4$	8.28	1.82	440,530		0.1		100
LAr	1.4	1.29	120-170	0.005/0.860		a 170 nm	
LKr	2.41	1.40	120-170	0.002/0.085		a 170 nm	
LXe	3.06	1.60	120-170	0.003/0.022		a 170 nm	4x10^4

- NOBLE GAS SCINTILLATORS

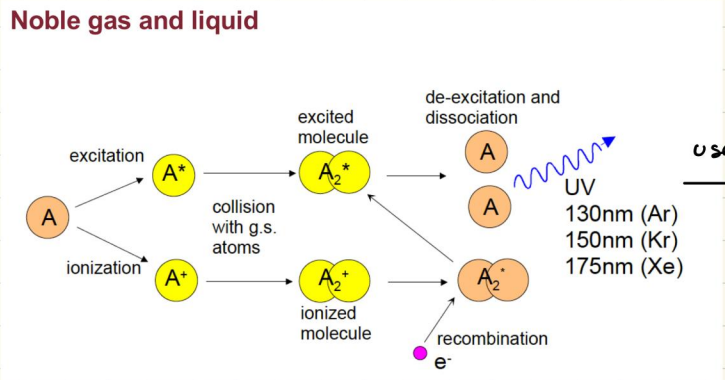

useful for PID →

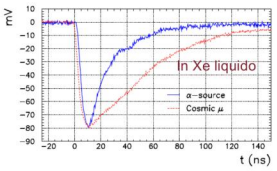

Triplet states excited by **larger** dE/dx
(delayed fluorescence)

Recombination time is 45 ns

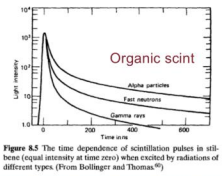

Figure 8.5 The time dependence of scintillation pulses in stilbene (equal intensity at time zero) when excited by radiations of different types. (From Bollinger and Thomas[40])

- SCINTILLATION EFFICIENCY : price to pay to produce one carrier of information (analogous of W for gas)

  INORGANIC : to create a γ we need an e-h pair: we need to pay E_{gap} ~ 20 eV (in NaI(Ti))
  (In NaI(Ti) ~12% of E_{dep} is converted into light → $E_\gamma \simeq 3$ eV)

  ORGANIC : 100 eV per photon

LIGHT GUIDE

- Rem. scintillation light is emitted isotropically (Cherenkov light is emitted in a precise direction).

- The light collection needs to be maximized
- The light can go directly to the photosensor or can be guided through the internal reflection process:

Angle for internal reflection : $\theta_c = \arcsin\left(\frac{n_1}{n_0}\right)$

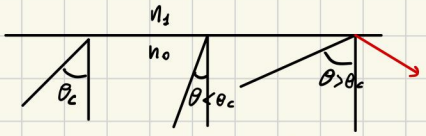

- the light guide must mechanically match the size of the photosensor (no air in between, use optical glue or grease)

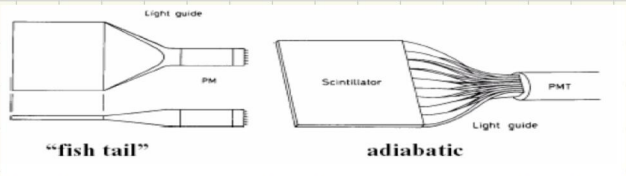

- Examples :

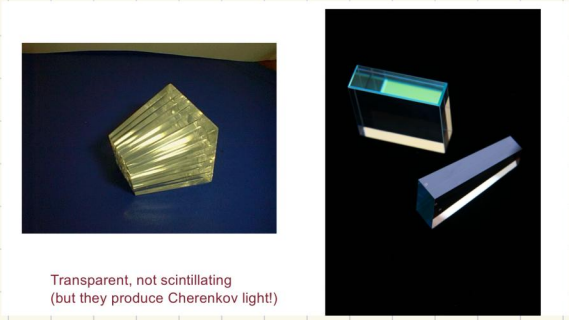

Transparent, not scintillating
(but they produce Cherenkov light!)

SCINTILLATING FIBERS

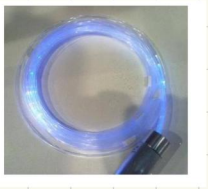

- They are at the same time either scintillator and light guide
- Can be very small (200 μm diameter) (round or squared)

- The fraction of solid angle is equal to the maximal theoretical fraction of light at one end

$$F = \frac{\Omega}{4\pi} = \frac{1}{4\pi}\int_{\phi=0}^{\phi=\phi_c} d\Omega = \frac{1}{4\pi}\int_0^{\phi_c} 2\pi \sin\phi \, d\phi = \frac{1}{2}(1-\cos\phi_c) = \frac{1}{2}(1-\sin\theta_c) = \frac{1}{2}\left(1-\frac{n_1}{n_0}\right)$$

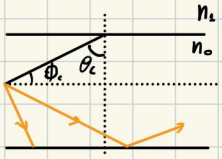

- CLADDING : external material to protect the internal scintillating core

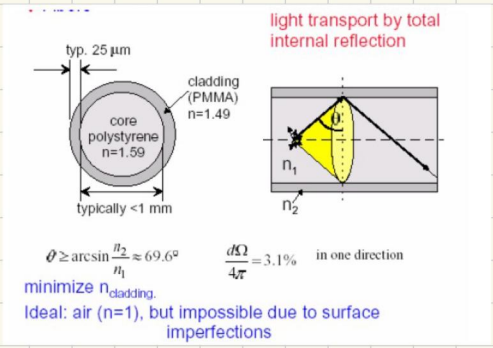

- MULTI-CLADDING :

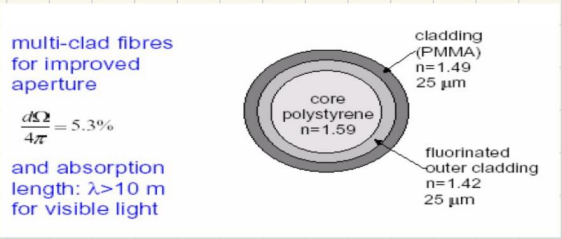

- LIGHT PROPAGATION

  - Any imperfections at the core-cladding interface may disturb the total internal reflection
  - Some of the scintillation light may be reabsorbed in the fiber due to overlap of the emission and absorbtion bands of the fluorescent species
  - Rayleigh scattering from small density fluctuations in the core can deflect an optical ray that is not longer totally internally reflected

  ⟶ attenuation length L (depends on λ) L ~ 10 cm - few m ⟶ $I = I_0 e^{-\frac{x}{L}}$

  - Hence to the PHT are arriving few photons

- TRACKING WITH FIBERS

  - Fine granularity
  - Low mass
  - Fast signal (ns)
  - Can be adapted to various geometry

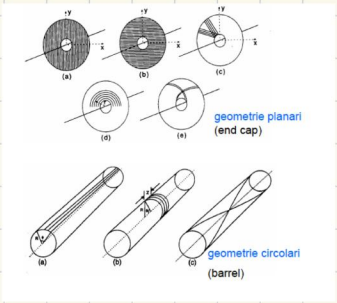

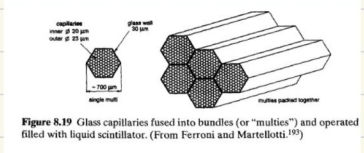

Figure 8.19 Glass capillaries fused into bundles (or "multies") and operated filled with liquid scintillator. (From Ferroni and Martellotti.[193])

DETECT PHOTONS

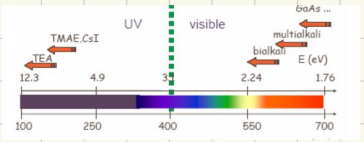

- Goal: convert light into an electric signal
- Remember that the light wavelength can range from UV to RED
- The trick is using the photoelectric effect.
- QUANTUM EFFICIENCY: ability to convert photon in a detectable electron

PMT - PHOTOMULTIPLIER TUBE

- **HOW DOES IT WORK?** the dynodes are kept at higher and higher voltages

photo-sensitive material at a negative potential →

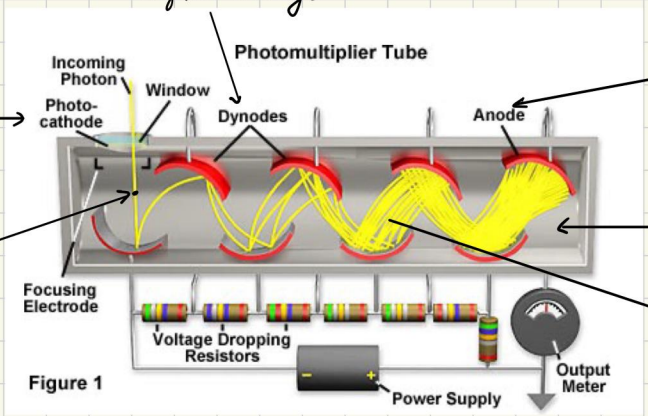

Figure 1

← pick-up signal, grounded

← vacuum tube

the emitted photoelectron goes into a collection field and it's accelerated (~100eV) and focused on the 1st dinode where there is a secondary emission of electrons.

Multiplication stage: on each dynode further secondary emissions take place → avalanches

- **PHOTO - CATHODE**

- It produces an e^- from a γ via photoelectric effect
- Actually 3 steps:

1) The molecule/atom is ionized (via photoelectric effect)
2) A very small kinetic energy e^- should find its way out of the material
3) Escape into the vacuum of the PMT tube

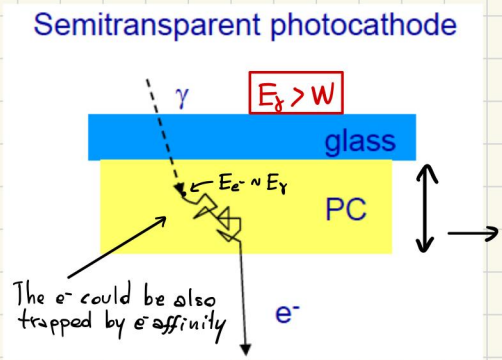

Typically: $E_\gamma \sim 3eV$
Work function: (metals) 3-4eV / (semiconductors) 1.5eV

- must be quite thin otherwise e^- just lose its kinetic energy in the material. For this reason is better to use semiconductors since the active region can be few 10 nm
- however if it's very thin is also transparent to the photon (because the thickness can be ~ abs length) → no γ absorption

- BAND MODEL

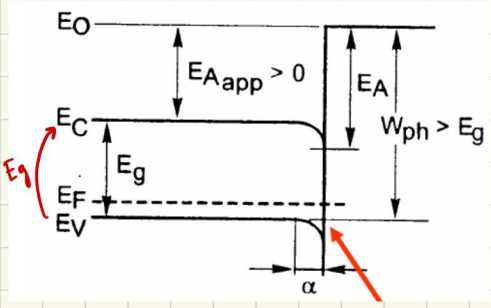

Photon energy has to be sufficient to bridge the band gap E_g but also to overcome the electron affinity E_A, so that the electron can be released into the vacuum.

Low work function (as for semiconductors) means thermoionic emission (exponential with temperature)

- THERMOIONIC EMISSION (PMT NOISE contribution)

  - the photocatode can emit e^- for thermal fluctuations → noise!
  - current thermoionic density: $J = A_G T^2 e^{\frac{-W}{KT}}$ $\quad A_G = 1.21 \cdot 10^6 \frac{A\,m^2}{K^2}$ $\quad KT = 25\,meV$

- PMT WINDOW

  - Photocathode must be in vacuum → there must be a window to hold the vacuum
  - The window must be transparent to the light that goes through it → usually glass or better, fused silica. Of course there is a minimun energy under which it is no more transparent

Transmission of various PM windows

not shown:
MgF_2: cut @115 nm
LiF: cut @105 nm

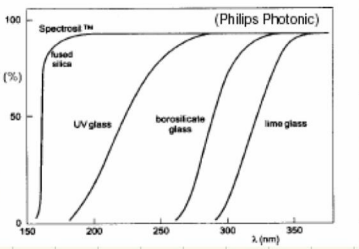

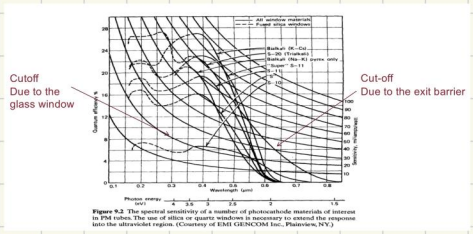

Figure 9.2 The spectral sensitivity of a number of photocathode materials of interest in PM tubes. The use of silica or quartz windows is necessary to extend the response into the ultraviolet region. (Courtesy of EMI GENCOM Inc., Plainview, NY.)

- QUANTUM EFFICIENCY

  - Above some cut-off energy one photo-electron has a chance to exit the cathode. This chance depends on the energy of photon.
  - An empiric definition of overall efficiency for this detection is: (depends on λ)

$$\text{Quantum efficiency (QE)} = \frac{\#\,photoelectrons}{\#\,incident\,photons}$$

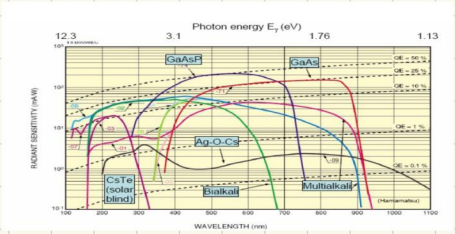

  - Radiant sensitivity: $S = \frac{I}{P(\lambda)}$ ← emitted e^- current / ← incident power of γ $\quad \left[\frac{A}{W}\right]$; for a given λ: $S = \frac{\lambda QE}{1240}$

- DYNODES

  - MULTIPLICATION: one electron extracts more than one electron from the dynode

Low kin energy
Few sec electrons from the surface

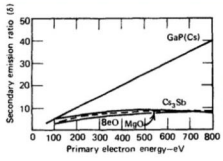

High kinetic energy
Several secondaries but deeper in the bulk of the dynodes

Figure 9.3 Variation of the secondary emission yield with primary electron energy for standard dynode materials (lower three curves) and an NEA material [GaP(Cs)]. (From Krall et al.[6])

  - NEGATIVE e^- AFFINITY

    - Dynodes made with NEA materials (oxydes)
      1) More e^- per stage and hence less dynodes for the same ampl.
      2) Kinetic energy distr. less spread out (less variation in the transit time)

- VOLTAGE DIVIDERS & GAIN UNCERTAINTY

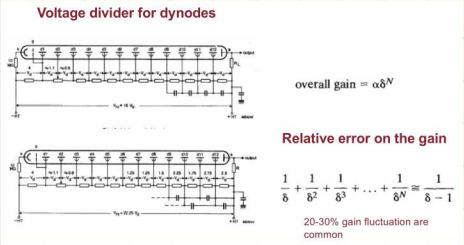

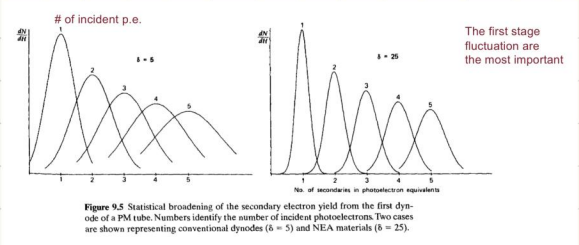

Figure 9.5 Statistical broadening of the secondary electron yield from the first dynode of a PM tube. Numbers identify the number of incident photoelectrons. Two cases are shown representing conventional dynodes ($\delta = 5$) and NEA materials ($\delta = 25$).

• PMT EQUIVALENT RC CIRCUIT

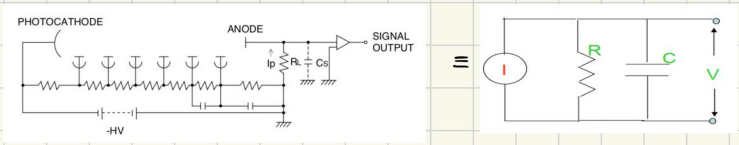

R = anodic resistance ⊕ load resistence (50 Ω)
C = capacitance
$\tau = RC$; τ_s : scintillation time

$$\rightarrow I(t) = \frac{V}{R} + C\frac{dV}{dt} \longrightarrow I(t) = \frac{GNe}{\tau_s} e^{-\frac{t}{\tau_s}} \longrightarrow V(t) = \begin{cases} -\frac{GNeR}{\tau-\tau_s}\left[e^{-\frac{t}{\tau_s}} - e^{-\frac{t}{\tau}}\right] & \tau \neq \tau_s \\ \frac{GNeR}{\tau_s^2}\, t\, e^{-\frac{t}{\tau_s}} & \tau = \tau_s \end{cases}$$

• TYPICAL PMT ANODE PULSE

- Typical waveform properties

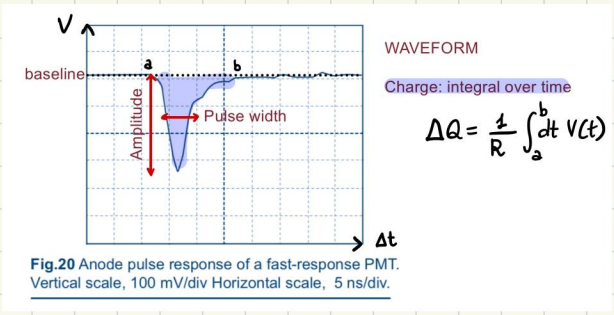

Fig.20 Anode pulse response of a fast-response PMT. Vertical scale, 100 mV/div Horizontal scale, 5 ns/div.

• For the signal fit:

$$V(t) = \begin{cases} B, & t < a \\ A\left(e^{-\frac{t-c}{\tau_s}} - e^{-\frac{t-c}{\tau}}\right) & t \geq a \end{cases}$$

with A, c, τ_s 3 parameters and $\tau = RC$,
B : baseline

- Timing performances : transit time (spread)

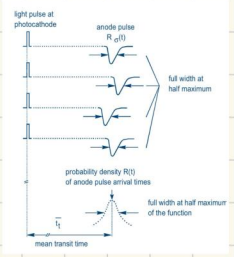

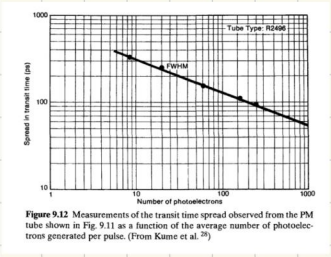

Figure 9.12 Measurements of the transit time spread observed from the PM tube shown in Fig. 9.11 as a function of the average number of photoelectrons generated per pulse. (From Kume et al. [28])

$\rightarrow$ FWHM ~ 1 ns - 10 ns

- Various anodic pulses

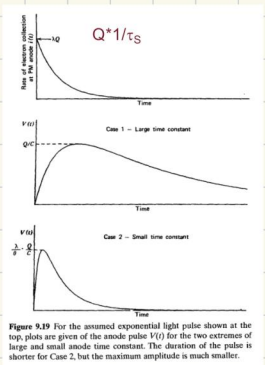

Figure 9.19 For the assumed exponential light pulse shown at the top, plots are given of the anode pulse V(t) for the two extremes of large and small anode time constant. The duration of the pulse is shorter for Case 2, but the maximum amplitude is much smaller.

Exponential light pulse

Classical light pulse with $\tau \gg \tau_s$

Classical light pulse with $\tau \ll \tau_s$

- ## LED LIGHT MEASUREMENT

  - We shine light on a PMT using a LED (mimic scint. light)
  - Charge of the PMT pulse : $q = G \cdot QE \cdot N + q_0$ ← pedestal (quantum eff., gain, incident photons)

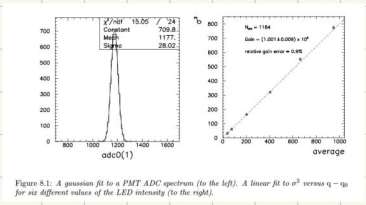

Figure 8.1: A gaussian fit to a PMT ADC spectrum (to the left). A linear fit to σ^2 versus $q - q_0$ for six different values of the LED intensity (to the right).

  - Fluctuation of the charge : $\sigma^2 = G(QE)^2 N + \sigma_0^2 \rightarrow \boxed{\sigma^2 = QE\,(q - q_0) + \sigma_0^2}$

- ## POSITION RECONSTRUCTION IN A SCINTILLATING BAR WITH 2 PMTs

- METHOD 1

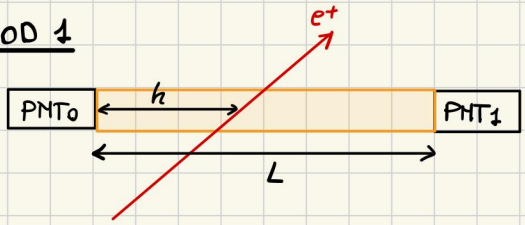

v_{eff} : effective light velocity ~ 15 $\frac{cm}{ns}$
T : starting time

$$\begin{cases} t_0 = T + \dfrac{C_0}{\sqrt{A_0}} + \dfrac{h}{v_{eff}} + b_0 \\ t_1 = T + \dfrac{C_1}{\sqrt{A_1}} + \dfrac{L-h}{v_{eff}} + b_1 \end{cases}$$

$$\boxed{h = v_{eff}\,\frac{t_0 - t_1}{2} + const}$$

- METHOD 2 : charge unbalance

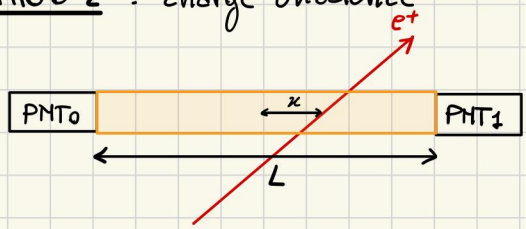

E_γ : energy deposited by γ ray
QE : quantum efficiency
$\mathcal{E}$: energy deposited per light photon created in scintillator
α : attenuation light coefficient

$$\begin{cases} E_0 = \dfrac{E_\gamma \cdot QE}{\mathcal{E}} \exp\left[-\alpha\left(\frac{L}{2} + x\right)\right] \\ E_1 = \dfrac{E_\gamma \cdot QE}{\mathcal{E}} \cdot \exp\left[-\alpha\left(\frac{L}{2} - x\right)\right] \end{cases} \rightarrow \boxed{x = \frac{1}{2\alpha} \ln\left(\frac{E_1}{E_0}\right)}$$

SUMMARY OF PRODUCTION AND SIGNAL PROCESS

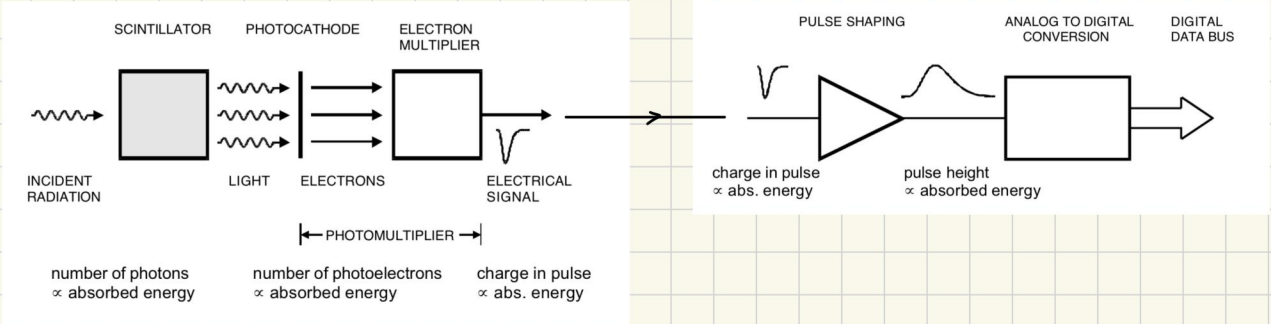

SEMICONDUCTORS

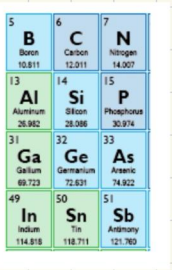

- **SEMICONDUCTORS**: A semiconductor is a system where I have the valence band completely filled, and the conduction band completely empty at T=0 and such that at T>0 there is a promotion and so conduction.
  (see CM-notes)

  - INTRINSIC SEMICONDUCTORS : - # e^- in the conduction band = # holes in the valence band
    $\longrightarrow n_c(T) = p_V(T) \equiv n_I$

    $\longrightarrow n_I = \sqrt{n_c p_v}\, e^{-\beta \frac{E_{gap}}{2}}$ at T=20°C $\begin{cases} n_I = 2\cdot 10^{10}\,cm^3 \ (Si) \\ n_I = 2\cdot 10^{13}\,cm^3 \ (Ge) \end{cases}$

    - conduction is possible only between the valence and the conduction band

  - EXTRINSIC SEMICONDUCTORS : doped semiconductors

- **DOPING** : is a trick to make easier the conduction

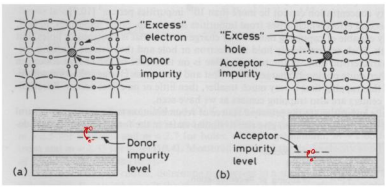

  - n-doping : creating an excess of e^- through the insert of a donor material (with more valence e^-) $\longrightarrow$
    - example: Si (4 valence e^-) + P (5 valence e^-)

  - p-doping : creating an excess of hole through the insert of an acceptor material (with less valence e^-)
    - example: Si (4 valence e^-) + B or Al

- **p-n junction** :

  - What is it: junction between a p-doped piece and a n-doped piece

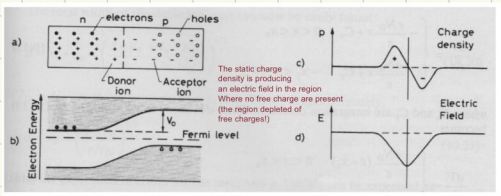

  - What happens: free charges are moving to the other side of the junction leaving behind the dopant atoms with their static charge.
    - donor ions are positive (they have lost the electron) on the n side
    - acceptor ions are negative (they have lost the hole) on the p side

  - Depletion region : region around the junction interface, majority of charge carriers are here

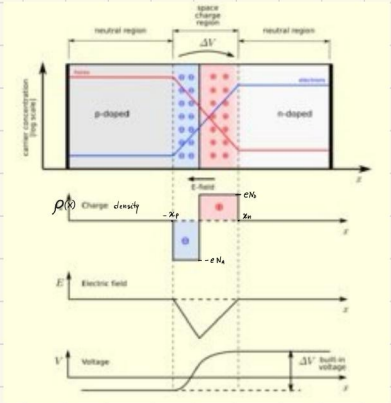

$\longrightarrow \rho(x) = \begin{cases} eN_D & 0 < x < x_n \\ -eN_A & -x_p < x < 0 \end{cases}$

$\longrightarrow \frac{d^2V}{dx^2} = -\frac{\rho(x)}{\varepsilon} \longrightarrow \frac{dV}{dx} = \begin{cases} -\frac{eN_D}{\varepsilon}x + C_n & 0 < x < x_n \\ \frac{eN_A}{\varepsilon}x + C_p & -x_p < x < 0 \end{cases}$

SEMICONDUCTOR DETECTORS

- **PROs:**
  - Dense, compact → μm resolution
  - Good energy resolution (for Si the e-h cost is ~3.6 eV)
  - Relatively fast: >10 ns
- **CONs:**
  - Cannot cover large surface (too expensive)
  - Subject to radiation damage (crystal lattice dislocation)

• PHOTODIODE

- **What is it:** it is a semiconductor diode sensitive to photon radiation. It produces an electrical current if it absorbs the photon. (not for single photon: very noisy)
- **How is it made:** PIN: p-n junction structure with long intrinsic region
- **How does it work:** if the photon has $E > E_{gap}$ and it is absorbed in the depletion region it forms an e-h pair. The hole moves toward the anode and the e^- toward the cathode thanks to $\vec{E}$ between the donor side (+ charge) and the acceptor side (- charge)

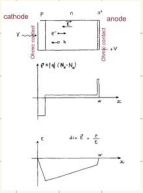

Q.E. ~ 80% G = 1

- **SPECTRAL RESPONSE:**

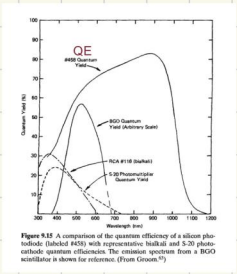

Figure 9.15 A comparison of the quantum efficiency of a silicon photodiode (labeled #456) with representative bialkali and S-20 photocathode quantum efficiencies. The emission spectrum from a BGO scintillator is shown for reference. (From Groom.[9])

- AVALANCHE PD (APD)

- **What is it:** a photodiode which, using the avalanche effect, provides an high gain effect to the induced photo current
- **How is it made:** p-n structure or PIPN structure
- **How does it work:** it is applied an high polarization voltage which induces an avalanche after the formation of the e-h pair

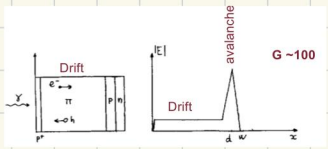

- $V_0 \sim 100-200$ V : linear behaviour : amplitude $\propto$ # γ
- $V_0 > 300$ V : Geiger mode i.e. no linearity anymore: amplitude ~ const

(n.b. Gain is very sensitive to voltage stability and temperature)

- HYBRID PD (HPD)

- **How is it made:** photocathode + p.e. acceleration + silicon detector (photodiode)
- **How does it work:** the photocathode absorbs a γ and produces pe^-. The p.e^- is accelerated with an external $\vec{E}$ field. The photodiode detects the accelerated pe^-

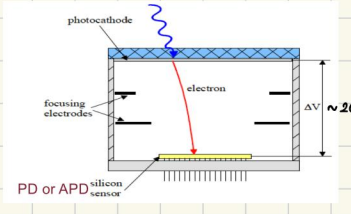

$$G = \frac{e\Delta V}{W_{Si}} = \frac{20\ keV}{3.6\ eV} \approx 5 \cdot 10^3$$

- PRO : single p.e. detection with high resolution

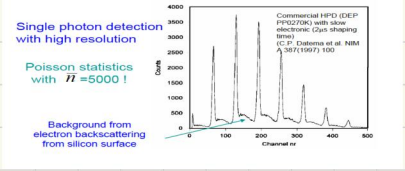

- SILICON PHOTO MULTIPLIER (SiPM)

  - How is it made : matrix (1x1 mm²) of small APDs (10x10 μm²) working in Geiger mode.

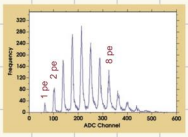

  - How does it work : the matrix is a digital counter : the APD analog signal is used only to generate ON/OFF information. Photons are counted by counting how many APD are ON.
  - PROs : high efficiency to see each single photon ; low gain fluctuation ; can sustain high rate ; very good timing performance.

- STRIP SENSORS

  - Charges are produced and moving in the depletion region (a ionization chamber)
  - Electrodes are realized with highly doped Si (larger doping, larger conductivity)

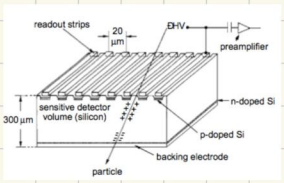

  - Induced charge on the strips builds up the signal. Very close amplifier is needed.

  - APPLICATION OF STRIP SENSORS : SILICON BASED VERTEX TRACKER

    ▸ VERTEX : point in space where a group of particles come from. There can be multiple vertexes in one collision event. There is one main vertex (collision point) in one collision event. There can be multiple multiple collision events with multiple collision vertexes (LHC).

    ▸ How is it made : The beam pipe is inside ; particles are colliding in the center.
    - Strips are running along z and along φ
    - Several coaxial layers

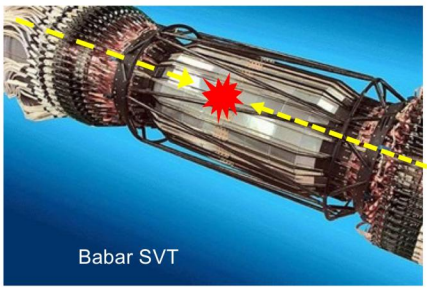

- PIXEL SENSORS

  - 2D matrices of Si sensors - 2D res : 10·10 μm²
  - electronics located under the sensors
  - single pixel analysis :

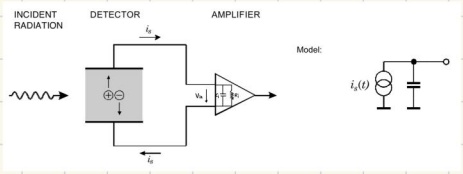

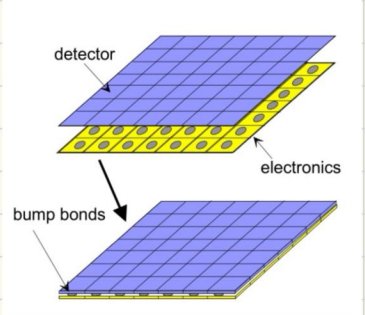

- DARK CURRENT

  - Electrons can go into the conduction band by thermal fluctuation

$$\longrightarrow \quad p(T) = c\,T^{3/2}\,e^{-\frac{E_g}{2K_0T}}$$

INDUCED CHARGE AND CURRENT

- Concept of induced current on electrode k:
  - rate of change of electrostatic flux on the electrode surface (not the collection of charge by the electrode)
  - requires to compute the total field $E(x,y,z,t)$ (due to bias voltages, fixed space charge, and moving charges) at every time instant, the integral of the flux on electrode surface.

- RAMO'S THEOREM
  - The charge q_A (and current I_A) induced on an electrode A by a moving point charge q with velocity v is given by
$$-q V_w(x) = -q_A v E_w(x)$$
where $V_w(x)$ is the weighting potential at point x i.e. the potential obtained in the point x, where the charge q is located, in an alternative setting: all the electrodes other than A are set to ground and the potential of A is set to the unit value.

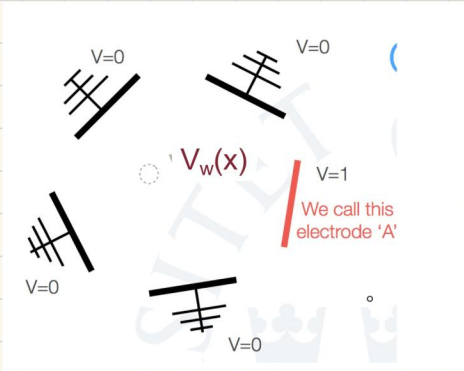

  - N.B. Charge q is moving with velocity v under the real $\vec{E}$ field due to all electrodes V.

Proof:

- We need to use the Green's identity $\int_V V' \nabla^2 V - \int_V V \nabla^2 V' = \int_{\partial V} V' \frac{dV}{dn} dS - \int_{\partial V} V \frac{dV'}{dn} dS$

Configuration 1

$V_A = V_B = V_C = V_D = V_E = V_F = 0$

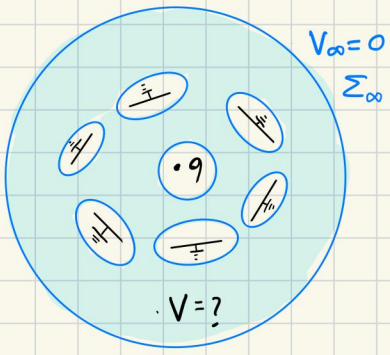

$\nabla^2 V = -4\pi\rho = 0$

Configuration 2

$V_A' = 1 \quad V_B' = V_C' = V_D' = V_E' = V_F' = 0$

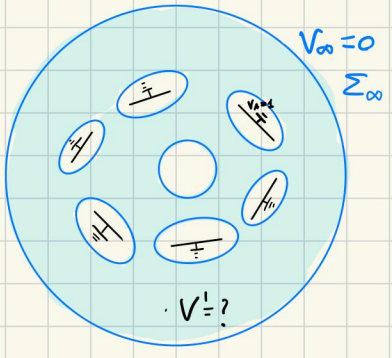

$\nabla^2 V' = 4\pi\rho' = 0$

$$\longrightarrow \int_{\partial V} V' \frac{dV}{dn} dS - \int_{\partial V} V \frac{dV'}{dn} dS = 0 \longrightarrow \int_{\Sigma_q} V_q' \frac{dV_q}{dn} dS - \cancel{\int_{\Sigma_q} V_q \frac{dV_q'}{dn} dS}^{\,0} + \int_{\Sigma_A} V_A' \frac{dV_A}{dn} dS - \cancel{\int_{\Sigma_A} V_A \frac{dV_A'}{dn} dS}^{\,0} = 0$$

$$\longrightarrow -V_q \cancel{4\pi} q + V_A' \cancel{4\pi} q_A = 0 \longrightarrow V_A q_A = -V_q' q \equiv -V_w(x) q \longrightarrow \boxed{q_A = -\frac{V_w(x) \cdot q}{V_A'}}$$

EXAMPLE: DRIFT TUBE

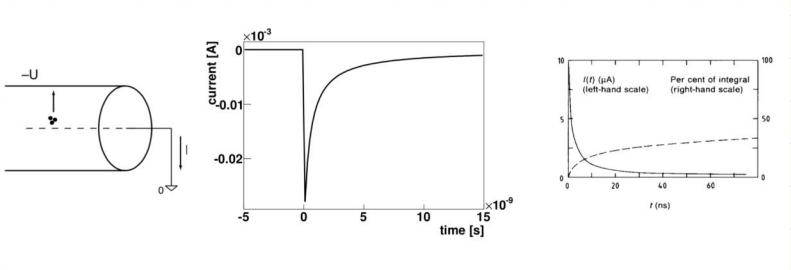

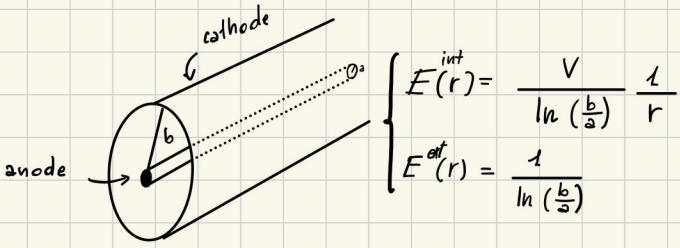

I want to compute the induced charge on the anode. First of all let's compute the radial position of the ion function of time:

$r(t=0) = a$

- $v_d = \mu E(r) \longrightarrow v_d = \frac{dr}{dt} = \mu \frac{V_0}{\ln(b/a)} \frac{1}{r} \longrightarrow r\,dr = \mu \frac{V_0}{\ln(b/a)} dt \Rightarrow \boxed{r(t) = a\sqrt{1 + \frac{2\mu_I V_0 t}{a^2 \ln(b/a)}}}$

- Typical values: $V_0 = 1\,kV$; $\mu_I \sim \frac{10\ cm/ms}{1\,kV} = 10^3 \frac{cm^2}{Vs}$; $a = 50\,\mu m$ $b = 1\,cm$

$\longrightarrow r(t_0) = 1\,cm \longleftrightarrow t_0 \sim 10\,ns$

Then the induced current is:

$$I_A = \frac{dq_A}{dt} = -\frac{dV_w}{dt} q = -\frac{dV_w}{dr_i} \frac{dr_i}{dt} q = -E_w v_d^I q = -q E_w \mu_I E$$

$$= -(Ge)\left(\frac{1}{\ln(b/a)} \frac{1}{r}\right)\left(\frac{V_0}{\ln(b/a)} \frac{1}{r}\right) \cdot \mu_I = -Ge\left[\frac{\mu_I V_0}{(\ln(b/a))^2}\right] \frac{1}{r^2} \equiv A \frac{1}{1 + \frac{t}{t_0}} \longrightarrow \boxed{I_A = A \frac{1}{1 + \frac{t}{t_0}}}$$

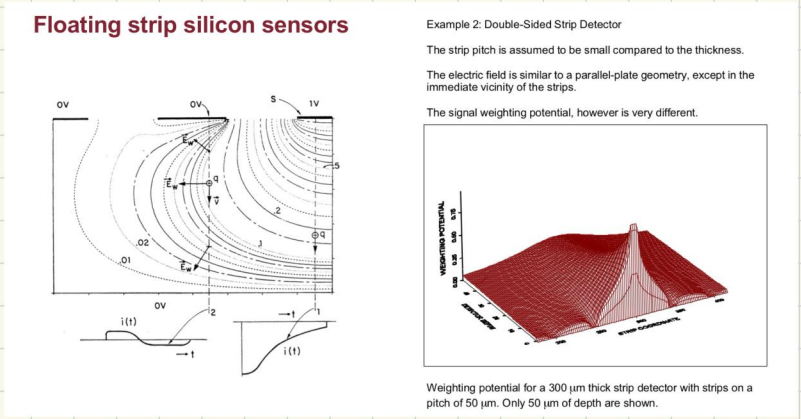

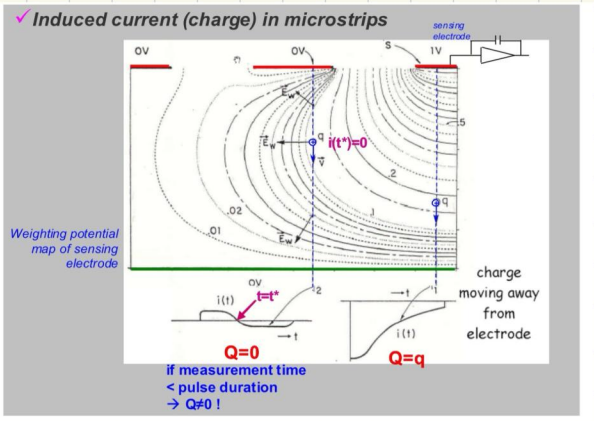

CALORIMETERS

- The goal is to measure the energy of a particle absorbing it totally (fully destructive) and also time and direction.

- 2 TYPES : HADRONIC CALORIMITERS , E.M. CALORIMITERS

- 2 CLASSES :

  - SAMPLING CALORIMITERS
    - Passive absorbing and active sampling materials
    - Pb - Co scintillators, ionization chambers etc.
    - Counts number of shower tracks in the active materials, shower tracks are mainly produced in the passive absorbing materialss

  - HOMOGENEUS CALORIMETERS
    - Same material where the shower is evolving and shower tracks are producing carriers of information

- ENERGY RESOLUTION OF A CALORIMETER

  - E_0 : energy to be detected $\longrightarrow$ $\frac{\sigma_E}{E_0} = \frac{a}{\sqrt{E_0}} \oplus \frac{b}{E_0} \oplus c$

  a : stochastic term (due to the fact that $E_0 \propto N_{pe} \rightarrow \left(\frac{1}{\sqrt{N}}\right)$)
  b : noise term (not related to E_0)
  c : constant term (imperfect calibration non uniformity, energy lost before the cal.)

  - 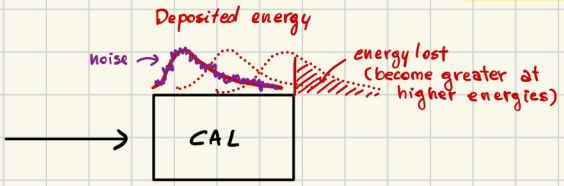

- BASIC OF SHOWER TRACKS DETECTION

  - Energy deposited in 1 rad. length : $E_c = \left(\frac{dE}{dx}\right)_{ion} \cdot X_0$
  - Total track length : $T_{tot} = \left(\frac{E_0}{E_c}\right) \cdot X_0$
  - $\frac{\sigma_E}{E_0} = \frac{1}{\sqrt{n}} = \sqrt{\frac{L_{sig}}{L_{TOT}}}$; $\frac{\sigma_E}{E_0} = \sqrt{\frac{F}{n}} = \sqrt{\frac{F L_{sig}}{L_{TOT}}}$

  L_{sig} : length necessary to produce 1 carrier of info.
  F : Fano's factor (1 for scint. materials, 0.1 for Si)

- CALORIMETER ANGULAR DISTRIBUTION :

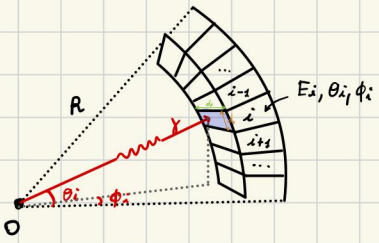

$$\begin{cases} \theta_\gamma = \dfrac{\sum \theta_i E_i}{\sum E_i} F_\theta(\phi, \theta, E) \\ \phi_\gamma = \dfrac{\sum \phi_i E_i}{\sum E_i} F_\phi(\phi, \theta, E) \end{cases}$$

$$\sigma(\theta_i) \simeq \frac{d_\theta}{R} \qquad \sigma(\theta) = \frac{\frac{d_\theta}{R}\sqrt{\sum E_i}}{\sum E_i} \cdot F_\theta = \frac{\frac{d_\theta}{R} \cdot F_\theta}{\sqrt{E}}$$

$$\sigma(\phi_i) \simeq \frac{d_\phi}{R} \qquad \sigma(\phi) = \frac{\frac{d_\phi}{R}\sqrt{\sum E_i} \cdot F_\phi}{\sum E_i} = \frac{\frac{d_\phi}{R} \cdot F_\phi}{\sqrt{E}}$$

• CMS ECAL (homogenous)

• HOW IS IT MADE:

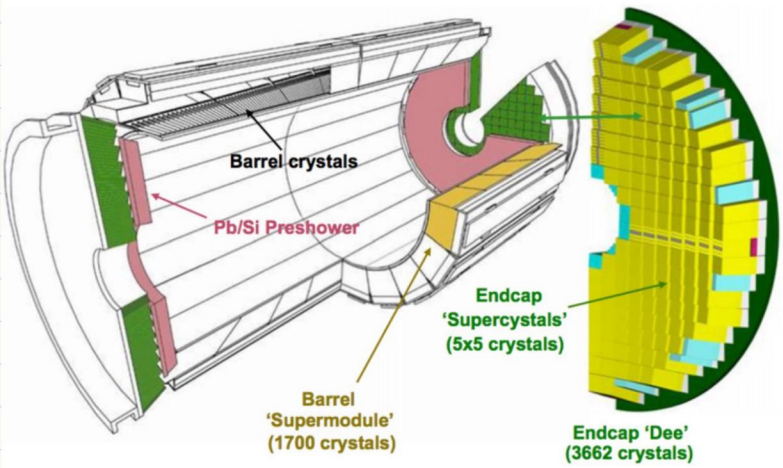

Lead tungstate crystals (25x25 mm^2)
(76000)
X_0 = 0.89 cm
R_M = 2.2 cm
Very dense, very compact!

Fast scintillation (80% light within 25 ns)
Blue light, well matched to photo-sensors
BUT
only 70 photons / MeV !!! (bad light yield in favor of fast scintillation)

Calorimeters are
inside the magnet coils

Minimize the material
in front of the ECAL !

More on CMS ECAL

- Radiation resistance, but light yield depends on the absorbed dose!
-

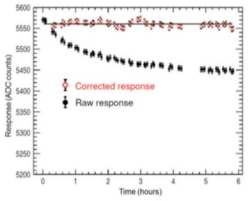

Example of calibration:
need to follow constantly the light yield changes!

Photo-sensors:
APD 5x10 mm^2 (partial coverage!)
G ~50
QE ~70%

CMS ECAL energy resolution

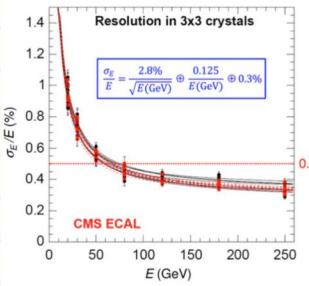

1 GeV particle

$a_{pe} = \sqrt{\frac{F}{n_{pe}}} = \sqrt{\frac{2.4}{4500}} \simeq 2.3\%$

BUT a shower can extend over more than a single crystal : Crystal "clusters" (3x3, 5x5,...)

Some "lateral" losses, add in quadrature 2%

- Noise term (b)
  - The APD waveform is sampled at 25 ns frequency (pedestal subtraction in each channel)
  - BUT, adding more crystal increases the noise ! (for 3x3 b is 120 MeV).
  - BUT APD are noiser and noiser (integrating dose) (add to b 30 MeV)
  - BUT there might be pile-up (high luminosity) (add to b 100 MeV)
- NB: add in quadrature

SAMPLING CALORIMETERS

• Different structure:

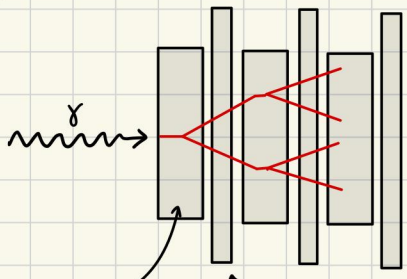

passive material (dense) Pb/Fe

active material
e.g scintillator + PMT
it samples the shower evolution detecting the charged particles

- LAr ATLAS CALORIMETER

- Accordion geometry
- How does it work:
  - shower particles generated in the Pb layers
  - ionization of LAr
  - collection of the charge (ions/e^- drift)

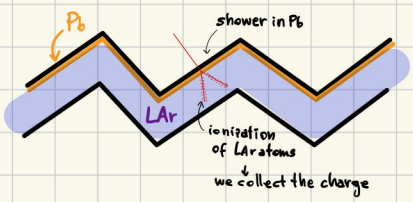

- PROs:
  - fast collection geometry
  - no dead spaces
  - 174000 electronic channels
  - Intrinsically radiation tolerant
  - better E resolution

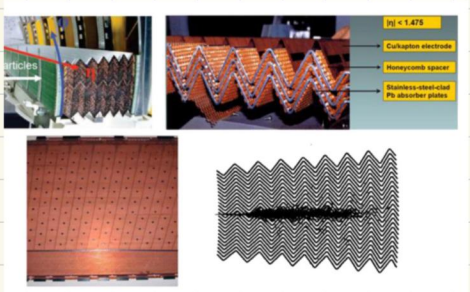

- KLOE SCINTILLATING FIBERS + LEAD SAMPLING CALORIMETER

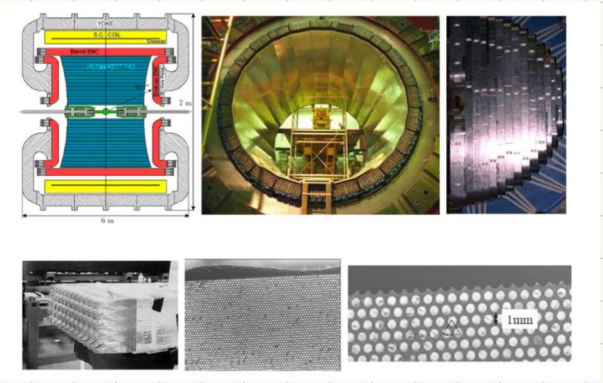

- Same concept of ATLAS calorimeter but without noble liquid
- It is made by Pb sheets interleaved with fibers (1mm diameter)

- LKR NA48 CALORIMETER / MEG LXe CALORIMETER

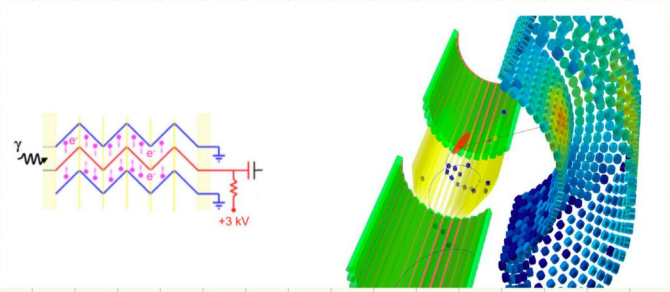

- MORE ON NOBLE LIQUID

	Z	A	T_{BP} (K)	Density (g/cm³)	X_0 (cm)	R_M (cm)	E_C (MeV)	dE/dx (min) (MeV/cm)	W_I (eV)	F
Argon	18	39.9	87.3	1.40	14.0	9.0	31.9	2.11	23.6	0.11
Krypton	36	83.8	119.9	2.42	4.7	5.9	16.5	3.28	18.4	0.06
Xenon	54	131.3	165.1	2.95	2.9	5.2	11.3	3.71	15.6	0.04

- Useful because they can be used for both scintillation and ionization
  - scintillation : for position measurement
  - ionization : for calorimeter measurements

  } Both provide PID (e.g. DN double phase TPC)

- HADRONIC SHOWERS AND HADRONIC CALORIMETERS

- Much more complicated than e.m. showers
- Main components : pions (but not only)
  - charged pions reinteract
  - neutral pions decay promptly $\pi^0 \to \gamma\gamma$ → e.m. subshowers

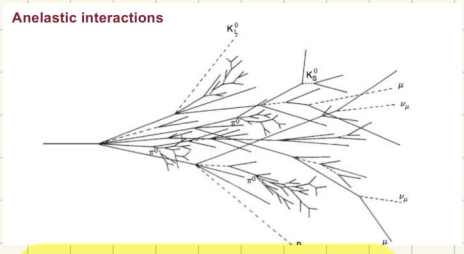

- Scale length given by interaction length (longer than X_0) $\lambda_I \sim 35\ g\,cm^{-2} \cdot A^{1/3}$
- Larger lateral spread (due to strong interaction; typical E scale ~350MeV for transverse momentum)

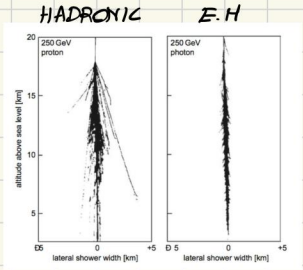

- SUMMARY PIC

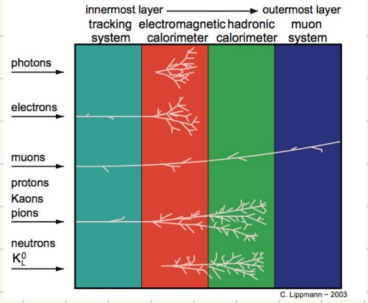

ELECTRONICS

- TYPE OF SIGNAL
  - Analog signal : (used into amplification, shaping, transmission...) variable amplitude

  - Digital signal : (used into bit conversion, data saving) constant amplitude, but variable timing

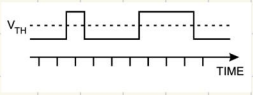

- BASIC ABOUT DIGITAL LOGIC

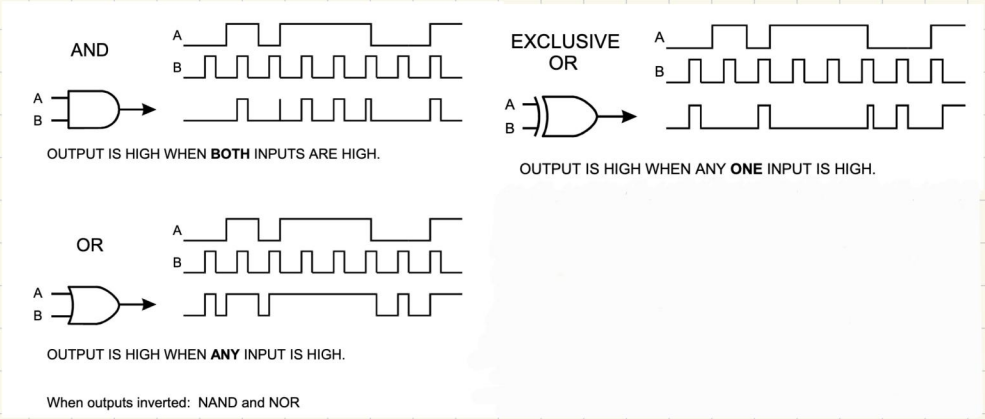

- BASIC MODEL FOR A DETECTOR

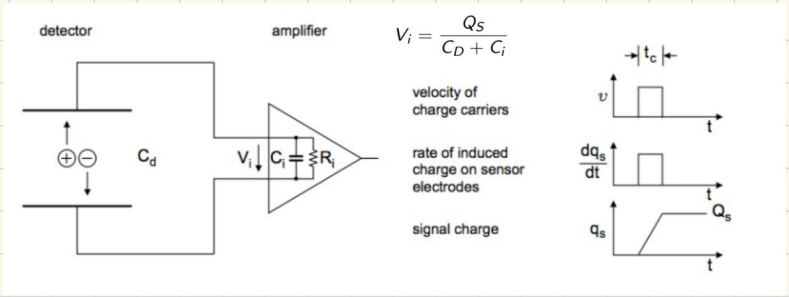

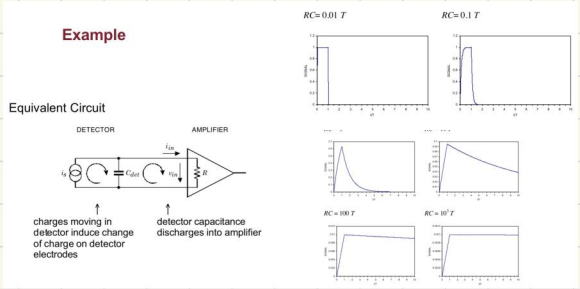

- PULSE SHAPING
  - 2 conflicting objectives:
    1) Limit the bandwidth to match the measurement time ⟶ too large bandwidth increases the noise
    2) Contain the pulse width so that successive signal pulses can be measured without overlap (pile-up) ⟶ short pulse duration increases the allowed signal rate but also the noise.

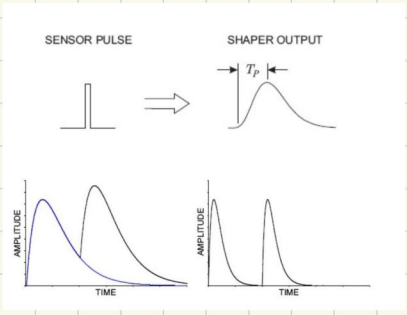

  - Example of a simple shaper : CR-RC
    - the high-pass filter sets the duration of the pulse to have a decay time τ_d
    - the low-pass filter increases the rise time to limit the noise bandwidth.
    - Key design parameter : peaking time ⟶ it dominates the noise bandwidth

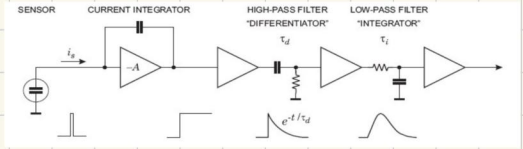

- **ADC**

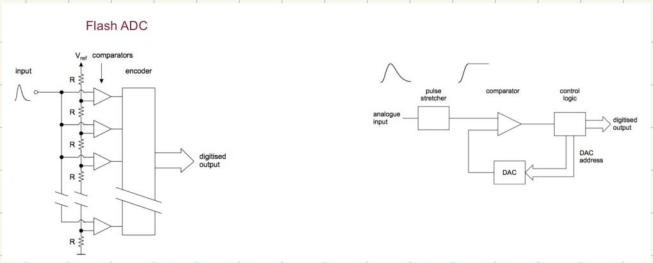

- **TDC**

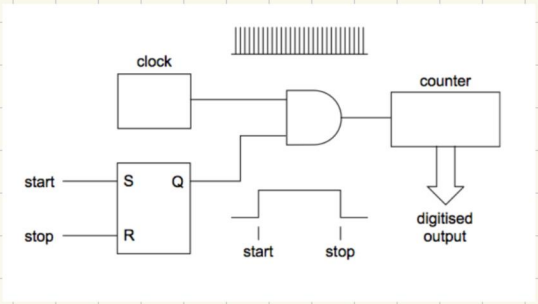

- WILKINSON : it transforms charge into number of clock (time over threshold)

WILKINSON ADC

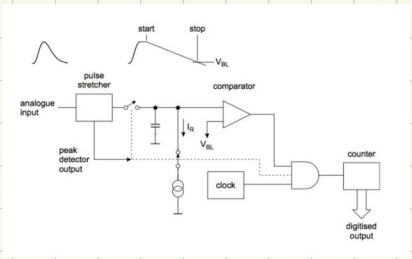

WILKINSON TDC